On Anterior Cruciate Ligament Injury Prevention: Utilizing Wearable Sensors to Track Potential High-Risk Knee Kinematics and Kinetics

by

Mirel Ajdaroski

A dissertation submitted in partial fulfillment
of the requirements for the degree of
Doctor of Philosophy
(Mechanical Sciences and Engineering)
in the University of Michigan-Dearborn
2023

Doctoral Committee:

Associate Professor Amanda O. Esquivel, Chair
Professor Alan Argento
Professor James A. Ashton-Miller, University of Michigan-Ann Arbor
Associate Professor Samir Rawashdeh

Acknowledgements

This dissertation would not have been possible without my advisor Dr. Amanda Esquivel who gave me invaluable guidance throughout both my undergraduate and graduate pursuits. She allowed me to freely work on my research but gave important suggestions and support whenever I needed it. Without her guidance and support, completing this work would've been impossible. I owe you a tremendous amount of gratitude.

I would also like to sincerely thank the Ann Arbor team - Dr. James Ashton-Miller, Dr. Mélanie L. Beaulieu, Dr. Payam Mirshams Shahshahani, and Dr. So Young Baek. Their interest in our study and their kind and welcoming attitudes made working together one of the most enjoyable experiences of my life. I look forward to working together with them in future studies.

I would like to thank my committee members: Dr. Alan Argento, Dr. James Ashton-Miller, and Dr. Samir Rawashdeh. Each has given vital comments and suggestions during the proposal of my work that have helped shape my research.

And lastly, I would like to thank my lab team member at the University of Michigan-Dearborn, who have helped with data collection and given me priceless feedback on my ideas.

Thank you all

Preface

Chapters 3 through 6 have been written as separate manuscripts for publication. There may be some repetition of the presented material for each chapter.

Table of Contents

List of Tables

List of Figures

List of Abbreviations

ACL..... Anterior cruciate ligament

ADL ..... Activities of daily living

AMB ..... Anteromedial bundle

aTT .....Anterior tibial translation

BA ..... Bland-Altman

BW .....Body weight

CI.....Confidence interval

CLS ..... Certus/load cell system

COD .....Change-of-direction

CRS .....Cardan rotation sequence

FATC ..... Femur-ACL-tibia complex

GPR..... Gaussian process regression

GRF..... Ground reaction force

GRM .....Generalized regression model

H ..... Height

ICC .....Interclass correlation

IMC .....Inertial motion capture

IMUs .....Inertial measurement units

IQR.....Interquartile range

KAM ..... Knee abduction/adduction moment

KRM ..... Knee rotation moment

LADF ..... Linear acceleration decay factor

LoAs ..... Bland-Altman limits of agreement

MAE ..... Mean absolute error

MAPE ..... Mean absolute percent error

MCS ..... Motion capture systems

MDDF ..... Magnetic disturbance decay factor

MEM ..... Mix effect model

MSE ..... Mean square error

N ..... Newtons

NED ..... North-east-down

NIOSH ..... National Institute of Occupational Safety and Health

NRMSE ..... Normalized root mean square errors

PLB ..... Posterolateral bundle

pVGRF ..... Peak vertical GRF

QC ..... Quaternion conversion

ReLU ..... Rectified linear unit

RMSE ..... Root mean square error

SA ..... Stair ascent

SD ..... Stair descent

StS ..... Sit-to-stand

SVM ..... Support vector machine

TQC ..... Tuned quaternion conversion

Abstract

Participation in competitive sports is on the rise, and along with this comes an increase in sports-related injuries. While these injuries can happen to any part of the body, some of the most common are lower limb injuries, particularly to ligaments, with one of the most common being the anterior cruciate ligament (ACL). Within this work, we examined soft tissue overuse injury mechanisms using a novel tool for identifying potentially injurious loading cycles that occur in adolescent athletes (predominantly female athletes) with the long-term goal of prevention of this unintentional injury. We used a commercially available inertial measurement units (IMUs) to develop post-collection equations that could accurately and reliably estimate ground reaction force, knee moments, and knee angles; each a crucial factor in determining potential ACL injury. We partitioned this study into two distinct stages, each with specific purposes and goals. In the first stage, we used *in vitro* models to estimate our required metrics. Here, we used two IMUs and machine learning algorithms and compared the estimates to values measured by a motion capture and load cell system. We determined that the equations could estimate ground reaction force, knee moments, and knee angles with moderate accuracy and reliability. We additionally found that a tuned quaternion conversion method provided more accurate knee angle measurements than a commercially available sensor fusion algorithm. These findings allowed us to proceed to the second stage, human subject testing, where we developed modifications to the first-stage equations. Here we used four IMUs (two on each limb), the models developed in the first stage, and machine learning to construct a modified model; we then compared the estimates for these modified models to measurements of a motion capture system and force plate

measurements. These modified models could estimate metrics with moderate accuracy; however, the knee moment reliability was not satisfactory. We then developed a confusion matrix to examine if these estimates could distinguish between low-risk and potentially damaging events, and results showed high classification accuracy, precision, specificity, and sensitivity. We also adjusted the quaternion conversion method for human subject use and found the tuned algorithm provided more accurate and reliable knee angle measurements. Our results show the potential of IMUs for tracking gameplay events and distinguishing between low-risk and potential-risk events. While we acknowledged several limitations within our work, we ultimately believe that IMUs may be able to aid coaches and sports physicians in preventing some athletes from sustaining ACL injuries.

Chapter 1: The Purpose of the Study

Over the last two decades, the participation of adolescents and children in organized sports has experienced a boom in popularity, with involvement occurring at younger ages and expectations of individuals being higher [1, 2]. While organized sports have many benefits for those who regularly engage in them, such as improved physical and mental health, negative effects such as an increased risk of injuries can also occur [3]. Nearly 30 million people are injured every year while participating in some sports [4]. And while injury can happen to any part of the body, some of the most common are those to the lower limbs, which include stress fractures, tendinopathy, ligament tears, and, depending on the sport, joint dislocations [5]. However, among these possible lower limb injuries, some of the most debilitating are those to ligaments, specifically, to the ACL. In the United States, some 100,000 to 200,000 ACL ruptures are reported every year [6, 7]. To address this concern, it is important to understand the mechanics involved in ACL injuries. In this chapter, we will begin with an introduction to the structure of the ACL, including its mechanical properties, and other defining characteristics. This will be followed by a discussion of the potential injury mechanisms, how tracking of kinematics and kinetics of the knee may help prevent injuries, the technology used as well as their drawbacks, and finally discuss the various gaps in knowledge that this research was designed to address.

1.1 The Anterior Cruciate Ligament

The primary function of the ACL is to resist anterolateral displacement and internal rotation of the tibia relative to the femur [8]. It's also one of the most injured ligaments in sports, and once

ruptured, surgical intervention is often required [8-10]. With its origin on the posteromedial aspect of the fossa on the lateral femoral condyle and its insertion on the anterolateral aspect of the intercondylar fossa of the tibia, the ACL runs anteromedially and distally from the femur toward the tibia [11-13]. In an adult the typical length of this ligament is 32 mm with a typical width range of 7 to 12 mm [13]. At the site of insertion, the ACL passes beneath the transverse (also known as anterior) mensicomeniscal ligament (the ligament that attaches the anterior horn of the lateral meniscus to the anterior horn of the medial meniscus), and in some cases the posterior fascicles of the ACL it may blend with the posterior attachment of the lateral meniscus and become indistinguishable [11].

Although the ACL has been modeled as a single bundle and even three-bundle structure, in general, it is considered a two-bundle system that includes the anteromedial bundle (AMB) and the posterolateral bundle (PLB) [11, 14]. The AMB is comprised of the fascicles on the anteromedial aspect of the insertion site of the ACL, and under relaxed conditions, exhibits a more vertical orientation than that of the PLB (approximately 70° from the tibial head compared to 55°) [15, 16]. The PLB fascicles are located on the posterolateral aspect of the insertion of the ligament, and during extension, experience more stress, leaving the AMB slacker [15, 16]. As the knee flexes, the ACL begins to become parallel to the superior tibia, and while experiencing rotation, tends to exhibit a greater lengthening under internal rotation than external; a discrepancy that is more prominent while the joint is in flexion [16]. However, it is worth noting that, because it's composed of differing fascicles and in different orientations, various parts of the ACL are stretched in different directions throughout the knee's total range of motion [17]. Therefore, while the two-bundle is widely accepted and indicates that the AMB is active during

flexion and the PLB is active during extension, this is an oversimplification of the system; at any position of the knee, some tension will be present on both bundles due to leg muscle activity. While the ACL's primary function is to resist anteroposterior movement of the tibia to the femur, studies have also illustrated that its secondary function is resisting internal rotation during knee extension [18-20].

The stress/strain curve associated with most biological tissues is unique when compared to other materials in that three distinct regions are readily observed; 1) the toe region, 2) the linear region, and 3) the yield/failure region [20]. For most activities of daily living (ADL), ligaments remain in the in toe or in the linear region [20, 21]. In the toe region of the relaxed ligament, the collagenous fibers of the ligament/tendon are in what is called a *crimped* state due to disorganized fibers [22]. Within the stress strain curve, this first region is distinct and exhibits a lower stiffness compared to the other regions [20, 21]. This is important because, when a load is applied and collagen fibers begin straightening, a portion of that stress is dissipated in a process known as *uncrimping* [22]. The toe region accounts for about 2% of the strain, after which point, the ligament enters the linear region [22]. Within the linear region, the uncrimped collagen fibers, in response to continued strain, start to stretch, and begin to deform in a linear manner as inter-molecular sliding of collagen triple helices begin to occur [20, 21]. Generally, if the strain is below 4% , the tissue will return to its original, uncrimped state once the load is removed with no damage to the fibers; this portion is thus elastic and reversible [22]. Beyond this 4% limit, some fibrils begin failing as the intramolecular cross-links between collagen fibers breaks. Continuing to strain the ligament can cause an accumulation of these micro failures, ultimately

reducing the stiffness of the tissue. When strain is greater than 8% of its original length, macroscopic failures are observed until ultimate failure of the ligament is reached [22].

During biomechanical testing of the ACL, various testing conditions such as pre-conditioning and the age of the specimen can affect the outcome. During loading-unloading cycles in tissues, the stress-strain curve differs in the initial few iterations; each new iteration shifts the curve rightward [20, 23]. Along with shifting, subsequent cycles decrease the peak stress achieved in the ligament during the same applied load [23]. These characteristic changes of the tissue can occur even while the tissue is under viscoelastic recovery, and it's these characteristic changes that are termed the hysteresis of the system [20, 23]. To address the effect of these changes, *preconditioning* is frequently used in the testing of biological tissues [23]. While there is no standardized method through which preconditioning is conducted, most studies that have examined the use of some tissue preconditioning report that a state of stability (the point at which subsequent testing causes no characteristic changes) can be achieved after 3-10 testing cycles [24-26]. Although standardized preconditioning methods do not exist, various studies have presented generalized guidelines that should be followed. During tissue preconditioning, it has been suggested that the load in the preconditioning protocol should be similar to the testing protocol; [27, 28]. The overall structural and mechanical properties of the ACL are heavily influenced by the age of the individual; older persons have been shown to have decreases in the upper limits of important properties associated with the ACL and the femur-ACL-tibia complex (FATC) such as linear stiffness, ultimate load, and the energy the system can withstand before failure [29-31]. Cadaveric testing has shown the average linear stiffness of ACLs belonging to young specimens (22-35 yrs.) to be 242 ± 28 N/mm, with a 26% decrease when observing ACLs

of older (60-97 yrs.) specimens [29]. Woo et al. observed that the mean ultimate load in younger ACL specimens was 2160 ± 157 N and decreased with age to a mean value of 1160 ± 104 N when testing older specimens, representing a 46% decrease [29]. Energy absorption, defined as the area beneath the stress-strain curve to the point of failure, was observed to be 11.6 ± 1.7 Nm in young specimens and decreased sharply to 1.8 ± 0.5 Nm when observing older specimens [29].

1.2 Mechanism of ACL Injury

ACL injury can fall into one of two distinct categories: 1) contact (30% of all cases); 2) non-contact (70% of all cases) [32-35]. Contact injuries are the result of a transfer of a force onto the knee from an external source (usually from another player or player equipment), which causes an abnormally large anteroposterior knee displacement to occur [32, 33]. Given the functional role of the ACL, it's theorized that under these conditions, the ACL experiences a significant strain as it attempts to resist the movement which causes failure of the tissue [32, 33]. Because these injuries transpire acutely during gameplay, the only means through which they can be addressed is either through the introduction of additional protective equipment (affecting player capabilities) or the implementation of additional rules (affecting gameplay). However, because these injuries are less than half as common as non-contact injuries, it is non-contact injures that should be focused upon.

As the name suggests, non-contact injuries involve no contact or load transfer from an external source save the ground reaction and/or moment under the foot, so the load on the knee is generated internally by the player in response to that reaction force or moment. Non-contact

ACL injuries can be further subdivided into two distinct categories: 1) acute, and 2) those that may be the result of possible tissue fatigue [36]. Recent studies using cadaveric specimens have suggested that some non-contact ACL injuries may be attributable to overuse of the ligament, where repetitive high stress/strain-inducing activities result in micro-failures of the tissue, and continued performance without adequate rest leads to propagation of these failures which ultimately leads to an ACL rupture [36]. If this is the case, then the prediction of some ACL failures may be possible. In the next sections, we will discuss the knee kinematics through which a non-contact ACL injury can occur, followed by a discussion on the methods through which knee kinematics are measured.

1.2.1 Kinematics of the Knee During Non-Contact ACL Injuries

Various studies have examined the kinematics of the knee during non-contact ACL injuries using a combination of data captured on-field, in laboratory testing, and computer simulations, and have been able to note the typical kinematics [37, 38]. Generally, it has been reported that during non-contact injuries, the knee is in an externally rotated and more extended position (20° or less in flexion); slight valgus may also be present [37, 38]. It's been theorized that once these conditions are met, and load (ground reaction force) is applied across the knee, a powerful quadriceps contraction causes anterior displacement of the tibia to the femur [37, 38]. This displacement may lead to increases in ACL strain to above the tolerable threshold as the ACL attempts to resist the movement [37, 38]. Although, this is one of many possible mechanisms other studies have reported that a fully extended knee, in neutral internal rotation and valgus orientation, subjected to high loading (such as landing from a jump) can significantly strain the ligament [37]. Some studies have also noted the effect of strong muscle actions, such as an

eccentric contraction of the quadriceps during high-speed sudden stopping actions has also been linked to non-contact injuries [39].

While the above-mentioned theory emphasizes the load and knee orientation or the contractile strength of the muscle groups in the thigh, many studies have also shown a correlation between knee moments and stress/strain of ACL, particularly internal rotation and valgus; thus, the ability to track knee moments may also be important [16, 40-42]. Increases in the valgus moment in conjunction with an increase in the antero-tibial shear have been shown to increase the stress sustained by the ACL; it's also been noted that the stress due to this combination is greater than that of either component acting individually [16, 40]. With the addition of a load (ground reaction force), the effect of valgus moment grows considerably, causing significant increases in the strain of the ligament to or above its threshold limits [41]. A meta-analysis conducted by Hewett et al. examined six different studies that focused on non-contact ACL injuries throughout a normal season of play across differing sports, to determine potential predictive factors that could be used in understanding the risk factors for female athlete non-contact ACL injuries [32, 33]. They found that athletes that sustained an ACL injury had up to a 2.5x greater knee valgus moment at the time of injury ($p < 0.01$) and that the magnitude of knee valgus moment was able to predict ACL injury status (73% specificity and 78% sensitivity) [32, 33]. Though, they remarked on ACL injuries having a multifactorial etiology, with various contributing factors. They also add to this that the subject they observed had been playing sports for multiple years, and that it may take years of excessive valgus moments before an ACL injury occurs. This poses the question of whether it was valgus moments that led to the injuries, or if another of these

contributing factors is responsible for the injury and changes in valgus are the results of an already damaged ACL.

Internal rotational moments have also been linked to increases in the stress sustained by the ligament, and when combined with antero-tibial shear and a valgus moment, this stress further increases; the addition of a load has also been observed as contributing to the stress of the ACL while under an internal rotational moment [40-42]. Shin et al. utilized *in vivo* human data and computer simulation to quantify theoretical ACL strain experienced during a single-legged landing and noted the correlations of the valgus and internal rotational moment increases with increases in the ligament's strain [42]. A combination of maximum physiological valgus and internal rotational moments was observed to produce peak strains of 0.105 [42]. The reported range for ACL rupture due to strain is 0.09 to 0.15 [42]. When Shin et al. expanded the parameters to include conditions akin to game scenarios, they recorded peak strains as high as 0.115 [42]. However, when examining overuse as a possible ACL injury mechanism, Wojtys et al. found that high internal rotation moments contributed to failure, whereas abduction moment did not place large strains on the ACL [36].

The importance of the ground reaction force (GRF), the knee orientation, and the internal rotational and valgus moments in the quantification of stress/strain in ACL can be easily understood, but other, non-kinematic/kinetic factors may also influence potential overuse injuries. And while we will not be considering them during our study, it is important to recognize and briefly discuss their influence.

1.2.2 Non-Kinematic/Kinetic Factors That Also Contribute to Overuse Injuries

While both males and females are susceptible to ACL injuries, females on average are 3x more likely to be affected [32, 33]. The exact reason for this difference between the sexes is still being researched, but to date, various possible explanations have been discussed. The smaller, slightly narrower shape of the intercondylar notch of the female femur may cause the ACL to sustain greater degrees of strain when subjected to similar conditions as their male counterparts [37, 43-45]. Alternatively, the wider pelvis of females causes their quadriceps angle (q-angle) to be larger, thus, forcing the femur into a larger valgus angle toward the knee [46]. Various studies have shown that this larger angle decreases the muscular support of the knee, and thus, the stability of the joint is more heavily influenced by the ligaments [47, 48]. There are also hormonal differences between the sexes, and these differences may affect the laxity and other mechanical properties of the ligament [49]. Other factors include the type of footwear and the surface of play, with various studies reporting that certain shoes, designed to improve a player's on-field effectiveness through providing additional field traction, have the unintended effect of increasing stress on the ligament and have been correlated with a higher incidence rate [37, 38, 50, 51]. While the anatomical reason for the increased risk of ACL injury cannot be controlled, other factors relating to kinematics and volume of exposure are controllable factors.

1.3 Measuring the Forces and Moments Placed on the Knee, and Knee Angles Involved

Traditionally, lower limb joint kinematics/kinetics have been quantified in laboratory settings using camera-based motion capture systems (MCS) combined with force plates. During a session, a subject can be asked to perform various actions that are recorded. This data is then processed using a combination of force and marker positional data, which allows for the

determination of ground reaction force, joint moments, and angles. In general, this system is not ideal to capture on-field kinematic and kinetic data as this system is bulky and there is an inability to measure rotations accurately due to the presence of soft tissue. However, in recent years the development of wearable sensors has emerged as an alternative to motion capture and has been employed in various applications such as gait analysis and rehabilitation assistance [52-58]. Wearable sensors are smart electronic devices that can be directly worn by a person to allow for the detection and transmission of various signals concerning the body such as vital signs or pedometers for health purposes. In more recent years, growing interest in IMU technologies, a particular type of wearable sensor, has emerged in the field of sports medicine as a possible means to track subject data without the cost and hindrances of MSCs.

1.3.1 Inertial Measurement Units

IMUs are small, wearable sensors that consist of orthogonal accelerometers, rate gyroscopes, and magnetometers that allow for the direct measurement of a body segment's linear acceleration, angular velocity, and environmental magnetic field strength. Three-dimensional joint angles can be obtained through sensor fusion algorithms; these algorithms use knowledge of their dynamics to estimate orientation changes based on gyroscope information and fuse these estimates with orientations determined through a combination of accelerometer and magnetometer information. However, there are limitations in the direct measurements of certain data, and because of this, post-collection equations are required if IMUs are to be used for the assessment of the forces and/or moments that could lead to injuries like ACL ruptures.

1.4 Summary of the Problem and Purpose of the Study

The increase in the frequency of ACL injuries is a growing concern, and the need to be able to prevent them has garnered much attention in sports medicine. Most ACL injuries are non-contact in nature, and in some cases may be due to ligament overuse. Fortunately, if overuse is the reason, there is a way to prevent them through the tracking of certain kinematic/kinetic data: GRF, moments, and angles, especially during training and practices. While traditional methods have limited practical use outside the laboratory, the emergence of IMUs may be a viable on-field approach to tracking these parameters. We propose to study soft tissue overuse injury mechanisms using these novel tools for identifying potentially injurious loading cycles that occur in adolescent athletes (predominantly female athletes) with the long-term goal of preventing this unintentional injury.

Various studies have reported upon the correlation between linear acceleration and GRF and have used IMU data to estimate GRF with varying success [59-61]. However, many of these studies have focused on linearly modeling the relationship. Other factors, such as angular acceleration, skin laxity, as well as landing angle, may influence the relationship. It may be that the relationship between linear acceleration and experienced GRF is not purely linear, but instead a more complex, affected by multiple variables either directly or indirectly. Thus, the first purpose of our study was to develop a model that can be applied to an IMU's data to obtain the magnitude GRF.

While a set of adjacent IMUs can report tibiofemoral angles, such angles may be questionable. Because IMUs have been extensively used in rehabilitation and gait analysis, it's hypothesized

that the sensor fusion algorithm's specific parameters are tuned for these less intense activities and, as such, may be less accurate when employed in more dynamic ones such as sports, where larger changes in joint angles and velocities may occur. The widespread and proven success of sensor fusion algorithms is known, but it may be that certain parameters need to be fine-tuned for dynamic actions. Thus, the second purpose of this study was to fine-tune specific parameters of a sensor fusion algorithm and determine if these modified parameters demonstrate improved accuracy and reliability in angle measuring capabilities over those used by a sensor.

The correlation between increases in valgus and/or internal rotational moments and stress experienced by the ACL has been noted previously. Studies have attempted to correlate IMU data with moments but have done so utilizing gyroscope data and single-variable, linear modeling [62, 63]. Examining moments in terms of rigid body dynamics states the moments are related to some force acting some distance from the point of rotation as well as some angular rate acting upon the mass moment of inertia. Therefore, a multivariable model may be needed to determine moments more accurately. Furthermore, other variables such as skin laxity may also contribute to the relationship in live subjects. Thus, the third purpose of this study was to develop a mathematical model that can be applied to IMU data to obtain moments, specifically, those of valgus and internal rotation.

The fourth and final purpose of this study was to determine if the estimates obtained for force and moments could be used to classify an event as either low-risk or potentially injurious. This ability to classify events may be crucial for injury-tracking purposes as we are not necessarily

concerned with the values for force/moments, but instead, if the force/moment experienced is sufficient to potentially be injurious or not.

1.5 Dissertation Overview

With the understanding of what we wished to achieve, we developed our study to answer several important scientific questions: Can linear and angular accelerations and/or angles measured at the lower leg and upper leg indicate ground reaction force, knee internal tibial torque, and flexion moment values? How can IMUs be used to identify potentially dangerous loading conditions in a laboratory setting *in vivo*? And can the fine-tuning of specific parameters in a sensor fusion algorithm lead to more accurate and reliable tibiofemoral angle measurements? The study was separated into two distinct stages, each with specific purposes and goals. Stage 1: Identify injurious loading cycles using a wearable IMU based on kinematic inputs of impact force, knee moments, and angles in an *in vitro* model. Stage 2: Estimate various parameters such as GRF and knee moments to IMU measurements and examine errors due to soft tissue motion. Models and algorithm parameters developed in Stage 1 were applied to Stage 2 data and modified to account for the effects of tissue artifact and different dynamic movements. Following the modification of our models, a final assessment of the practicality of our models and algorithm to estimate GRF, knee moments, and knee angles was examined, along with our ability to distinguish between low-risk and potentially injurious events. How these models may be implemented in the field, and possible limitations were also discussed.

1.6 References

[1] D. Caine, L. Purcell, and N. Maffulli, "The child and adolescent athlete: a review of three potentially serious injuries," (in eng), *BMC Sports Sci Med Rehabil,* vol. 6, p. 22, 2014, doi: 10.1186/2052-1847-6-22.

[2] E. R. Dodwell, L. E. Lamont, D. W. Green, T. J. Pan, R. G. Marx, and S. Lyman, "20 years of pediatric anterior cruciate ligament reconstruction in New York State," (in eng), *Am J Sports Med,* vol. 42, no. 3, pp. 675-80, Mar 2014, doi: 10.1177/0363546513518412.

[3] C. Malm, J. Jakobsson, and A. Isaksson, "Physical Activity and Sports-Real Health Benefits: A Review with Insight into the Public Health of Sweden," (in eng), *Sports (Basel),* vol. 7, no. 5, May 2019, doi: 10.3390/sports7050127.

[4] S. Habelt, C. C. Hasler, K. Steinbruck, and M. Majewski, "Sport injuries in adolescents," *Orthop Rev (Pavia),* vol. 3, no. 2, p. e18, Sep 6 2011, doi: 10.4081/or.2011.e18.

[5] W. Bruns and N. Maffulli, "Lower limb injuries in children in sports," (in eng), *Clin Sports Med,* vol. 19, no. 4, pp. 637-62, Oct 2000, doi: 10.1016/s0278-5919(05)70230-1.

[6] W. Alghamdi *et al.*, "Prevalence of Cruciate Logaments Injury among Physical Education Students of Umm Al-Qura University and the Relation betwen the Dominant Body Side and Ligament Injury Side in Non-Contact Injury Type," *American Journal of Medicine and Medical Sciences,* vol. 7, no. 1, pp. 14-19, 2017.

[7] I. O. Saeed, "MRI Evaluation for Post-Traumatic Knee Joint INjuries," *Journal of Nursing and Health Science,* vol. 7, no. 2, pp. 48-51, 2018.

[8] G. G. Arliani, C. Astur Dda, M. Kanas, C. C. Kaleka, and M. Cohen, "Anterior Cruciate Ligament Injury: Treatment and Rehabilitation. Current Perspectives and Trends," *Rev Bras Ortop,* vol. 47, no. 2, pp. 191-6, Mar-Apr 2012, doi: 10.1016/S2255-4971(15)30085-9.

[9] Y. Nagano, H. Ida, M. Akai, and T. Fukubayashi, "Biomechanical characteristics of the knee joint in female athletes during tasks associated with anterior cruciate ligament injury," *Knee,* vol. 16, no. 2, pp. 153-8, Mar 2009, doi: 10.1016/j.knee.2008.10.012.

[10] B. R. Bach, Jr., M. E. Levy, J. Bojchuk, S. Tradonsky, C. A. Bush-Joseph, and N. H. Khan, "Single-incision endoscopic anterior cruciate ligament reconstruction using patellar tendon autograft. Minimum two-year follow-up evaluation," *Am J Sports Med,* vol. 26, no. 1, pp. 30-40, Jan-Feb 1998, doi: 10.1177/03635465980260012201.

[11] V. B. Duthon, C. Barea, S. Abrassart, J. H. Fasel, D. Fritschy, and J. Menetrey, "Anatomy of the anterior cruciate ligament," *Knee Surg Sports Traumatol Arthrosc,* vol. 14, no. 3, pp. 204-13, Mar 2006, doi: 10.1007/s00167-005-0679-9.

[12] M. L. Purnell, A. I. Larson, and W. Clancy, "Anterior cruciate ligament insertions on the tibia and femur and their relationships to critical bony landmarks using high-resolution

volume-rendering computed tomography," *Am J Sports Med,* vol. 36, no. 11, pp. 2083-90, Nov 2008, doi: 10.1177/0363546508319896.

[13] R. v. Zyl, A. N. v. Schoor, P. J. d. Toit, and E. M. Louw, "Clinical anatomy of the anterior cruciate ligament and pre-operativeprediction of ligament length," *SA Orthopaedic Journal,* vol. 15, no. 4, pp. 47-52, 2016.

[14] E. Stieven-Filho, E. T. Garschagen, M. Namba, J. L. Silva, O. Malafaia, and L. A. Cunha, "Anatomic study of the double-bundle of the anterior cruciate ligament with the knee in 90 masculine flexion," *Rev Col Bras Cir,* vol. 38, no. 5, pp. 338-42, Sep-Oct 2011.

[15] A. A. Amis and G. P. Dawkins, "Functional anatomy of the anterior cruciate ligament. Fibre bundle actions related to ligament replacements and injuries," *J Bone Joint Surg Br,* vol. 73, no. 2, pp. 260-7, Mar 1991.

[16] J. M. Hollis, S. Takai, D. J. Adams, S. Horibe, and S. L. Woo, "The effects of knee motion and external loading on the length of the anterior cruciate ligament (ACL): a kinematic study," *J Biomech Eng,* vol. 113, no. 2, pp. 208-14, May 1991, doi: 10.1115/1.2891236.

[17] T. J. Mommersteeg, J. G. Kooloos, L. Blankevoort, J. M. Kauer, R. Huiskes, and F. Q. Roeling, "The fibre bundle anatomy of human cruciate ligaments," *J Anat,* vol. 187 (Pt 2), pp. 461-71, Oct 1995.

[18] H. Matsumoto, Y. Suda, T. Otani, Y. Niki, B. B. Seedhom, and K. Fujikawa, "Roles of the anterior cruciate ligament and the medial collateral ligament in preventing valgus instability," *J Orthop Sci,* vol. 6, no. 1, pp. 28-32, 2001, doi: 10.1007/s007760170021.

[19] D. B. Lipps, Y. K. Oh, J. A. Ashton-Miller, and E. M. Wojtys, "Effect of increased quadriceps tensile stiffness on peak anterior cruciate ligament strain during a simulated pivot landing," (in eng), *J Orthop Res,* vol. 32, no. 3, pp. 423-30, Mar 2014, doi: 10.1002/jor.22531.

[20] K. Robi, N. Jakob, K. Matevz, and V. Matjaz, "The Physiology of Sports Injuries and Repair Processes," ed, 2013, pp. 42-86.

[21] S. L. Woo, R. E. Debski, J. Zeminski, S. D. Abramowitch, S. S. Saw, and J. A. Fenwick, "Injury and repair of ligaments and tendons," (in eng), *Annu Rev Biomed Eng,* vol. 2, pp. 83-118, 2000, doi: 10.1146/annurev.bioeng.2.1.83.

[22] M. L. Killian, L. Cavinatto, L. M. Galatz, and S. Thomopoulos, "The role of mechanobiology in tendon healing," *J Shoulder Elbow Surg,* vol. 21, no. 2, pp. 228-37, Feb 2012, doi: 10.1016/j.jse.2011.11.002.

[23] T. K. Tonge, B. J. Murienne, B. Coudrillier, S. Alexander, W. Rothkopf, and T. D. Nguyen, "Minimal preconditioning effects observed for inflation tests of planar tissues," (in eng), *J Biomech Eng,* vol. 135, no. 11, p. 114502, Nov 2013, doi: 10.1115/1.4025105.

[24] M. J. Muñoz *et al.*, "An experimental study of the mouse skin behaviour: damage and inelastic aspects," (in eng), *J Biomech,* vol. 41, no. 1, pp. 93-9, 2008, doi: 10.1016/j.jbiomech.2007.07.013.

[25] Y. J. Zeng, Y. H. Liu, C. Q. Xu, X. H. Xu, H. Xu, and G. C. Sun, "Biomechanical properties of skin in vitro for different expansion methods," (in eng), *Clin Biomech (Bristol, Avon),* vol. 19, no. 8, pp. 853-7, Oct 2004, doi: 10.1016/j.clinbiomech.2004.05.009.

[26] M. C. Lee, Y. C. Fung, R. Shabetai, and M. M. LeWinter, "Biaxial mechanical properties of human pericardium and canine comparisons," (in eng), *Am J Physiol,* vol. 253, no. 1 Pt 2, pp. H75-82, Jul 1987, doi: 10.1152/ajpheart.1987.253.1.H75.

[27] Y. Lanir and Y. C. Fung, "Two-dimensional mechanical properties of rabbit skin. II. Experimental results," (in eng), *J Biomech,* vol. 7, no. 2, pp. 171-82, Mar 1974, doi: 10.1016/0021-9290(74)90058-x.

[28] E. O. Carew, A. Garg, J. E. Barber, and I. Vesely, "Stress relaxation preconditioning of porcine aortic valves," (in eng), *Ann Biomed Eng,* vol. 32, no. 4, pp. 563-72, Apr 2004, doi: 10.1023/b:abme.0000019176.49650.19.

[29] S. L. Woo, J. M. Hollis, D. J. Adams, R. M. Lyon, and S. Takai, "Tensile properties of the human femur-anterior cruciate ligament-tibia complex. The effects of specimen age and orientation," *Am J Sports Med,* vol. 19, no. 3, pp. 217-25, May-Jun 1991, doi: 10.1177/036354659101900303.

[30] S. L. Woo, C. Wu, O. Dede, F. Vercillo, and S. Noorani, "Biomechanics and anterior cruciate ligament reconstruction," *J Orthop Surg Res,* vol. 1, p. 2, Sep 25 2006, doi: 10.1186/1749-799X-1-2.

[31] J. Hashemi, H. Mansouri, N. Chandrashekar, J. R. Slauterbeck, D. M. Hardy, and B. D. Beynnon, "Age, sex, body anthropometry, and ACL size predict the structural properties of the human anterior cruciate ligament," (in eng), *J Orthop Res,* vol. 29, no. 7, pp. 993-1001, Jul 2011, doi: 10.1002/jor.21245.

[32] T. E. Hewett, K. R. Ford, and G. D. Myer, "Anterior cruciate ligament injuries in female athletes: Part 2, a meta-analysis of neuromuscular interventions aimed at injury prevention," *Am J Sports Med,* vol. 34, no. 3, pp. 490-8, Mar 2006, doi: 10.1177/0363546505282619.

[33] T. E. Hewett, G. D. Myer, and K. R. Ford, "Anterior cruciate ligament injuries in female athletes: Part 1, mechanisms and risk factors," *Am J Sports Med,* vol. 34, no. 2, pp. 299-311, Feb 2006, doi: 10.1177/0363546505284183.

[34] G. D. Myer, M. V. Paterno, K. R. Ford, C. E. Quatman, and T. E. Hewett, "Rehabilitation after anterior cruciate ligament reconstruction: criteria-based progression through the return-to-sport phase," *J Orthop Sports Phys Ther,* vol. 36, no. 6, pp. 385-402, Jun 2006, doi: 10.2519/jospt.2006.2222.

[35] M. V. Paterno *et al.*, "Biomechanical measures during landing and postural stability predict second anterior cruciate ligament injury after anterior cruciate ligament reconstruction and return to sport," *Am J Sports Med,* vol. 38, no. 10, pp. 1968-78, Oct 2010, doi: 10.1177/0363546510376053.

[36] E. M. Wojtys, M. L. Beaulieu, and J. A. Ashton-Miller, "New perspectives on ACL injury: On the role of repetitive sub-maximal knee loading in causing ACL fatigue failure," (in eng), *J Orthop Res,* vol. 34, no. 12, pp. 2059-2068, 12 2016, doi: 10.1002/jor.23441.

[37] L. Y. Griffin *et al.*, "Noncontact anterior cruciate ligament injuries: risk factors and prevention strategies," *J Am Acad Orthop Surg,* vol. 8, no. 3, pp. 141-50, May-Jun 2000, doi: 10.5435/00124635-200005000-00001.

[38] O. E. Olsen, G. Myklebust, L. Engebretsen, and R. Bahr, "Injury mechanisms for anterior cruciate ligament injuries in team handball: a systematic video analysis," *Am J Sports Med,* vol. 32, no. 4, pp. 1002-12, Jun 2004, doi: 10.1177/0363546503261724.

[39] P. Renstrom *et al.*, "Non-contact ACL injuries in female athletes: an International Olympic Committee current concepts statement," *Br J Sports Med,* vol. 42, no. 6, pp. 394-412, Jun 2008, doi: 10.1136/bjsm.2008.048934.

[40] K. L. Markolf, D. M. Burchfield, M. M. Shapiro, M. F. Shepard, G. A. Finerman, and J. L. Slauterbeck, "Combined knee loading states that generate high anterior cruciate ligament forces," *J Orthop Res,* vol. 13, no. 6, pp. 930-5, Nov 1995, doi: 10.1002/jor.1100130618.

[41] B. Yu and W. E. Garrett, "Mechanisms of non-contact ACL injuries," (in eng), *Br J Sports Med,* vol. 41 Suppl 1, pp. i47-51, Aug 2007, doi: 10.1136/bjsm.2007.037192.

[42] C. S. Shin, A. M. Chaudhari, and T. P. Andriacchi, "Valgus plus internal rotation moments increase anterior cruciate ligament strain more than either alone," *Med Sci Sports Exerc,* vol. 43, no. 8, pp. 1484-91, Aug 2011, doi: 10.1249/MSS.0b013e31820f8395.

[43] B. Geng *et al.*, "Narrow Intercondylar Notch and Anterior Cruciate Ligament Injury in Female Nonathletes with Knee Osteoarthritis Aged 41-65 Years in Plateau Region," *Chin Med J (Engl),* vol. 129, no. 21, pp. 2540-2545, Nov 5 2016, doi: 10.4103/0366-6999.192771.

[44] H. C. Smith *et al.*, "Risk factors for anterior cruciate ligament injury: a review of the literature - part 1: neuromuscular and anatomic risk," *Sports Health,* vol. 4, no. 1, pp. 69-78, Jan 2012, doi: 10.1177/1941738111428281.

[45] H. C. Smith *et al.*, "Risk factors for anterior cruciate ligament injury: a review of the literature-part 2: hormonal, genetic, cognitive function, previous injury, and extrinsic risk factors," *Sports Health,* vol. 4, no. 2, pp. 155-61, Mar 2012, doi: 10.1177/1941738111428282.

[46] R. R. Khasawneh, M. Z. Allouh, and E. Abu-El-Rub, "Measurement of the quadriceps (Q) angle with respect to various body parameters in young Arab population," (in eng), *PLoS One,* vol. 14, no. 6, p. e0218387, 2019, doi: 10.1371/journal.pone.0218387.

[47] S. G. McLean, X. Huang, and A. J. van den Bogert, "Association between lower extremity posture at contact and peak knee valgus moment during sidestepping: implications for ACL injury," *Clin Biomech (Bristol, Avon),* vol. 20, no. 8, pp. 863-70, Oct 2005, doi: 10.1016/j.clinbiomech.2005.05.007.

[48] S. B. Mountcastle, M. Posner, J. F. Kragh, Jr., and D. C. Taylor, "Gender differences in anterior cruciate ligament injury vary with activity: epidemiology of anterior cruciate ligament injuries in a young, athletic population," *Am J Sports Med,* vol. 35, no. 10, pp. 1635-42, Oct 2007, doi: 10.1177/0363546507302917.

[49] K. O'Malley, A. Rubinstein, and W. Postma, "Anterior Cruciate Ligament Injury: Current Understanding of Risk Factors," *Orthopedics and Rheumatology Open Access Journal,* vol. 1, no. 3, pp. 1-8, 2015, doi: 10.19080/OROAJ.2015.01.555565.

[50] V. R. Carlson, F. T. Sheehan, and B. P. Boden, "Video Analysis of Anterior Cruciate Ligament (ACL) Injuries: A Systematic Review," *JBJS Rev,* vol. 4, no. 11, Nov 29 2016, doi: 10.2106/JBJS.RVW.15.00116.

[51] A. Thomson, R. Whiteley, and C. Bleakley, "Higher shoe-surface interaction is associated with doubling of lower extremity injury risk in football codes: a systematic review and meta-analysis," *Br J Sports Med,* vol. 49, no. 19, pp. 1245-52, Oct 2015, doi: 10.1136/bjsports-2014-094478.

[52] C. J. Anderson, C. G. Ziegler, C. A. Wijdicks, L. Engebretsen, and R. F. LaPrade, "Arthroscopically pertinent anatomy of the anterolateral and posteromedial bundles of the posterior cruciate ligament," (in eng), *J Bone Joint Surg Am,* vol. 94, no. 21, pp. 1936-45, Nov 2012, doi: 10.2106/JBJS.K.01710.

[53] M. Arif and A. Kattan, "Physical Activities Monitoring Using Wearable Acceleration Sensors Attached to the Body," (in eng), *PLoS One,* vol. 10, no. 7, p. e0130851, 2015, doi: 10.1371/journal.pone.0130851.

[54] A. G. Cutti, A. Ferrari, P. Garofalo, M. Raggi, and A. Cappello, "'Outwalk': a protocol for clinical gait analysis based on inertial and magnetic sensors," (in eng), *Med Biol Eng Comput,* vol. 48, no. 1, pp. 17-25, Jan 2010, doi: 10.1007/s11517-009-0545-x.

[55] J. Favre, X. Crevoisier, B. M. Jolles, and K. Aminian, "Evaluation of a mixed approach combining stationary and wearable systems to monitor gait over long distance," (in eng), *J Biomech,* vol. 43, no. 11, pp. 2196-202, Aug 2010, doi: 10.1016/j.jbiomech.2010.03.041.

[56] A. Ferrari *et al.*, "First in vivo assessment of "Outwalk": a novel protocol for clinical gait analysis based on inertial and magnetic sensors," (in eng), *Med Biol Eng Comput,* vol. 48, no. 1, pp. 1-15, Jan 2010, doi: 10.1007/s11517-009-0544-y.

[57] J. F. Lin and D. Kulić, "Human pose recovery using wireless inertial measurement units," (in eng), *Physiol Meas,* vol. 33, no. 12, pp. 2099-115, Dec 2012, doi: 10.1088/0967-3334/33/12/2099.

[58] P. Picerno, A. Cereatti, and A. Cappozzo, "Joint kinematics estimate using wearable inertial and magnetic sensing modules," (in eng), *Gait Posture,* vol. 28, no. 4, pp. 588-95, Nov 2008, doi: 10.1016/j.gaitpost.2008.04.003.

[59] N. G. Elvin, A. A. Elvin, and S. P. Arnoczky, "Correlation between ground reaction force and tibial acceleration in vertical jumping," (in eng), *J Appl Biomech,* vol. 23, no. 3, pp. 180-9, Aug 2007, doi: 10.1123/jab.23.3.180.

[60] R. D. Gurchiek, R. S. McGinnis, A. R. Needle, J. M. McBride, and H. van Werkhoven, "The use of a single inertial sensor to estimate 3-dimensional ground reaction force during accelerative running tasks," (in eng), *J Biomech,* vol. 61, pp. 263-268, 08 2017, doi: 10.1016/j.jbiomech.2017.07.035.

[61] U. Meyer *et al.*, "Validation of two accelerometers to determine mechanical loading of physical activities in children," (in eng), *J Sports Sci,* vol. 33, no. 16, pp. 1702-9, 2015, doi: 10.1080/02640414.2015.1004638.

[62] J. M. Konrath, A. Karatsidis, H. M. Schepers, G. Bellusci, M. de Zee, and M. S. Andersen, "Estimation of the Knee Adduction Moment and Joint Contact Force during Daily Living Activities Using Inertial Motion Capture," (in eng), *Sensors (Basel),* vol. 19, no. 7, Apr 2019, doi: 10.3390/s19071681.

[63] A. Karatsidis *et al.*, "Predicting kinetics using musculoskeletal modeling and inertial motion capture,"

Chapter 2: A Literature Review & Preliminary Work

In this chapter, we examined previous works that have utilized IMUs to correlate or estimate the GRF, knee moments, and knee angles. A brief synopsis of each study is given, along with how their results informed our current work. Together with the literature review portion, a summary of our preliminary work on using IMUs to track high forces and knee moments in cadaveric specimens is presented, along with the pitfalls and limitations we determined and how we addressed them in this new work.

2.1 Estimating GRF: Mathematical Model Development

Table 2-1 Overview of studies that have utilized IMUs to estimate GRF. The model used by each study, the fit between measured and estimate (R^2), root mean square error (RMSE), and mean absolute percent error (MAPE) are presented when possible. RMSE is presented in terms of either newtons (N) or normalized via body weight (BW).

Studies using IMUs to estimate GRF

Study	IMU	Model Type	R^2	RMSE	MAPE
Elvin et al. [1]	-	Linear Regression	(0.75, 0.90)	-	-
Meyer et al. [2]	ActiGraph GT3X+	Linear Regression	0.62	-	-
Meyer et al. [2]	GENEA	Linear Regression	0.65	-	-
Gurchiek et al. [3]	YOST Data Logger 3-Space Sensor (SS)	Linear Regression	0.24	466.3 N	-
Gurchiek et al. [3]	YOST Data Logger 3-Space Sensor (COD)	Linear Regression	0.24	600.4 N	-
Thiel et al. [4]	SABELSense	Multivariable Linear Regression	0.50	-	(3.29%, 33.32%)
Neugebauer et al. [5]	BioTrainer AM	Linear Regression	0.88		9.0 ± 4.2%
Neugebauer et al. [5]	BioTrainer AM	MEM	0.97		5.2 ± 1.6 %
Alcantara et al. [6]	IMeasureU	Multivariable Linear Regression	-	0.14 BW	4.0 ± 2.6%
Alcantara et al. [10]	IMeasureU	Machine Learning		0.16 ± 0.04 BW	

Various studies have constructed mathematical models through either linear regression modeling, implementation of mix effect modeling (MEM), or complex machine learning algorithms to predict GRF using only data that could be obtained from an IMU and have done so

with a wide range of correlations, though in most cases, a strong correlation was observed [1-6]. Studies such as those by Elvin et al. and Meyer et al. found strong correlations between IMU data and GRF when using linear regression modeling, but failed to report some measure of model accuracy, such as RMSE or MAPE [1, 2]. Without this key piece of information, it is unknown how close estimated forces were to measured. The use of individually developed models is also troublesome as it presents the potential to skew correlations toward stronger fits; important subject-specific parameters may have been ignored. Thus, for our study, to develop robust and universally applicable models, data across multiple specimens/subjects was used to account for potential specimen/subject variations.

Gurchiek et al. and Thiel et al. also used some type of regression modeling, but reported some measurement of accuracy for their models, albeit correlations between their estimated and measured values ranged from low to moderate [3, 4]. Gurchiek et al. using linear regression modeling, reported low correlations and RMSE values of up to 600 N, indicating a poor degree of accuracy [3]. However, what makes the Gurchiek et al. study interesting is their implementation of change-of-direction (COD) actions. In theory, COD actions would produce more artifact as the directional changes would cause more soft tissue motion. Theil et al. reported moderate correlations and MAPE values up to 33%, illustrating poor estimated force accuracy [4]. However, unlike the previously discussed studies which used simple, single-variable linear regression, Thiel et al. used a multivariable linear regression model which assumed vertical GRF was a function of the IMU's linear acceleration components, with least square coefficients of the model being adjusted through the number of previously recorded strides (i.e., the coefficients

where adjusted based on the number of steps the subject had taken) [4]. However, this study also had an extremely small sample size (N=3) [4].

Neugebauer et al. developed a model to estimate peak vertical GRF (pVGRF) in youth gait [5]. The IMU sensor was placed over the iliac crest of their hip, participants were asked to perform several walking actions at differing speeds across a force plate-embedded floor [5]. GRF was modeled using a generalized regression model (GRM) as well as a MEM. MEMs can be thought of as a more complex version of a regression model in which interactions between terms are noted as well as possible grouping term effects (random effects). In both cases, they reported strong correlations between predicted and measured pVGRF (R^2=0.97 MEM; R^2=0.88 GRM) [5]. They also reported that when using the MEM, the MAPE between measured and predicted pVGRF was 5.2 ± 1.6% while that for a GRM was 9.0 ± 4.2% [5]. This may indicate that other variables, not directly related to GRF measurement, should be considered to account for possible subject variation (such as sex of subject, leg circumference, etc.). Furthermore, there was a significant dependence on mass as a fixed effect (predictor variable) and subject as a random effect (grouping variable) ($p < 0.05$) [5]. However, this study only used accelerometers, and thus could not consider the possible contribution(s) of angular motion(s) [5]. Neugebauer et al. factored in the speed of action as a fixed effect within their MEM and found it to be statistically significant ($p<0.01$) [5]. This study by Neugebauer et al. indicates that a more complex modeling technique such as MEM may be useful.

In 2021, a study conducted by Alcantara et al. quantified the accuracy of a linear regression model to estimate GRF via sacral-mounted accelerometers across multiple running speeds [6]. In

this study, they used a training set (N=28) to develop the model and a testing set (N=9) to test the model's validity [6]. This is crucial, as the results presented by Alcantara et al. are not subject to potential bias. They constructed the model using linear acceleration obtained via the IMU, subject's body mass, step frequency, and running speed as predictor variables [6]. Alcantara et al. reported their model produced predicted values with an RMSE of 0.139 BW and a MAPE of 4.04 ± 2.57% [6]. However, several limitations should be mentioned concerning this study, chief among them were the trends reported by Alcantara et al.; It was noted that the model tended to overestimate lower pVGRF while underestimating higher ones [6]. This may problematic if implementing this model on-field. However, their use of an independent testing set to test model validity was noteworthy and was therefore implemented throughout our study.

2.1.1 Use of Neural Networks to Estimate GRF

Recently, various studies have created neural networks, or machine learning algorithms, to estimate GRF via IMU data [7-11]. Neural Networks have numerous advantages over traditional regression modeling such as increased flexibility (due to integration of approximation functions in the algorithm) as well as being able to deal with nonlinear data with multiple inputs and layers [12]. However, disadvantages with neural networks do exist, such as an inability to quantify the influence of independent variables on dependent ones (the "black box" phenomenon), computational expense, and the dependence on the training data [12]. This latter disadvantage is particularly important as dependency on training data may lead to problems of over-fitting and generalization in which the neural network is highly tuned to the training data [12]. However, implementing an independent validation set may alleviate this issue of the training set dependence [6]. And while the "black box" phenomenon prevents us from quantifying the

influence of a variable, F-tests may allow us to circumvent this issue by illustrating the influence of a variable in estimates compared to all other variables.

In 2021, Alcantara et al. again evaluated the performance of a model's ability to estimate GRF but used feedforward neural networks, non-level ground running (up/downhill) conditions, and sacral and shoe-mounted IMUs [7]. Here, they reported an RMSE of 0.16 ± 0.04 xBW [7]. They also noted a proportional relationship between running speed and RMSE, with low-speed actions resulting in lower RMSE values [7]. This should be expected, as speed increases, the effects of soft tissue artifact causing noise contamination may be magnified. However, Alcantara et al. also noted the neural network's inability to account for changes in impact peaks across inclines as a possible contributing factor to the poorer performance of their machine learning algorithm compared to their previously developed regression model; impact peak was a significant feature in their algorithms [6, 7]. The authors also mentioned that the inclusion of acceleration of the lower leg in the neural network may improve the accuracy of the predictions, as impact peak in GRF waveforms may be affected by subject-specific lower extremity kinematics, an observation supported by the studies conducted by Gottschall and Kram, and Vernillo et al. [7, 13, 14]. Several limitations were noted such as the method of attaching the IMUs to the subjects, noting that using tape may introduce movement artifact in the measured signal. Johnson et al. observed affixing IMUs to the lower leg using commercial straps produced a peak acceleration of 1.2 g greater than when utilizing a combination of athletic tape/elastic wrap [7, 15]. This meant we needed to consider the method by which our sensors were secured on a subject; both subject comfort as well as mitigation of sensor movement needed to be ensured. A study conducted by Baggaley et al. in 2019 reported that the lower leg experiences larger accelerations than the

sacrum (where a sensor was placed by Alcantara et al.), which may mean an increased sensitivity to motion artifact [16]. Other factors to consider include the placement of the IMU. Tan et al. found that placement/orientation error could reduce accuracy by as much as 20.8%. Therefore, a method to quantify sensor placement differences across subjects could be important.

2.2 Estimating Moments

Table 2-2 | Overview of studies that have utilized IMUs to estimate knee abduction/adduction moments (KAM) or knee rotation moments (KRM). The model used by each study, the fit between measured and estimated (R^2), and RMSE normalized via BW and height (H) is presented.

Studies using IMUs to estimate KAM & KRM

Study	IMU	Model Type	R^2	RMSE
KAM				
Favre et al. [27]	Physiolog	Linear Regression	0.18	
Konrath et al. [28]	Xsens Awinda (Stair Ascent)	Linear Regression	0.73	1.0% BW*H
Konrath et al. [28]	Xsens Awinda (Stair Descent)	Linear Regression	0.55	1.4% BW*H
Konrath et al. [28]	Xsens Awinda (Sit-to-Stand)	Linear Regression	0.96	0.6% BW*H
Lee et al. [30]	Trigno Avanti	Feedforward neural network	0.46	17.2 ± 9.85 % BW*H
KRM				
Favre et al. [27]	Physiolog	Linear Regression	< 0.01	
Karatsidis et al. [29]	Xsens MVN Link	Linear Regression	0.67	0.2% ± 0.1% BW*H
Lee et al. [30]	Trigno Avanti	Feedforward neural network	0.20	21.5 ± 11.5 % BW*H

Numerous studies have examined the relationship between knee moments and the strain experienced by the ACL and found that increases in KAM and/or KRM correlate with

proportional increases in strain [17-20]. Because of this correlation, there has been an emergence of studies that have used IMU data in the development of models for KAM and KRM estimates, with varying degrees of success [21-24]. Konrath et al. estimated KAM using regression modeling and IMU data obtained from commonly performed rehabilitation activities [22]. Three participants were fitted with two IMUs placed on the thigh and shank and asked to perform a stair ascent/descent (SA/SD) as well as a sit-to-stand (StS) action. They reported a strong to very strong correlation between their estimated and measured values and low normalized root mean square errors (NRMSE) (normalized in terms of the subject's body weight and height) (NRMSE: SA: 0.01; SD: 0.014; StS: 0.006) [22]. It's important to note that this study examined only slower actions and not more dynamic movements such as those observed during participation in a sport [22] These less dynamic actions would presumably result in less soft tissue artifact and in turn lead to better results. Because the purpose of our study was to track potential injurious cycles on-field, where highly dynamic actions are enacted, we needed to ensure that all testing actions were highly dynamic.

Karatsidis et al. estimated KRM during walking using a full body inertial motion capture (IMC) method [23]. Strong correlations between their estimated and measured values were reported ($R = 0.82$) and an NRMSE value of 0.002 ± 0.001 BW*H [23]. While this was highly accurate, the use of an IMC system on-field may not be practical in a real-world application because it would likely hinder the performance of athletes. Within our study, optimization of the number of IMUs was considered such that the minimum number of IMUs was used whilst maintaining an estimate's accuracy and reliability. A study by Lee et al. used machine learning to develop algorithms to estimate joint torques of the lower limbs during normal walking using only

feedforward neural networks. It was not clear whether other algorithms were considered [24]. Negligible fits between estimated and measured KAM and KRM were reported., with NRMSE values of more than 20%, illustrating poor levels of accuracy [24]. Whether this poor accuracy was due to the modeling method or due to the sensors they selected is unknown; within our study, various modeling types were examined per parameter (GRF, KAM, or KRM) as we theorized that different parameters may require different models. While both Lee et al. and Alcantara et al. found feedforward models were able to estimate GRF accurately, Lee et al. found them to be insufficient for KAM or KRM estimates [7, 24].

2.3 Our Previous Laboratory Work Using IMUs To Estimate Force & Moments

In 2020, we published work correlating data obtained by an IMU to measured forces and moments during cadaveric testing to determine whether the selected IMUs hold the potential for field testing and tracking potential fatigue levels of the ACL [25]. Ten cadaveric knee specimens were instrumented with two wearable IMUs (APDM Opal, APDM Wearable Technologies, Portland, OR) and placed into a custom-built testing apparatus designed to simulate a one-legged landing of approximately 3-4x BW; this apparatus, which includes simulated trans-knee muscle forces, has been validated and used in other studies (Figure 2-1) [26, 27].

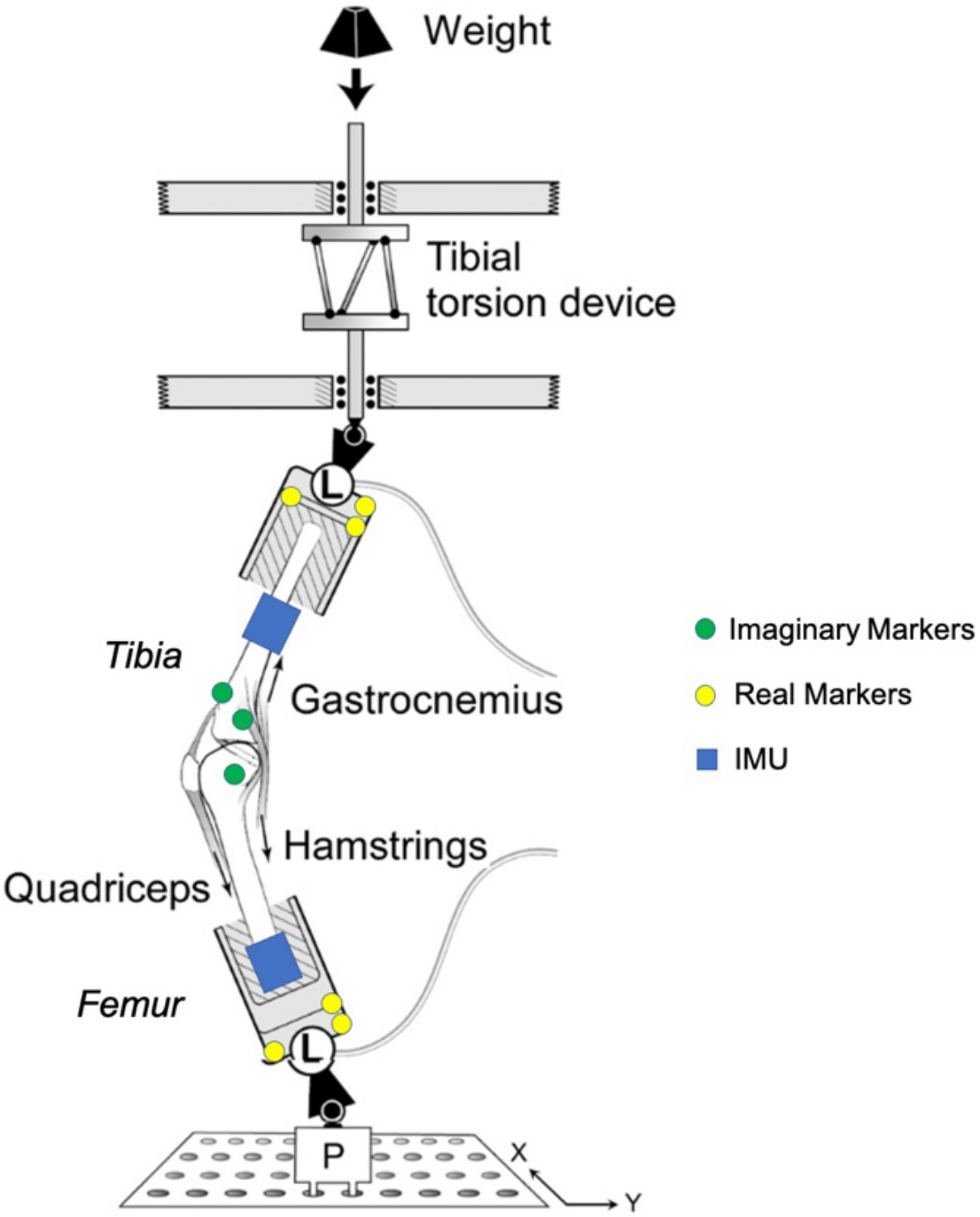

Figure 2-1 | Schematic of the testing rig. IMU placement and digital marker location labeled. Reproduced with permission.

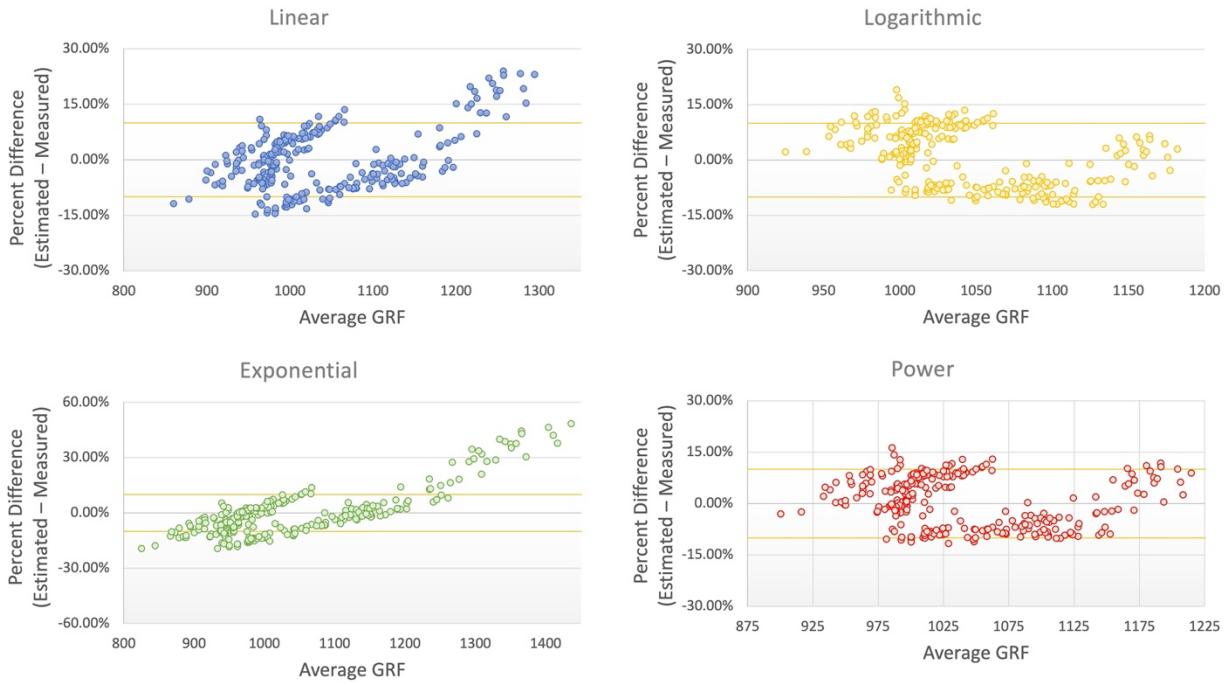

Figure 2-2 | BA plots relating the average GRF to the percent difference between estimated and measured GRF for the linear (blue), logarithmic (yellow), exponential (green), and power (red) models. Average GRF is the average between measured GRF and estimated.

While GRF could not be directly obtained during cadaveric testing, peak tibial force was used as a proxy; in theory, peak tibial force would be most like GRF [25]. Four unique regression models were applied to the data to obtain correlations: linear, exponential, logarithmic, and power (Table 2-3). Given the relationship between linear acceleration and force (i.e., one that is linearly dependent), we understood that a linear regression model may be the most appropriate. However, it was theorized that other models could account for various other variables indirectly such as height, specimen rigidity, age, etc. [25]. Surprisingly, the power model was the only one to exhibit a very strong fit (R^2=0.96), though strong fits were observed in the other three model types (Table 2-3) [25]. Similarly, the RMSE and MAPE were lowest within the power model. This corroborates our initial theory that the relationship between force and IMU data is not so simple as to be modeled via a single variable linear regression model, but instead, is more

complex and may require additional variables and higher order regressions. In the Bland-Altman (BA) plots, both the linear and exponential models exhibited upward trends; as the magnitude of the measured GRF increased, the percent difference increased as the IMU's overestimations increased (Figure 2-2) [25]. This trend is particularly important for injury tracking as it may lead to greater instances of false positives. No discernable trends were observed in either the power or logarithmic models (Figure 2-2) [25].

Table 2-3 | Results of our preliminary work in using an IMU to estimate GRF, KAM, and KRM. The model types used, the fit between measured and estimated (R^2), RMSE, and MAPE are presented.

Results of our preliminary work

Model Type	R^2	RMSE	MAPE
GRF			
Linear	0.88	86.9 N	6.49% ± 4.81%
Exponential	0.87	140 N	9.04% ± 9.13%
Power	0.96	76.4 N	6.46% ± 3.30%
Logarithmic	0.89	83.5 N	7.25% ± 3.49%
KAM			
Linear	0.44	3.60 Nm	36.7% ± 28.8%
Multivariable Linear	0.65	2.93 Nm	35.5% ± 32.7%
KRM			
Linear	0.78	13.5 Nm	16.4% ± 14.0%
Multivariable Linear	0.45	5.10 Nm	7.05% ± 4.40%

Comparing IMU data to measured KAM a moderate fit level was reported when using multivariable first-order regression modeling (R^2=0.65) (Table 2-3) [25]. While fitting a similar model to KRM resulted in a low fit level (R^2=0.45), the implementation of a single variable linear regression in which only angular velocity about the vertical axis was considered, saw a strong fit level (Table 2-3) (R^2=0.78). However, while fit levels are important in determining possible relationships, in both KAM and KRM, the use of the multivariable first-order regression model resulted in smaller RMSE and MAPE values, indicating a greater degree of accuracy (Table 2-3) [25]. Bland-Altman (BA) plots showed that the multivariable first-order regression model resulted in more trials falling within the preestablished ±10% Bland Altman Limits of Agreement (LoAs) for both KAM and KRM estimates, thus, illustrating a better degree of reliability (Figure 2-3). However, in both cases, clear trends were observed in KAM and KRM estimates – as the moment decreased in magnitude, variation between measured and estimated values increased (Figure 2-3).

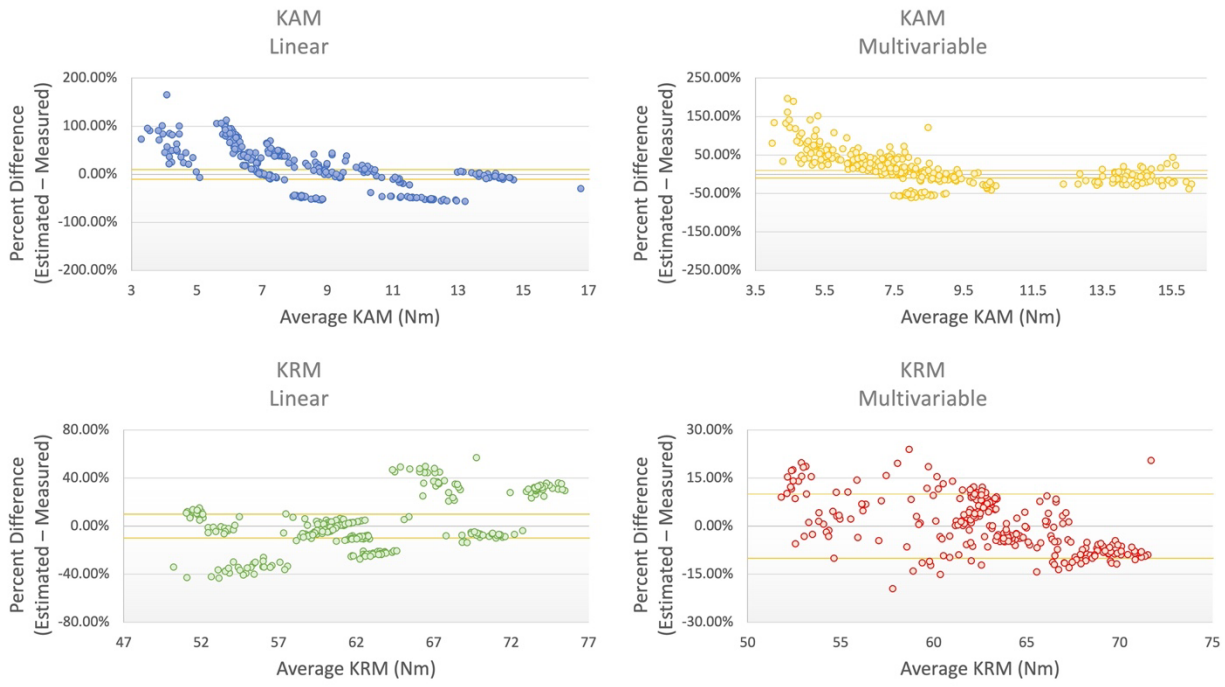

Figure 2-3 | BA plots relating the average KAM or average KRM to the percent difference between estimated and measured KAM or KRM. Average KAM/ KRM is the average between measured KAM/KRM and estimated.

2.3.1 Previous pitfalls To Be Avoided

We acknowledge several limitations in our preliminary work, which may have influenced our results or their application to future endeavors. Among these limitations is our exclusive use of in-vitro models, which omit soft tissue motion that could affect the coupling of the sensor to a body segment *in vivo*. We also did not have two independent data sets to develop the equations first and then test the accuracy and reliability of our models when applied to new data; this may mean the preliminary models skew toward higher accuracy and reliability. Limitations of the rig prevented observing actions that were not jump-landings; this may mean these models do not apply to events beyond this particular action. Furthermore, our preliminary work exclusively observed high-loading cycles. While our goal is to identify high-loading conditions by using IMU data, we must also be able to distinguish between low-loading (low injury risk) and those that carry some potential for ACL damage; we can accomplish this by observing multiple

loading condition intensities and develop the models accordingly. All models developed within our preliminary work are simple, and while we were able to obtain high accuracy and reliability, their simplicity may mean they are insufficient for on-field event tracking. The quadriceps tendon freezing cycle also potentially hindered our results; with no set number of trials between freezings, we used our best judgment to determine whether the tendon thawed, thus opening our testing to inconsistencies between "groups" (tests between subsequent freezings), as the thaw level of the tendon may have varied. The lower sampling rate of the sensor may have led to missed information and potential aliasing.

2.4 Estimating Angles from IMUs

Table 2-4 | Overview of studies that have compared IMU obtained angles to those of a MCS. The method through which IMU angles were obtained, the fit between IMU and MCS angles (R^2) and the RMSE is presented when possible. Note: the results of Zügner et al. were presented in terms of interclass correlation (ICC).

Studies comparing IMU-obtained angles to an MCS

Study	IMU	Method	R^2	RMSE
Tong et al. [112]	ENC-05EA	Integration & Inclination Subtraction	0.86	6.42°
Watanabe et al. [111]	WAA-006 Wireless Technologies	Integration		(3.00°, 4.00°)
Bakhshi et al. [113]	SparkFun Electronics	Integration		
Bell et al. [115]	3-Space Bluetooth Sensor Yost Labs	Sensor Fusion Algorithm		(2.00°, 2.90°)
Zügner et al. [114]	GaitSmart	Sensor Fusion Algorithm		
Ajdaroski et al. [116]	APDM Opal (Flexion)	Sensor Fusion Algorithm	0.34	8.11°
Ajdaroski et al. [116]	APDM Opal (Abduction)	Sensor Fusion Algorithm	0.08	4.61°
Ajdaroski et al. [116]	APDM Opal (Rotation)	Sensor Fusion Algorithm	0.24	4.60°

Various studies have calculated joint angles, particularly those of the knee, through IMU-derived data [28-35]. However, the focus of many of these studies has been on examining differences in flexion angles; possibly due to the knee flexion angle exhibiting the largest change during an action, and subsequently easiest to measure reliably. But while that may be the case, it precludes the potential effects that knee abduction and rotational angles may play in knee injuries, specifically, in ACL injuries. Many studies have proposed there is a correlation between ACL

strain and the abduction/adduction and rotational orientation of the joint [18-20, 36-40]. Because of this possible correlation, to improve knee injury tracking, it is important to estimate all three tibiofemoral angles. Furthermore, the method by which joint angles are determined through IMUs also varies widely from study to study, with some integration of angular rates while others used Euler angles.

Studies such as those by Watanabe et al., Tong et al., and Bakhshi et al. have calculated knee joint angles by integrating angular rates, though without the conversion to Euler angles and limiting themselves to only determining flexion angles [30-32]. This process may be problematic as angles obtained do not describe the orientation of the joint with respect to a fixed coordinate system, but rather to some arbitrary coordinate system. As such, each study's estimated angles may not represent the knee's true orientation, and comparisons between estimated and MSC-measured values may not be accurate. However, these studies have shown their methods to be accurate in knee flexion estimates as the least accurate of these studies (Tong et al.) demonstrated a low RMSE value (RMSE of 6.4°) [31]. These studies observed actions associated with rehabilitation and would not necessarily translate to more dynamic actions. Various studies have noted the potential effects soft tissue artifact may have on the validity of results [41-43].

Bell et al. and Zügner et al. compared angles estimated via a sensor's proprietary sensor fusion algorithm (Euler angles) and those of an MCS [33, 34]. In the study by Bell et al., the range of RMSE values between estimated and measured knee flexion angles were low (RMSE between 2° and 2.9°) [34]. While this shows high accuracy for flexion angle estimates, neither the accuracy for abduction/adduction nor rotational estimates were reported. For Zügner et al., while RMSE

values were not examined, ICC was determined as well as the statical significance in the difference between estimated and measured angles [33]. Zügner et al. reported that they found no significance in the mean difference between estimated and measured knee flexion angles ($p=0.7$) and determined, a high ICC was observed ($ICC>0.8$) [33]. Because they did not report RMSE, it is not possible to determine the accuracy of these angle estimates. Mean difference comparisons and ICC compare data sets as groups, and as such, mitigate the effects of gross differences; if the algorithm over- and underestimates angles similarly, the mean difference would be relatively small, and could be misleading as to the performance of an algorithm. Approaches such as RMSE or MAPE remove this pitfall and may be much better indicators of accuracy.

In a previous study performed using APDM Opal^{TM} IMUs, highly dynamic activities (jumps) were observed in all three knee angles [44]. A moderate relationship between the IMU and MCS was reported when examining flexion/extension at pVGRF ($R=0.58$), while those of abduction/adduction and internal/external rotation were low to negligible. It was concluded that for both abduction/adduction and rotation, the APDM Opal^{TM} algorithm was able to perform well under certain conditions, particularly those of smaller angle displacements, and experienced greater variability as the magnitude of the measured angle increased [44]. This trend in abduction/adduction and internal/external rotation may mean that the sensor fusion algorithm of APDM Opal^{TM} may be tuned toward smaller angle measurements; this is understandable given the use of IMUs in rehabilitation where small angles are common. Thus, this allowed us to pose the hypothesis that commercially available IMUs employ sensor fusion algorithms that may not necessarily be accurate when used in more dynamic activities such as sports, where larger changes in joint angles, angular velocities, and linear accelerations occur and that a new

algorithm, tuned for these activities, is needed. However, we should note that increases in abduction movements/orientation may the result of injury and not the cause of it.

2.5 Literature Review Summary

As stated at the beginning of the chapter, a review of other studies that have utilized IMUs for the tracking of knee kinematic/kinetics becomes central, as each study gives important insight into potential modeling techniques, methods of data collection, and significant parameters that could be considered in model development. Particularly, each study helped in narrowing down the potential parameters to be considered, as we could only use those that could be quantified during on-field usage from data obtained solely from the IMU. This meant that parameters such as step count could not be considered. Also, from the studies, we saw that across most cases, multi-variable models (models of increased complexity) provided better overall correlations and lower RMSE values, however, there is a delicate balance; as model complexity increases there is also an increase in the likelihood of training data dependence, something we considered carefully throughout our study. For GRF, multiple studies reported moderate to strong correlations with IMUs. Our previous work also showed there to be a strong correlation, and smaller RMSE and MAPE values demonstrated the possibility that a commercially available IMU can estimate force from inertial data. KAM and KRM estimates proved slightly more difficult, as most studies found there to be only moderate or poor correlations. While we found implementing a linear regression model to KRM allowed for a strong correlation between estimated and measured, an additional examination into possible ways to estimate KAM/KRM accurately and reliably is needed. It may be that the modeling techniques employed by various studies were insufficient, and terms of importance were not considered. Previous studies tended to focus on flexion and

ignored abduction/adduction and rotation. Because of our focus on injury prevention, our emphasis is on ab/adduction and rotational angle measurements.

In the following chapters, we will present the results of this current study, beginning with Stage 1: the development of *in vitro* models. This will begin with examining work where the goal was to tune a quaternion conversion (QC) method for calculating the three orthogonal knee angles during the high velocities associated with a jump landing using commercially available IMUs. We then developed models using IMU data to estimate key parameters that could identify possibly injurious loading cycles to the ACL. Following this, we examined our results in Stage 1 and applied this to human subjects' data to develop potential modifications that may reduce the effects of soft tissue artifact and account for a variety of dynamic movements that could not be replicated *in vitro*. Following this, the final comment on the practical use of our findings, possible pitfalls, future directions, and considerations is presented.

2.6 References

[1] N. G. Elvin, A. A. Elvin, and S. P. Arnoczky, "Correlation between ground reaction force and tibial acceleration in vertical jumping," (in eng), *J Appl Biomech,* vol. 23, no. 3, pp. 180-9, Aug 2007, doi: 10.1123/jab.23.3.180.

[2] U. Meyer *et al.*, "Validation of two accelerometers to determine mechanical loading of physical activities in children," (in eng), *J Sports Sci,* vol. 33, no. 16, pp. 1702-9, 2015, doi: 10.1080/02640414.2015.1004638.

[3] R. D. Gurchiek, R. S. McGinnis, A. R. Needle, J. M. McBride, and H. van Werkhoven, "The use of a single inertial sensor to estimate 3-dimensional ground reaction force during accelerative running tasks," (in eng), *J Biomech,* vol. 61, pp. 263-268, 08 2017, doi: 10.1016/j.jbiomech.2017.07.035.

[4] D. V. Thiel *et al.*, "Predicting Ground Reaction Forces in Sprint Running Using a Shank Mounted Inertial Measurement Unit," *Proceedings,* vol. 2, no. 6, p. 199, 2018.

[5] J. M. Neugebauer, D. A. Hawkins, and L. Beckett, "Estimating youth locomotion ground reaction forces using an accelerometer-based activity monitor," (in eng), *PLoS One,* vol. 7, no. 10, p. e48182, 2012, doi: 10.1371/journal.pone.0048182.

[6] R. S. Alcantara, E. M. Day, M. E. Hahn, and A. M. Grabowski, "Sacral acceleration can predict whole-body kinetics and stride kinematics across running speeds," (in eng), *PeerJ,* vol. 9, p. e11199, 2021, doi: 10.7717/peerj.11199.

[7] R. S. Alcantara, W. B. Edwards, G. Millet, and M. Grabowski, "Predicting continuous ground reaction forces from accelerometers during uphill and downhill running: A recurrent neural network solution," *bioRxiv,* 2021.

[8] F. J. Wouda *et al.*, "Estimation of Vertical Ground Reaction Forces and Sagittal Knee Kinematics During Running Using Three Inertial Sensors," (in eng), *Front Physiol,* vol. 9, p. 218, 2018, doi: 10.3389/fphys.2018.00218.

[9] E. Dorschky, M. Nitschke, C. F. Martindale, A. J. van den Bogert, A. D. Koelewijn, and B. M. Eskofier, "CNN-Based Estimation of Sagittal Plane Walking and Running Biomechanics From Measured and Simulated Inertial Sensor Data," (in eng), *Front Bioeng Biotechnol,* vol. 8, p. 604, 2020, doi: 10.3389/fbioe.2020.00604.

[10] M. Pogson, J. Verheul, M. A. Robinson, J. Vanrenterghem, and P. Lisboa, "A neural network method to predict task- and step-specific ground reaction force magnitudes from trunk accelerations during running activities," (in eng), *Med Eng Phys,* vol. 78, pp. 82-89, 04 2020, doi: 10.1016/j.medengphy.2020.02.002.

[11] W. R. Johnson, A. Mian, M. A. Robinson, J. Verheul, D. G. Lloyd, and J. A. Alderson, "Multidimensional Ground Reaction Forces and Moments From Wearable Sensor Accelerations via Deep Learning," (in eng), *IEEE Trans Biomed Eng,* vol. 68, no. 1, pp. 289-297, Jan 2021, doi: 10.1109/TBME.2020.3006158.

[12] G. Ciaburro and B. Venkateswaran, *Neural Networks with R*. Packt, p. 270.

[13] J. S. Gottschall and R. Kram, "Ground reaction forces during downhill and uphill running," (in eng), *J Biomech,* vol. 38, no. 3, pp. 445-52, Mar 2005, doi: 10.1016/j.jbiomech.2004.04.023.

[14] G. Vernillo *et al.*, "Biomechanics of graded running: Part I - Stride parameters, external forces, muscle activations," (in eng), *Scand J Med Sci Sports,* vol. 30, no. 9, pp. 1632-1641, Sep 2020, doi: 10.1111/sms.13708.

[15] C. D. Johnson, J. Outerleys, A. S. Tenforde, and I. S. Davis, "A comparison of attachment methods of skin mounted inertial measurement units on tibial accelerations," (in eng), *J Biomech,* vol. 113, p. 110118, 12 2020, doi: 10.1016/j.jbiomech.2020.110118.

[16] M. Baggaley *et al.*, "Step length and grade effects on energy absorption and impact attenuation in running," (in eng), *Eur J Sport Sci,* vol. 20, no. 6, pp. 756-766, Jul 2020, doi: 10.1080/17461391.2019.1664639.

[17] J. M. Hollis, S. Takai, D. J. Adams, S. Horibe, and S. L. Woo, "The effects of knee motion and external loading on the length of the anterior cruciate ligament (ACL): a kinematic study," (in eng), *J Biomech Eng,* vol. 113, no. 2, pp. 208-14, May 1991, doi: 10.1115/1.2891236.

[18] K. L. Markolf, D. M. Burchfield, M. M. Shapiro, M. F. Shepard, G. A. Finerman, and J. L. Slauterbeck, "Combined knee loading states that generate high anterior cruciate ligament forces," (in eng), *J Orthop Res,* vol. 13, no. 6, pp. 930-5, Nov 1995, doi: 10.1002/jor.1100130618.

[19] B. Yu and W. E. Garrett, "Mechanisms of non-contact ACL injuries," (in eng), *Br J Sports Med,* vol. 41 Suppl 1, pp. i47-51, Aug 2007, doi: 10.1136/bjsm.2007.037192.

[20] C. S. Shin, A. M. Chaudhari, and T. P. Andriacchi, "Valgus plus internal rotation moments increase anterior cruciate ligament strain more than either alone," (in eng), *Med Sci Sports Exerc,* vol. 43, no. 8, pp. 1484-91, Aug 2011, doi: 10.1249/MSS.0b013e31820f8395.

[21] J. Favre, A. V. Dowling, and T. P. Andriacchi, "The Relationship between Segment Angular Velocity and Knee Abduction Moment during a Drop Jump:Implications for ACL Injury Risk Prediction," in *11th Annual Orthopaedic Research Society*, 2010.

[22] J. M. Konrath, A. Karatsidis, H. M. Schepers, G. Bellusci, M. de Zee, and M. S. Andersen, "Estimation of the Knee Adduction Moment and Joint Contact Force during Daily Living Activities Using Inertial Motion Capture," (in eng), *Sensors (Basel),* vol. 19, no. 7, Apr 2019, doi: 10.3390/s19071681.

[23] A. Karatsidis *et al.*, "Predicting kinetics using musculoskeletal modeling and inertial motion capture,"

[24] M. Lee and S. Park, "Estimation of Three-Dimensional Lower Limb Kinetics Data during Walking Using Machine Learning from a Single IMU Attached to the Sacrum," (in eng), *Sensors (Basel),* vol. 20, no. 21, Nov 04 2020, doi: 10.3390/s20216277.

[25] M. Ajdaroski, "Validation of an Internal Measurement Unit to Measure Knee Kinematics and ACL Fatigue in Cadaveric Specimens During Simulated One-Legged Landing," Master of Science in Engineering, Bioengineering, University of Michigan-Dearborn, 2020.

[26] D. B. Lipps, E. M. Wojtys, and J. A. Ashton-Miller, "Anterior cruciate ligament fatigue failures in knees subjected to repeated simulated pivot landings," (in eng), *Am J Sports Med,* vol. 41, no. 5, pp. 1058-66, May 2013, doi: 10.1177/0363546513477836.

[27] D. B. Lipps, Y. K. Oh, J. A. Ashton-Miller, and E. M. Wojtys, "Effect of increased quadriceps tensile stiffness on peak anterior cruciate ligament strain during a simulated pivot landing," (in eng), *J Orthop Res,* vol. 32, no. 3, pp. 423-30, Mar 2014, doi: 10.1002/jor.22531.

[28] R. Takeda, S. Tadano, A. Natorigawa, M. Todoh, and S. Yoshinari, "Gait posture estimation using wearable acceleration and gyro sensors," (in eng), *J Biomech,* vol. 42, no. 15, pp. 2486-94, Nov 2009, doi: 10.1016/j.jbiomech.2009.07.016.

[29] J. M. Barrett, D. Viggiani, J. Park, and J. P. Callaghan, "Expressing angles relative to reference postures: A mathematical comparison of four approaches," (in eng), *J Biomech,* vol. 104, p. 109733, May 2020, doi: 10.1016/j.jbiomech.2020.109733.

[30] T. Watanabe and H. Saito, "Tests of wireless wearable sensor system in joint angle measurement of lower limbs," (in eng), *Annu Int Conf IEEE Eng Med Biol Soc,* vol. 2011, pp. 5469-72, 2011, doi: 10.1109/IEMBS.2011.6091395.

[31] K. Tong and M. H. Granat, "A practical gait analysis system using gyroscopes," (in eng), *Med Eng Phys,* vol. 21, no. 2, pp. 87-94, Mar 1999, doi: 10.1016/s1350-4533(99)00030-2.

[32] S. Bakhshi, M. H. Mahoor, and B. S. Davidson, "Development of a body joint angle measurement system using IMU sensors," (in eng), *Annu Int Conf IEEE Eng Med Biol Soc,* vol. 2011, pp. 6923-6, 2011, doi: 10.1109/IEMBS.2011.6091743.

[33] R. Zügner, R. Tranberg, J. Timperley, D. Hodgins, M. Mohaddes, and J. Kärrholm, "Validation of inertial measurement units with optical tracking system in patients operated with Total hip arthroplasty," (in eng), *BMC Musculoskelet Disord,* vol. 20, no. 1, p. 52, Feb 2019, doi: 10.1186/s12891-019-2416-4.

[34] K. M. Bell *et al.*, "Verification of a Portable Motion Tracking System for Remote Management of Physical Rehabilitation of the Knee," (in eng), *Sensors (Basel),* vol. 19, no. 5, Feb 2019, doi: 10.3390/s19051021.

[35] B. Fan, H. Xia, J. Xu, Q. Li, and P. B. Shull, "IMU-based knee flexion, abduction and internal rotation estimation during drop landing and cutting tasks," (in eng), *J Biomech,* vol. 124, p. 110549, Jul 19 2021, doi: 10.1016/j.jbiomech.2021.110549.

[36] T. E. Hewett, G. D. Myer, and K. R. Ford, "Anterior cruciate ligament injuries in female athletes: Part 1, mechanisms and risk factors," (in eng), *Am J Sports Med,* vol. 34, no. 2, pp. 299-311, Feb 2006, doi: 10.1177/0363546505284183.

[37] T. E. Hewett, K. R. Ford, and G. D. Myer, "Anterior cruciate ligament injuries in female athletes: Part 2, a meta-analysis of neuromuscular interventions aimed at injury prevention," (in eng), *Am J Sports Med,* vol. 34, no. 3, pp. 490-8, Mar 2006, doi: 10.1177/0363546505282619.

[38] S. G. McLean, S. W. Lipfert, and A. J. van den Bogert, "Effect of gender and defensive opponent on the biomechanics of sidestep cutting," (in eng), *Med Sci Sports Exerc,* vol. 36, no. 6, pp. 1008-16, Jun 2004, doi: 10.1249/01.mss.0000128180.51443.83.

[39] S. M. Sigward and C. M. Powers, "Loading characteristics of females exhibiting excessive valgus moments during cutting," (in eng), *Clin Biomech (Bristol, Avon),* vol. 22, no. 7, pp. 827-33, Aug 2007, doi: 10.1016/j.clinbiomech.2007.04.003.

[40] M. L. Beaulieu, J. A. Ashton-Miller, and E. M. Wojtys, "Loading mechanisms of the anterior cruciate ligament," (in eng), *Sports Biomech,* vol. 22, no. 1, pp. 1-29, Jan 2023, doi: 10.1080/14763141.2021.1916578.

[41] A. Peters, B. Galna, M. Sangeux, M. Morris, and R. Baker, "Quantification of soft tissue artifact in lower limb human motion analysis: a systematic review," (in eng), *Gait Posture,* vol. 31, no. 1, pp. 1-8, Jan 2010, doi: 10.1016/j.gaitpost.2009.09.004.

[42] T. Y. Tsai, T. W. Lu, M. Y. Kuo, and C. C. Lin, "Effects of soft tissue artifacts on the calculated kinematics and kinetics of the knee during stair-ascent," (in eng), *J Biomech,* vol. 44, no. 6, pp. 1182-8, Apr 2011, doi: 10.1016/j.jbiomech.2011.01.009.

[43] L. B. Wood and H. Asada, "Low variance adaptive filter for cancelling motion artifact in wearable photoplethysmogram sensor signals," (in eng), *Annu Int Conf IEEE Eng Med Biol Soc,* vol. 2007, pp. 652-5, 2007, doi: 10.1109/IEMBS.2007.4352374.

[44] M. Ajdaroski, J. A. Ashton-Miller, S. Y. Baek, P. M. Shahshahani, and A. Esquivel, "Testing a Quaternion Conversion Method to Determine Human 3D Tibiofemoral Angles During an in Vitro Simulated Jump Landing," (in eng), *J Biomech Eng,* Sep 22 2021, doi: 10.1115/1.4052496.

Chapter 3: Testing a Quaternion Conversion Method to Determine Human 3D Tibiofemoral Angles During an *In Vitro* Simulated Jump Landing

This chapter is published in the ASME Journal of Biomechanics and should be referred to as:

> M. Ajdaroski, J. A. Ashton-Miller, S. Y. Baek, P. M. Shahshahani, and A. Esquivel, "Testing a Quaternion Conversion Method to Determine Human 3D Tibiofemoral Angles During an in Vitro Simulated Jump Landing," (in eng), J Biomech Eng, Sep 22, 2021, doi: 10.1115/1.4052496.

3.1 Abstract

Lower limb joint kinematics have been measured in laboratory settings using fixed camera-based motion capture systems; however, recently IMUs have been developed as an alternative. The purpose of this study was to test a QC method for calculating the three orthogonal knee angles during the high velocities associated with a jump landing using commercially available IMUs. Nine cadaveric knee specimens were instrumented with APDM Opal IMUs to measure knee kinematics in one-legged 3-4x BW simulated jump landings, four of which were used in establishing the parameters (training) for the new method and five for validation (testing). We compared the angles obtained from the QC method to those obtained from a commercially available sensor and algorithm (APDM Opal) with those calculated from an active marker motion capture system. Results showed a significant difference between both IMU methods and the motion capture data in most orthogonal angles ($p<0.01$), though the differences between the QC method and Certus system in the testing set for flexion and rotation angles were smaller than the APDM Opal algorithm, indicating an improvement. Additionally, in all 3 directions both the

limits of agreement and root mean square error between the QC method and the motion capture system were smaller than between the commercial algorithm and the motion capture.

3.2 Introduction

Over the last 20 years in the United States, the rate of ACL tears in young athletes has seen an annual increase of 2.3%, accounting for nearly half of all knee injuries [1, 2]. Additionally, young female athletes sustain ACL injuries at a higher rate, with anatomic, hormonal, and biomechanical differences between the sexes being potential risk factors [3-6]. While anatomical and hormonal factors are not easily modifiable, identifying and modifying the biomechanical factors may be possible. ACL tears are generally divided into two categories: contact or non-contact in nature, with the latter defined as involving no direct contact with another player or equipment. These non-contact ACL injuries can be caused by a singular event (an acute failure), but recently repetitive, high stress- and strain-inducing activities have also been shown to lead to non-contact ACL injuries (a material fatigue failure) [7].

The majority (75%) of reported ACL injuries are non-contact injuries [8, 9]. In one injury scenario, the knee is externally rotated with a slight flexion and a slight valgus angle at the time of injury [3, 10]. It has been theorized that once these conditions are met and the ground reaction force is applied across the knee, a powerful quadriceps contraction can cause sufficient anterior displacement of the tibia relative to the femur that increases ACL strain above its injury threshold [3, 10]. So, the magnitudes of the ground reaction and quadriceps forces, along with the 3D tibiofemoral angles are important factors [3, 11].

Traditionally, lower limb joint kinematics have been observed in laboratory settings using fixed camera-based motion capture systems; however, in recent years wearable sensors worn on selected body segments have been developed as an alternative and employed in various applications such as gait analysis and rehabilitation assistance [12-18]. One type of wearable sensor, an IMU, consisting of 3 orthogonal accelerometers, rate gyroscopes, and magnetic field sensors, provides direct measures of body segment linear acceleration, angular velocity, and magnetic field strength. Additionally, 3D joint angle kinematics can be determined through methods similar to those of camera-based systems and have been evaluated and confirmed in previous studies [16, 19]. IMUs provide the opportunity to monitor joint kinematics in real-world settings.

A commercially available IMU, APDM Opal (APDM Wearable Technologies, Portland, OR), uses a proprietary sensor fusion algorithm, whereby the orientation of the device can be tracked in inertial space. The algorithm uses knowledge of its dynamics to propagate the orientation changes based on gyroscope data and fuses the estimate with orientation estimates determined through its accelerometer and magnetometer information, thereby determining the orientation of the sensors in space. However, because this algorithm was developed for gait analysis, we hypothesized that it may not necessarily be accurate when used in more dynamic activities such as sports when larger changes in joint angles, velocity, and acceleration occur. So, the purpose of this study was to develop an algorithm to calculate the 3D tibiofemoral angles and compare those calculated angles as well as those obtained through the APDM fusion algorithm, to those from a standard motion capture system at a specific moment in time. Our goal was to determine if the new algorithm demonstrated improved accuracy and reliability in the ability to measure angles

during more dynamic activities. Improvements in the ability to measure tibiofemoral angles accurately and reliably during dynamic actions could be vital in identifying and tracking potentially injurious loading cycles during on-field activities and help prevent catastrophic failures such as ACL ruptures.

3.3 Materials and Methods

3.3.1 Subjects and Instrumentation

Nine cadaveric knee specimens were used for this study (Table 3-1). Each specimen was dissected leaving the ligamentous capsular intact as well as the muscle tendons of the quadriceps, hamstrings, and gastrocnemius. After dissection, the distal tibia/fibula and proximal femur were cut to a standard length of 20 cm from the center of the knee joint, then potted in polymethylmethacrylate cylinders. Once prepared, each specimen was rigidly fixed in a custom-built testing rig that was designed to simulate a one-legged jump landing of 3x-4x bodyweight (Figure 2-1). This testing rig, which includes simulated trans-knee muscle forces, has been validated in previous studies [20, 21].

Table 3-1 | Specimen Demographics. The total number of testing trials denotes how many trials the specimen was able to undergo before failure occurred, while trials analyzed consist of all trials in which refreezing of the tendon clamps was not performed nor any other noted deviations from the normal testing procedures occurred.

Demographics of the Specimens Used in the Testing Algorithm

Specimen #	Sex	Age	Side	Weight (kg)	Total Testing Trials	Trials Analyzed
1	F	20	L	86.6	100	80
2	M	32	R	68.0	100	96
3	M	32	R	88.4	100	98
4	M	25	R	86.2	100	96
5	M	33	R	49.9	100	96

Demographics of Specimens Used for Determining QC Method Parameters

Specimen #	Sex	Age	Side	Weight (kg)	Total Testing Trials	Trials Analyzed
6	M	39	L	54.4	100	96
7	F	30	R	82.1	53	50
8	M	29	R	74.8	100	96
9	F	28	R	63.5	100	98

A Certus optoelectronic tracking system (Optotrak Certus; Northern Digital Inc, Waterloo, Ontario, Canada) was used to track the changes in 3D tibiofemoral angles during the jump landing. A total of 20 Certus markers were used. Two sets of 3 “real” markers (physical markers affixed to a rigid body) were placed on the tibial and femoral load cells. An additional 14 “imaginary” markers were used that represented the anatomic landmarks of the knee being tested. This allowed for the capture of tibiofemoral kinematics such as 3D translation and rotation of the tibia with respect to the femur. The use of a 3D digitizing wand allowed for the defining and tracking of each imaginary marker. The sampling rate for the Certus system was set to 2 kHz. An APDM Opal sensor was rigidly attached to the medial aspect of the mid-tibia and another to the lateral aspect of the mid-femur using Co-flex bands and elastic ties (Figure 2-1).

The sampling rate for the APDM Opal sensors was 256 Hz but was expanded through linear interpolation to have a sampling rate of 2048 Hz to compare with the Certus system.

3.3.2 Testing Procedure

Before testing began, the IMU sensors were calibrated through the predefined calibration conditions used by the Moveo Mobility software developed by APDM. This initialization process was used by the software to establish initial conditions and minimize the influence that drift may have on data validity. Once initialized, the sensors continuously recorded data. After initialization, the quadriceps, hamstring, and gastrocnemius muscles were pre-tensioned to 180 N, 70 N, and 70 N, respectively, the initial knee angle adjusted to 15 degrees, and clamped securely in place with mechanical grips cooled by liquid nitrogen. This last step had to be repeated periodically throughout the testing, so knee angle and muscle tensions were recorded before each test and adjusted back to the above values, if necessary.

Drop height and weight were adjusted to match the target tibial ground reaction impact force of 4x BW (for larger specimens, this was reduced to 3x BW so as not to exceed test rig capacity). Once established, impacts were initiated by releasing a large weight to impact the distal end of the tibial load cell (Figure 2-1) guided via two parallel linear bearings. At least 5 preconditioning trials were conducted before the activation of the tibial torsional device to allow for any adjustments and potential uncrimping of collagen fibers. The tibial torsional device allowed for some of the impact force to be converted to internal tibial torque, as can happen in a live subject when the ground reaction causes internal tibial rotation at the knee [20, 21]. After the activation of the tibial torsional device, each specimen was subjected to up to 100 trials or until knee failure

occurred, clinically defined as anterior tibial displacement above 3 mm. Peak impact force was typically reached around 70 ms, so each trial consisted of 200 ms of data.

3.3.3 Data Analysis

In this study, we compared changes in tibiofemoral flexion, abduction, and internal rotation angles at peak impact with the three measurement modalities: 1) the Certus measurements which we considered the 'gold standard' for this study, and APDM wearable sensors - 2) using their proprietary algorithm and 3) our proposed algorithm. It was assumed that maximum vertical linear acceleration as measured by the APDM Opal sensors occurred at the same time as the maximum vertical force as measured by the Certus system. This assumption was made based on previous studies that showed a strong correlation between ground reaction force and linear acceleration [22].

3.3.4 Calculating the Euler Angles

A nine-axis indirect Kalman filter using the quaternion conversions of the IMU accelerometer, gyroscope, and magnetometer data was used in this study. This process is detailed at greater length in the paper by Stanley et al. [23]. Briefly, data were filtered using a fourth-order, zero-lag, low-pass Butterworth filter. The optimum cutoff frequency for the Butterworth low-pass digital filter was obtained by applying Winters' method to the sum squared difference between the unfiltered data and filtered data at a given frequency lying within the range of $1 \leq x < \frac{\text{sampling rate}}{2}$, divided by the sum squared difference between unfiltered data and the unfiltered mean; this process is outlined further by Yu et al. [24]. Average optimal cutoff frequencies were determined as: 12 Hz for the accelerometer (X=19 Hz; Y=11 Hz; Z=7 Hz); 20 Hz for the

gyroscope (X=10 Hz; Y=42 Hz; Z=9 Hz); and 8 Hz for the magnetometer (X=5 Hz; Y=10 Hz; Z=10 Hz). After filtering, a predicted orientation, v_i, for the current frame from the angular change of the previous frame, v_{i-1}, was obtained and subsequently converted to a quaternion such that:

$$v_i = R_i^f H \otimes v_{i-1} \tag{3-1}$$

where $R_i^f H$ is a rotation matrix from the inertial frame to the body frame using quaternion elements. Initially, the predicted orientation was estimated to be north-east-down (NED). Additionally, the previous orientation estimate q^-, was updated by rotating it by v_i such that:

$$q^- = q^+ \left(\prod_{n=1}^{i} v_n \right) \tag{3-2}$$

Using the quaternion conversions, estimations of gravitational and magnetic field measurements were obtained using the linear acceleration and angular velocity. These estimates were used to correct the gravitational and magnetic field data obtained by the previous orientation and magnetometer. These corrected estimates became the innovation, y_k, for the indirect Kalman filter. As mentioned by Stanley et al., the indirect Kalman filter attempts to track errors rather than orientation as the data is updated through a recursive process [23]. Additionally, because the process is recursive, the a priori estimates of the error process and the state transition models are always zero [23]. Therefore, the Kalman equations utilized in this study were reduced to:

$$P_k^- = Q_k \tag{3-3}$$

$$S_k = R_k - H_k P_k^- H_k^T \tag{3-4}$$

$$K_k = P_k^- H_k^T (S_k)^{-1} \tag{3-5}$$

$$x_k^+ = K_k y_k \tag{3-6}$$

$$P_k^+ = P_k^- - K_k H_k P_k^- \tag{3-7}$$

where S_k is defined as the innovation covariance, R_k is the covariance of the observation model noise, H_k is the observation model, P_k^- is the predicted estimate covariance, K_k, is the Kalman Gain, P_k^+ is the updated estimate covariance, and x_k^+ is the *a posteriori* state estimate. The a posteriori state estimate's orientation was corrected by the previous estimation such that:

$$q_k^+ = (q_k^-)(x_k^+) \tag{3-8}$$

Because the orientation was still in quaternion format, subtraction of the data from two adjacent segments is mathematically valid. Therefore, the data attributed to the tibial IMU sensor was subtracted from the femoral IMU sensor. The resulting values were then converted into Euler angles through:

$$\phi = \operatorname{atan2}\big(2(q_1 q_2 + q_2 q_3), 1 - 2(q_2^2 + q_3^2)\big) \tag{3-9}$$

$$\theta = \operatorname{asin}\big(2(q_1 q_3 - q_4 q_2)\big) \tag{3-10}$$

$$\psi = \operatorname{atan2}\big(2(q_1 q_4 + q_2 q_3), 1 - 2(q_3^2 + q_3^2)\big) \tag{3-11}$$

where ϕ is the internal/external rotation, θ is the valgus/varus angle, and ψ is the flexion/extension angle [25][*].

[*] Amended from original published manuscript

3.3.5 Establishing the Parameters

The covariance of the observation model noise, R_k, as well as the predicted estimate covariance, P_k^-, consisted of several parameters unique to a sensor. These unique parameters included accelerometer noise (variance of accelerometer signal noise), linear acceleration noise (variance of linear acceleration noise; akin to gyroscope drift noise), gyroscope drift noise (variance of gyroscope offset drift), gyroscope noise (variance of gyroscope single noise), magnetic disturbance noise (variance of the magnetic disturbance noise), magnetometer noise (variance in the magnetometer signal noise), linear acceleration decay factor (decay factor for the linear acceleration), and magnetic disturbance decay factor (decay factor for the magnetic disturbance) [23]. APDM Opal documentation provided the values associated with accelerometer noise, gyroscope noise, and magnetometer noise. The parameters of gyroscope drift noise, linear acceleration noise, and magnetic disturbance noise were not detailed by the documentation, and instead default values based on the FRDM-FXS-Multi family of sensor boards (as used by the Freescale Toolbox of MATLAB) were used. The use of these default values was implemented due to the potential value ranges being theoretically infinite such that a process of trial and error would not be possible. Linear acceleration decay factor (LADF) and magnetic disturbance decay factor (MDDF) were unknown parameters that could be adjusted as their theoretical values ranged from 0 to 1. Therefore, of the nine specimens in this study, four were selected to establish the values of these parameters (training set) (Table 3-1). A trial-and-error approach was taken where adjustments to the LADF and/or MDDF were performed to minimize the difference in maximum angle between the QC method and the Certus system. These adjustments were performed on each of the three orthogonal angles resulting in 3 unique LADF and 3 unique MDDF values per specimen. An average for both LADF and MDDF was determined and used

when calculating the angles of the remaining five specimens (testing set). A trial-and-error approach was used as it requires no assumed knowledge of the system and allows for the determination of some valid working solution. MATLAB scripts were used to calculate specimen angles using the QC method for both the training set and testing set (MATLAB_R2019b; MathWorks, Natick, MA).

3.3.6 Statistical Analysis

Since the intermittent freezing of the patellar ligament clamp led to significant changes in linear acceleration and angular velocity and had the potential to affect the mechanical properties of the specimen immediately post-freezing, these trials were omitted from any analysis. A repeated measures ANOVA with a pairwise comparison was performed on both training and testing specimen sets to determine whether there was a difference between the QC method and the Certus data, the QC method and the APDM algorithm, and the APDM algorithm and the Certus data (IBM SPSS Statistics v 24.0). A Bonferroni correction was used to correct for multiple comparisons. Differences were considered significant if $p < 0.05$. LoA were constructed for the testing specimen set to examine each method's reliability; lower LoA values indicated a better degree of reliability [26]. Linear mixed effect models for both sets were constructed where the angle as measured by Certus was a linear function of the IMU angles (the QC method or the APDM algorithm) with a random intercept per specimen. The root mean square of the residuals of the linear mixed effect model was used as the RMSE between Certus and one of the IMU angle methods.

3.4 Results

The angles of interest were those that occurred at maximum vertical tibial force (Certus system) or at maximum vertical tibial linear acceleration (APDM Opal and QC method) during the simulated jump ‘landing’. Figure 3-1 illustrates the representative signals measured by the three systems as well as the timestamp of the angle of interest. The APDM Opal algorithm exhibited a phase lag, whereby the peak angle appeared later than the peak angle of either the Certus system or the QC method.

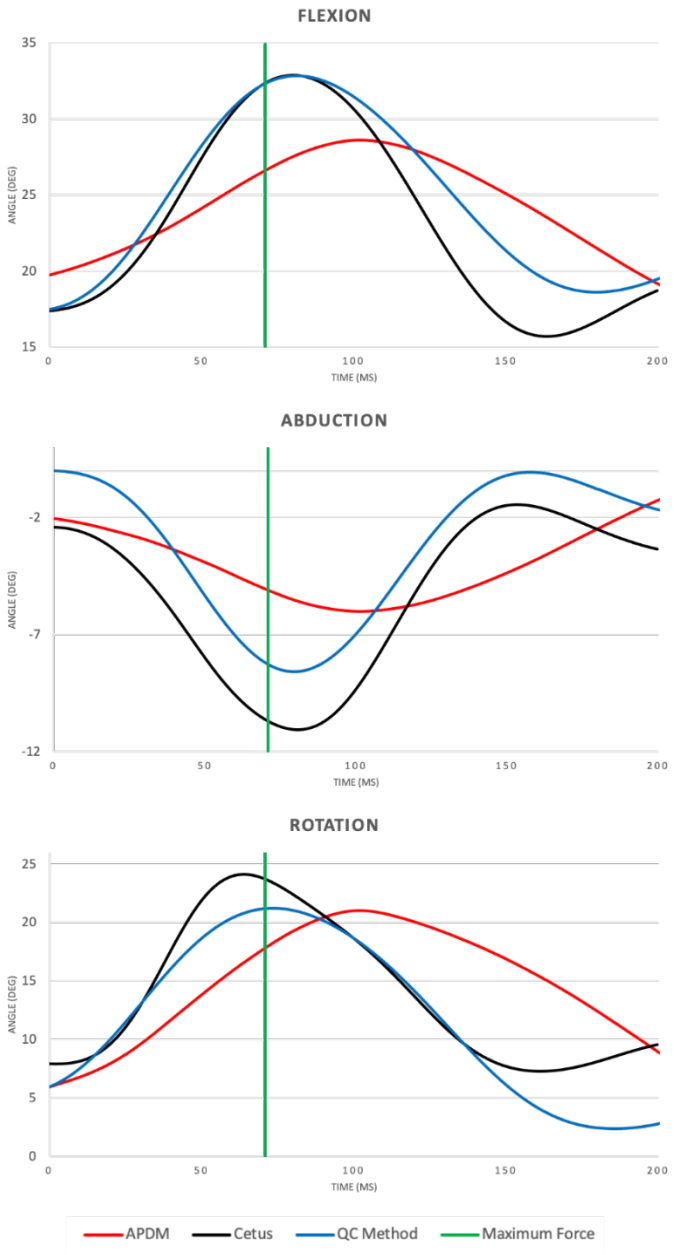

Figure 3-1 | Average time histories of the three orthogonal knee angles as measured by APDM algorithm (red curve), Certus (black curve), and QC method (blue curve) for a single knee specimen for (a) flexion, (b) abduction, and (c) rotation. The vertical green line indicates the time of the peak impact force. Note that the APDM algorithm (red) exhibited a phase lag relative to the Certus data and QC method.

3.4.1 Training Set

There was a significant difference in all three angles between the Certus and APDM Opal algorithm. The training set showed a mean difference in flexion/extension between the Certus

system and APDM Opal algorithm of 0.9° (95% CI: 0.6° to 1.2°)) (Table 3-2). For abduction/adduction, a mean difference of -1.1° (95% CI: -1.1° to -0.5°) between the Certus system and APDM Opal algorithm was observed, while the mean difference between the Certus system and the QC method was 0.2° (95% CI: 0.1° to 0.3°) (Table 2). The mean difference in rotation between the Certus system and the APDM Opal algorithm was 2.7° (95% CI: 2.1° to 3.3°) (Table 3-2). In each case both the LoA and RMSE associated with the QC method vs. Certus were observed to be smaller, indicating an increase in accuracy and reliability when using the QC method (Table 3-3).

Table 3-2 | Values of the pairwise comparison analysis performed for (a) flexion, (b) abduction, and (c) rotation in degrees. Mean (SD) and 95% confidence interval (CI) are based on the difference in angle measurement between compared systems for specimens in the training algorithm set (left) and for those in the testing algorithm set (right). *Statistically significant $p<0.05$

Repeated Measures ANOVA with Pairwise Comparison

		Training Set		Testing Set	
	Comparison	**Mean Diff. (SD)**	**95% CI[a]**	**Mean Diff. (SD)**	**95% CI[a]**
Flexion	Certus v APDM algorithm	0.9° (2.8°)*	(0.6°, 1.2°)	2.5° (0.2°)*	(1.9°, 3.1°)
	Certus v QC Method	-0.1° (0.9°)	(-0.2°,0.0°)	-0.7° (0.1°)*	(-1.1°, -0.4°)
	QC Method v APDM algorithm	-0.8° (2.8°)*	(-1.1°, -0.5°)	3.2° (0.3°)*	(2.6°, 3.8°)
Abduction	Certus v APDM algorithm	-1.1° (2.8°)*	(-1.4°, -0.8°)	-4.1° (0.1°)*	(-4.3°, -3.9°)
	Certus v QC Method	0.2° (0.7°)*	(0.1°, 0.3°)	-1.2° (0.1°)*	(-1.4°, -1.0°)
	QC Method v APDM algorithm	0.9° (2.7°)*	(0.7°, 1.2°)	-2.9° (0.1°)*	(-3.2°, -2.6°)
Rotation	Certus v APDM algorithm	2.7° (5.9°)*	(2.1°, 3.3°)	6.7° (0.4°)*	(5.8°, 7.6°)
	Certus v QC Method	0.1° (1.5°)	(-0.1°, 0.2°)	1.0° (0.2°)*	(0.6°, 1.4°)
	APDM algorithm v QC Method	-2.8° (5.9°)*	(-3.4°, -2.2°)	5.7° (0.4°)*	(4.8°, 6.5°)

[a]. Adjustment for multiple comparisons: Bonferroni

Table 3-3 | Comparison of the calculated knee angles between IMU-based methods (APDM Opal or QC Method) and the Certus motion capture system for specimens in the training algorithm set (left) and for those in the testing algorithm set (right).

Comparison of IMU Methods to Certus Values

		Training Set		Testing Set	
	Comparison	**RMSE**	**LoA**	**RMSE**	**LoA**
Flexion	Certus v APDM algorithm	1.0°	(-6.3, 4.6)	3.1°	(-12.1°, 7.0°)
	Certus v QC Method	0.7°	(-1.9, 1.8)	2.6°	(-4.5°, 5.8°)
Abduction	Certus v APDM algorithm	2.0°	(-4.4, 6.7)	1.1°	(0.2°, 8.0)
	Certus v QC Method	0.7°	(-1.3, 1.7)	0.8°	(-2.1°, 4.4°)
Rotation	Certus v APDM algorithm	3.4°	(14.2, 8.8)	6.0°	(-22.5°, 9.2°)
	Certus v QC Method	1.5°	(-2.9, 3.1)	2.4°	(-8.6°, 6.6°)

3.4.2 Testing Set

There was a statistically significant difference between the Certus measurements and both the QC Method and APDM Opal algorithm for all three angles. There was a mean difference in flexion/extension of 2.5° (95% CI: 2.0° to 3.1°) between the Certus system and APDM Opal algorithm while the mean difference between the Certus system and the QC method was -0.7° (95% CI: -1.1° to 0.4°) (Table 3-2). For abduction/adduction, the mean difference between the Certus system and APDM Opal algorithm was -4.1° (95% CI: -4.3° to -3.9°) while the mean difference between the Certus system and the QC method was -1.2° (95% CI: -1.4° to -1.0°) (Table 3-2). For rotation, the mean difference between the Certus system and APDM Opal algorithm was 6.7° (95% CI: 5.8° to 7.6°) while the mean difference between the Certus and the QC method was observed to be 1.0° (95% CI: 0.6° to 1.4°) (Table 3-2).

The Bland-Altman plot for flexion/extension of APDM algorithm vs. Certus cases showed a downward trend, indicating that the APDM algorithm method tended to overestimate the angle at lower angles and underestimate it at higher ones while no such trend was observed in the QC method vs. Certus (Figure 3-2a). Most trials for the APDM algorithm vs. Certus fell below the zero-difference line, indicating a tendency for underestimation while QC Method vs. Certus demonstrated a tendency for overestimation. For abduction/adduction, both the APDM algorithm vs. Certus and QC method vs. Certus showed a downward trend, however, the trend associated with the QC method vs. Certus was less pronounced (Figure 3-2b). Both APDM vs. Certus and QC Method vs. Certus exhibited most trials above the zero-difference line indicating a tendency for underestimation of the Certus absolute angle, though APDM algorithm vs. Certus exhibited a greater propensity (3.4% vs. 23.0%). In the Bland-Altman plot for rotation, both the APDM algorithm vs. Certus and QC method vs. Certus showed similar downward trends with both exhibiting most of their trials falling below the zero-difference line indicating a tendency of underestimation in both methods (Figure 3-2c). Though again, the APDM algorithm vs. Certus exhibited a greater propensity for underestimation (79.4% vs. 63.4%). Additionally, in each case, both the LoA and RMSE associated with the QC method vs. Certus were observed to be smaller than the opal algorithm, indicating an increase in accuracy and reliability when using the QC method and the training set LoA and RMSE were lower than the testing set. (Table 3-3)

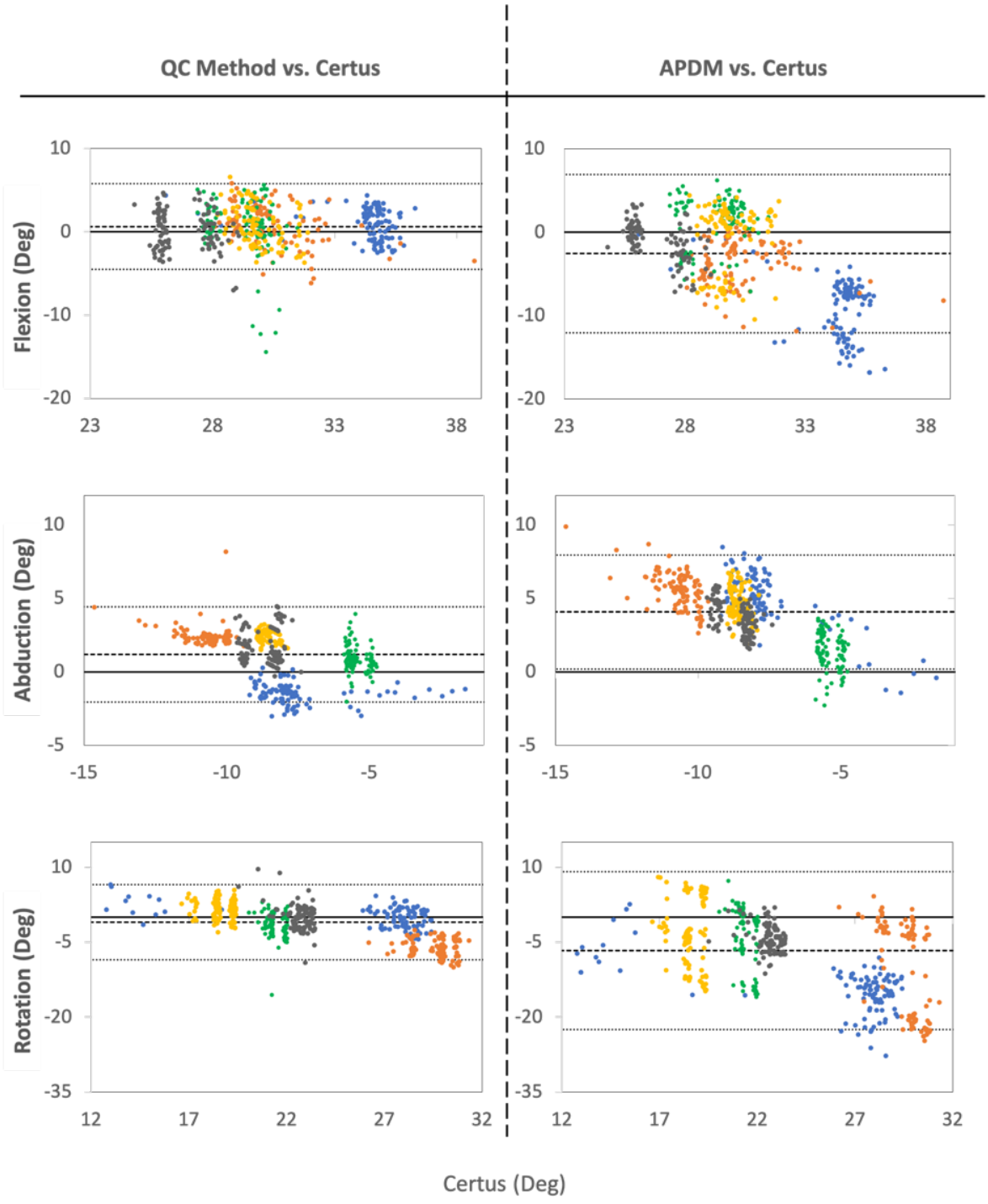

Figure 3-2 | Bland-Altman plot associated with the difference between the (a) flexion, (b) abduction, and (c) rotation angles using the QC method and Certus (left), and the APDM algorithm and the Certus system (right). The colors represent different knee specimens. The y-axis shows the difference in the measured angle.

3.5 Discussion

The purpose of this study was to determine whether the QC method could provide improved accuracy and reliability measurements of the changes in 3D knee angles during a dynamic activity consisting of a jump landing. In this study, we observed that across all cases and specimen sets, the QC method produced smaller differences than the APDM algorithm when compared to the 'gold-standard' Certus motion capture system. Although in the majority of cases, the difference between the QC method and Certus was statistically significant ($p < 0.01$), the mean difference for flexion (-0.7°) and rotation (1.0°) in the testing set between the two systems is clinically insignificant. For example, a review paper that examined the difference in knee flexion angles during documented ACL tears in male and female athletes reported differences in 10°-21.7° in knee flexion between injured and uninjured athletes and a laboratory study found a correlation of increased abduction angle of 8° in female athletes who went on to injure their ACL [27, 28]. Only the mean difference between the QC method and Certus for flexion (-0.1°) and rotation (0.1°) in the training set were observed as not being statistically significant, though this may be due to the algorithm being overly tuned for the training set. Furthermore, in every instance, the RMSE values associated with the difference between the QC method and the Certus system were smaller than those for the APDM algorithm, with the largest difference occurring in the testing set for rotation (2.4° compared to 6.0°). In every case the LoA associated with the difference between the QC method and the Certus system was smaller than those of APDM Opal, indicating a smaller range in differences and a better degree of reliability. A particular point of interest is the observation that the APDM Opal algorithm exhibited a phase lag compared to the Certus system, whereas the QC method did not (Table 3-2). This was also observed by Takeda et al. where a phase lag in peak flexion angle between the IMU and camera

system is visible [29]. Takeda et al. attributed this phase lag in their study to the use of a moving average filter to remove noise from the raw acceleration and angular velocity data [29].

Several studies have calculated joint angles using IMU sensors and compared the results to those from a motion capture system [29-32]. However, most focus has been on examining differences in knee flexion, the knee angle that exhibits the largest change. While determining an IMU's ability to measure flexion angles is important when observing knee injuries, several studies have noted the relationships between knee injuries (particularly ACL stress/strain) and valgus and rotational angles, rather than flexion angle [6, 33-38]. So, to improve knee injury prevention, it is important to be able to accurately measure all three tibiofemoral angles, not just flexion. Determining Euler angles from only linear acceleration and angular velocity is common practice because this process can smoothly measure rotation in 3D space. However, because it can only yield orientation to some random horizontal global frame of reference, it lacks a sense of magnetic north and thus cannot accurately measure angles perpendicular to that horizontal global frame [23]. Furthermore, in many of these studies, direct conversion of angular velocities into Euler angles through the implementation of a rotation matrix was performed [29, 30]. This approach poses several problems. First, rotation matrices do not commute and the order in which they are applied is important. Additionally, there is a possibility that during rotation, alignment of two of the axes may occur resulting in gimbal lock and loss of data. And finally, there is a potential distortion of the data that can occur. It should also be noted that Euler angles are not vectors. This poses the issue that, mathematically, subtraction of the Euler angles of adjacent segments to determine joint angles is not justifiable.

Studies such as those by Watanabe et al. and Tong et al. calculated knee flexion joint angles but did not convert these to Euler angles [31, 32]. This poses the problem that angles obtained by either study do not describe the orientation of the joint to a fixed coordinate system and thus may not represent the knee's true 3D angular orientation. In the study conducted by Tong et al., the difference between adjacent segment inclinations was determined which, when compared to their camera system, resulted in a RMSE value of 6.4°. This is larger than that observed within our study for either the APDM Opal (3.1°) or our QC Method (2.6°) [32]. Watanabe et al. performed a similar process to that of Tong et al. in that they used the difference in integrated angular velocity between two adjacent segments, however, they also made use of a Butterworth low-pass filter as well as a Kalman filter, as we used in our QC Method [31]. Watanabe et al. observed an RMSE between 3° and 4°, smaller than that reported by Tong et al. and comparable to that of the APDM Opal (3.1°), however, the RMSE associated with our QC Method was observed to be smaller (2.6°). Both studies examined gait, which has lower velocities and accelerations than the present jump landing activity. Slower movements, such as in gait may not have the same levels of movement artifact as those that are more dynamic such as those in the present study. Additionally, Tong et al. used a limited sample size (N=3) which is unlikely to suffice to establish a reliable methodology [32]. While the sample size used by Watanabe et al. was comparable to our study (N=6), they had significantly fewer total trials (N=18 compared to N=466) which may not capture the inter-trial variations and trends [31]. In addition, these studies calculated knee flexion angle only.

Takeda et al. used the angular velocity of an IMU to estimate the translational acceleration; this translational acceleration was subtracted from the IMU linear acceleration to obtain gravitational

acceleration which was then used to determine the flexional orientation of the joint [29]. Unlike the studies of either Watanabe et al. or Tong et al., Takeda et al. applied rotational matrices to obtain the Euler angles [29]. The process resulted in an observed RMSE between their method and camera system of 6.8°, comparable to that observed by Tong et al. and larger than that observed within our study for either the APDM Opal (3.1°) or our method (2.6°) [29]. The lag observed by Takeda et al. between their method and camera system is similar to the lag observed in our study between APDM Opal and Certus system: their method's peak flexion angle fell between 10-15% after the peak flexion angle of the camera system, and in our study, the average APDM Opal peak flexion angle was 40 ms (~20%) after the peak flexion angle of the camera system [29].

One previous study used APDM Opal sensors and compared the results to a camera system, but unlike many other studies made use of both highly dynamic activities (jumps) as well as live subjects [39]. Additionally, all three angles of the knee were measured and compared. The APDM Opal sensors performed well under certain conditions, primarily those of smaller angular displacement and in the ability to measure abduction/adduction and internal/external rotation [39]. This was not what was observed in our study which found abduction/adduction and internal/external rotation of either method exhibiting larger RMSE values. In nearly every case RMSE values observed in this study were smaller than those previously reported [39]. The only exception was in the comparison of internal/external rotation for APDM Opal vs. Certus which had the largest RMSE values among all comparisons (RMSE: 6.7° compared to 3.9° observed by Ajdaroski et al.) [39]. While artifact due to skin/muscle laxity of live subjects may have contributed to why the RMSE values observed were larger, in the case of internal/external

rotation of APDM Opal vs. Certus it may be drift and error accumulation due to the longer testing durations in the present study that could account for its larger RMSE value. The QC method has the potential for measuring more accurate and reliable angles than the method employed by the APDM Opal algorithm, although the application of the QC method on live subjects is still needed to confirm this.

3.5.1 Limitations

The present study examined a new algorithm for calculating knee angles in a 'best case scenario' without the ever-present soft tissue motion that affects the coupling of the sensor to the bone *in vivo*. That means that the present measurements of knee angle changes were conducted under the best possible conditions and future studies should examine how soft tissue motion can affect accuracy. Additional pre-/post filtering may be necessary for live subjects using the QC method. Additional variation may also be expected in live subjects because each individual will have more varied landing kinematics than the present instrumented apparatus provided. It is also true that limited ranges in flexion, abduction, and rotation angles were observed in the present study. Testing with smaller and larger knee angle changes will be required to understand the possible error that could occur in the full range of motion of the knee. Furthermore, maneuvers other than jump landings have been observed to lead to non-contact ACL injuries and as such, it may be possible that the QC method developed in this study is overly tuned for a jump landing scenario [11-13]. The trial-and-error approach used in the determination of LADF and MDDF values may be a source of potential error. A more robust method such as nonlinear programming with specific constraint conditions could have been used, although it should be noted that this can be expensive to perform and given the very small differences between the QC method and Certus,

the added precision in value may not be needed. The limited number of specimens (n=4) used to establish the parameters for the QC method is also a potential limitation. The lower sampling rate of the IMU may also be a limitation as this may have led to missed information and/or aliasing when compared to higher sampling rates. Finally, the presence of iron in the frame of the present apparatus might have affected the accuracy of the IMU magnetometer readings, a situation that would not exist on a large outdoor field.

3.6 Conclusions

The QC method was able to estimate knee angles more accurately during a simulated one-legged landing than the APDM Opal algorithm across all three tibiofemoral angles. The improvements in accuracy provided by the QC method demonstrate that it may be feasible to use IMUs to identify and track knee angle measurements that may be associated with ACL injury given the reported association between ACL stress/strain and knee valgus and internal rotation angles and moments. Further testing of the QC method is needed in live subjects and a variety of scenarios.

Acknowledgments

This material is based on work supported by the National Science Foundation under grant number 2003434 and the National Institutes of Health under award number AR054821. The authors wish to thank Dr. Melanie Beaulieu for her assistance with data collection.

3.7 References

[1] V. Musahl and J. Karlsson, "Anterior Cruciate Ligament Tear," (in eng), *N Engl J Med,* vol. 380, no. 24, pp. 2341-2348, 06 2019, doi: 10.1056/NEJMcp1805931.

[2] N. A. Beck, J. T. R. Lawrence, J. D. Nordin, T. A. DeFor, and M. Tompkins, "ACL Tears in School-Aged Children and Adolescents Over 20 Years," (in eng), *Pediatrics,* vol. 139, no. 3, Mar 2017, doi: 10.1542/peds.2016-1877.

[3] L. Y. Griffin *et al.*, "Noncontact anterior cruciate ligament injuries: risk factors and prevention strategies," (in eng), *J Am Acad Orthop Surg,* vol. 8, no. 3, pp. 141-50, 2000 May-Jun 2000, doi: 10.5435/00124635-200005000-00001.

[4] C. Y. Wild, J. R. Steele, and B. J. Munro, "Why do girls sustain more anterior cruciate ligament injuries than boys?: a review of the changes in estrogen and musculoskeletal structure and function during puberty," (in eng), *Sports Med,* vol. 42, no. 9, pp. 733-49, Sep 2012, doi: 10.1007/BF03262292.

[5] L. Yin, D. Sun, Q. C. Mei, Y. D. Gu, J. S. Baker, and N. Feng, "The Kinematics and Kinetics Analysis of the Lower Extremity in the Landing Phase of a Stop-jump Task," (in eng), *Open Biomed Eng J,* vol. 9, pp. 103-7, 2015, doi: 10.2174/1874120701509010103.

[6] B. Yu and W. E. Garrett, "Mechanisms of non-contact ACL injuries," (in eng), *Br J Sports Med,* vol. 41 Suppl 1, pp. i47-51, Aug 2007, doi: 10.1136/bjsm.2007.037192.

[7] E. M. Wojtys, M. L. Beaulieu, and J. A. Ashton-Miller, "New perspectives on ACL injury: On the role of repetitive sub-maximal knee loading in causing ACL fatigue failure," (in eng), *J Orthop Res,* vol. 34, no. 12, pp. 2059-2068, 12 2016, doi: 10.1002/jor.23441.

[8] B. P. Boden, F. T. Sheehan, J. S. Torg, and T. E. Hewett, "Noncontact anterior cruciate ligament injuries: mechanisms and risk factors," (in eng), *J Am Acad Orthop Surg,* vol. 18, no. 9, pp. 520-7, Sep 2010, doi: 10.5435/00124635-201009000-00003.

[9] F. Launay, "Sports-related overuse injuries in children," (in eng), *Orthop Traumatol Surg Res,* vol. 101, no. 1 Suppl, pp. S139-47, Feb 2015, doi: 10.1016/j.otsr.2014.06.030.

[10] O. E. Olsen, G. Myklebust, L. Engebretsen, and R. Bahr, "Injury mechanisms for anterior cruciate ligament injuries in team handball: a systematic video analysis," (in eng), *Am J Sports Med,* vol. 32, no. 4, pp. 1002-12, Jun 2004, doi: 10.1177/0363546503261724.

[11] P. Renstrom *et al.*, "Non-contact ACL injuries in female athletes: an International Olympic Committee current concepts statement," (in eng), *Br J Sports Med,* vol. 42, no. 6, pp. 394-412, Jun 2008, doi: 10.1136/bjsm.2008.048934.

[12] C. J. Anderson, C. G. Ziegler, C. A. Wijdicks, L. Engebretsen, and R. F. LaPrade, "Arthroscopically pertinent anatomy of the anterolateral and posteromedial bundles of the

posterior cruciate ligament," (in eng), *J Bone Joint Surg Am,* vol. 94, no. 21, pp. 1936-45, Nov 2012, doi: 10.2106/JBJS.K.01710.

[13] M. Arif and A. Kattan, "Physical Activities Monitoring Using Wearable Acceleration Sensors Attached to the Body," (in eng), *PLoS One,* vol. 10, no. 7, p. e0130851, 2015, doi: 10.1371/journal.pone.0130851.

[14] A. G. Cutti, A. Ferrari, P. Garofalo, M. Raggi, and A. Cappello, "'Outwalk': a protocol for clinical gait analysis based on inertial and magnetic sensors," (in eng), *Med Biol Eng Comput,* vol. 48, no. 1, pp. 17-25, Jan 2010, doi: 10.1007/s11517-009-0545-x.

[15] J. Favre, X. Crevoisier, B. M. Jolles, and K. Aminian, "Evaluation of a mixed approach combining stationary and wearable systems to monitor gait over long distance," (in eng), *J Biomech,* vol. 43, no. 11, pp. 2196-202, Aug 2010, doi: 10.1016/j.jbiomech.2010.03.041.

[16] A. Ferrari *et al.*, "First in vivo assessment of "Outwalk": a novel protocol for clinical gait analysis based on inertial and magnetic sensors," (in eng), *Med Biol Eng Comput,* vol. 48, no. 1, pp. 1-15, Jan 2010, doi: 10.1007/s11517-009-0544-y.

[17] J. F. Lin and D. Kulić, "Human pose recovery using wireless inertial measurement units," (in eng), *Physiol Meas,* vol. 33, no. 12, pp. 2099-115, Dec 2012, doi: 10.1088/0967-3334/33/12/2099.

[18] P. Picerno, A. Cereatti, and A. Cappozzo, "Joint kinematics estimate using wearable inertial and magnetic sensing modules," (in eng), *Gait Posture,* vol. 28, no. 4, pp. 588-95, Nov 2008, doi: 10.1016/j.gaitpost.2008.04.003.

[19] J. Favre, R. Aissaoui, B. M. Jolles, J. A. de Guise, and K. Aminian, "Functional calibration procedure for 3D knee joint angle description using inertial sensors," (in eng), *J Biomech,* vol. 42, no. 14, pp. 2330-5, Oct 2009, doi: 10.1016/j.jbiomech.2009.06.025.

[20] D. B. Lipps, E. M. Wojtys, and J. A. Ashton-Miller, "Anterior cruciate ligament fatigue failures in knees subjected to repeated simulated pivot landings," (in eng), *Am J Sports Med,* vol. 41, no. 5, pp. 1058-66, May 2013, doi: 10.1177/0363546513477836.

[21] D. B. Lipps, Y. K. Oh, J. A. Ashton-Miller, and E. M. Wojtys, "Effect of increased quadriceps tensile stiffness on peak anterior cruciate ligament strain during a simulated pivot landing," (in eng), *J Orthop Res,* vol. 32, no. 3, pp. 423-30, Mar 2014, doi: 10.1002/jor.22531.

[22] N. G. Elvin, A. A. Elvin, and S. P. Arnoczky, "Correlation between ground reaction force and tibial acceleration in vertical jumping," (in eng), *J Appl Biomech,* vol. 23, no. 3, pp. 180-9, Aug 2007, doi: 10.1123/jab.23.3.180.

[23] M. Pedley, M. Stanley, and Z. Baranski, "Freescale Sensor Fusion Kalman Filter," ed: Freescale S emiconductor 2014.

[24] B. Yu, D. Gabriel, L. Noble, and K.-N. An, "Estimate of the Optimum Cutoff Frequency for the Butterworth Low-Pass Digital Filter," *Journal of Applied Biomechanics,* vol. 15, pp. 319-329, 1999 doi: 10.1123/jab.15.3.318.

[25] E. Bernardes and S. Viollet, "Quaternion to Euler angles conversion: A direct, general and computationally efficient method," (in eng), *PLoS One,* vol. 17, no. 11, p. e0276302, 2022, doi: 10.1371/journal.pone.0276302.

[26] J. M. Bland and D. G. Altman, "Statistical methods for assessing agreement between two methods of clinical measurement," (in eng), *Lancet,* vol. 1, no. 8476, pp. 307-10, Feb 1986.

[27] J. Larwa, C. Stoy, R. S. Chafetz, M. Boniello, and C. Franklin, "Stiff Landings, Core Stability, and Dynamic Knee Valgus: A Systematic Review on Documented Anterior Cruciate Ligament Ruptures in Male and Female Athletes," (in eng), *Int J Environ Res Public Health,* vol. 18, no. 7, 04 2021, doi: 10.3390/ijerph18073826.

[28] T. E. Hewett *et al.*, "Biomechanical measures of neuromuscular control and valgus loading of the knee predict anterior cruciate ligament injury risk in female athletes: a prospective study," (in eng), *Am J Sports Med,* vol. 33, no. 4, pp. 492-501, Apr 2005, doi: 10.1177/0363546504269591.

[29] R. Takeda, S. Tadano, A. Natorigawa, M. Todoh, and S. Yoshinari, "Gait posture estimation using wearable acceleration and gyro sensors," (in eng), *J Biomech,* vol. 42, no. 15, pp. 2486-94, Nov 2009, doi: 10.1016/j.jbiomech.2009.07.016.

[30] J. M. Barrett, D. Viggiani, J. Park, and J. P. Callaghan, "Expressing angles relative to reference postures: A mathematical comparison of four approaches," (in eng), *J Biomech,* vol. 104, p. 109733, May 2020, doi: 10.1016/j.jbiomech.2020.109733.

[31] T. Watanabe and H. Saito, "Tests of wireless wearable sensor system in joint angle measurement of lower limbs," (in eng), *Annu Int Conf IEEE Eng Med Biol Soc,* vol. 2011, pp. 5469-72, 2011, doi: 10.1109/IEMBS.2011.6091395.

[32] K. Tong and M. H. Granat, "A practical gait analysis system using gyroscopes," (in eng), *Med Eng Phys,* vol. 21, no. 2, pp. 87-94, Mar 1999, doi: 10.1016/s1350-4533(99)00030-2.

[33] K. L. Markolf, D. M. Burchfield, M. M. Shapiro, M. F. Shepard, G. A. Finerman, and J. L. Slauterbeck, "Combined knee loading states that generate high anterior cruciate ligament forces," (in eng), *J Orthop Res,* vol. 13, no. 6, pp. 930-5, Nov 1995, doi: 10.1002/jor.1100130618.

[34] T. E. Hewett, G. D. Myer, and K. R. Ford, "Anterior cruciate ligament injuries in female athletes: Part 1, mechanisms and risk factors," (in eng), *Am J Sports Med,* vol. 34, no. 2, pp. 299-311, Feb 2006, doi: 10.1177/0363546505284183.

[35] T. E. Hewett, K. R. Ford, and G. D. Myer, "Anterior cruciate ligament injuries in female athletes: Part 2, a meta-analysis of neuromuscular interventions aimed at injury prevention," (in eng), *Am J Sports Med,* vol. 34, no. 3, pp. 490-8, Mar 2006, doi: 10.1177/0363546505282619.

[36] C. S. Shin, A. M. Chaudhari, and T. P. Andriacchi, "Valgus plus internal rotation moments increase anterior cruciate ligament strain more than either alone," (in eng), *Med Sci Sports Exerc,* vol. 43, no. 8, pp. 1484-91, Aug 2011, doi: 10.1249/MSS.0b013e31820f8395.

[37] S. G. McLean, S. W. Lipfert, and A. J. van den Bogert, "Effect of gender and defensive opponent on the biomechanics of sidestep cutting," (in eng), *Med Sci Sports Exerc,* vol. 36, no. 6, pp. 1008-16, Jun 2004, doi: 10.1249/01.mss.0000128180.51443.83.

[38] S. M. Sigward and C. M. Powers, "Loading characteristics of females exhibiting excessive valgus moments during cutting," (in eng), *Clin Biomech (Bristol, Avon),* vol. 22, no. 7, pp. 827-33, Aug 2007, doi: 10.1016/j.clinbiomech.2007.04.003.

[39] M. Ajdaroski, R. Tadakala, L. Nichols, and A. Esquivel, "Validation of a Device to Measure Knee Joint Angles for a Dynamic Movement," (in eng), *Sensors (Basel),* vol. 20, no. 6, Mar 2020, doi: 10.3390/s20061747.

Chapter 4: Predicating Leg Force and Knee Moment Using Inertial Measurement Units: An *In Vitro* Study

This chapter has been submitted for publication in the ASME Journal of Biomechanics

Mirel Ajdaroski, So Young Baek, James A. Ashton-Miller, Amanda O. Esquivel

4.1 Abstract

We compared the ability of seven machine learning algorithms to use wearable IMU data to identify the severe knee loading cycles known to induce microdamage associated with ACL rupture. Sixteen cadaveric knee specimens, dissected free of skin and muscle, were mounted in a rig simulating standardized jump landings. One IMU was located above and the other below the knee, the applied 3-D action and reaction loads were measured via 6-axis load cells, and the 3-D knee kinematics also recorded by a laboratory motion capture system. Machine learning algorithms were used to predict the knee moments and the tibial and femur vertical forces; 13 knees were utilized for training each model, while 3 were used for testing its accuracy (i.e., normalized root mean square error) and reliability (Bland-Altman limits of agreement). The results showed the models predicted force and knee moment values with acceptable levels of error and, although several models exhibited some form of bias, acceptable reliability. Further research will be needed to determine whether these types of models can be modified to attenuate the inevitable *in vivo* soft tissue motion artifact associated with highly dynamic activities like jump landings.

4.2 Introduction

In the United States, approximately 100,000 to 200,000 ACL ruptures are reported every year [1, 2]. Several studies have examined the mechanisms by which an ACL may be injured, usually during sports like basketball, football, soccer, and volleyball, including so-called 'contact' (30% of all cases) and 'non-contact' (70% of all cases) injuries [3-6]. Non-contact injuries involve no load transfer from another player but rather loads on the knee generated by limb muscles and passive structures as well the ground reaction force beneath the foot. Recent studies have suggested that some non-contact ACL injuries may be due to overuse of the ligament, whereby repetitive high stress/strain-inducing activities result in ACL collagen unravelling and multiscale damage thereby weakening the ligament; without adequate built in rest periods for repair, ACL rupture can occur [7-10]. So, counting the accumulated number of these potentially injurious loading cycles over a given period could have considerable clinical import, as we shall discuss later.

Older studies have reported the circumstances of non-contact ACL injury. These include landing with an externally rotated knee in an extended position (20° or less of flexion) in slight valgus, or with a powerful quadriceps contraction; this can cause anterior displacement of the tibia with respect to the femur via the patella-femoral mechanism, thereby increasing the ACL strain above its tolerable threshold [11, 12]. Other studies suggest that landing a jump with a fully extended knee in neutral, or internal rotation with valgus orientation, can excessively strain the ligament [11], with ACL stress being correlated with the magnitude of internal rotation and valgus knee moments [13-16].

Traditionally, lower limb joint kinematics and kinetics are measured in laboratory settings using camera-based motion capture systems and force plates. However, such systems are large and bulky, making them impractical for regular usage in the field. In recent years the development of wearable sensors has emerged as an alternative to camera-based motion capture systems, and they have usefully been employed in various applications including gait analysis and assistive rehabilitation [17-23]. IMUs are small, wearable sensors generally consist of orthogonal accelerometers, rate gyroscopes and magnetometers allowing direct measurement of a body segment's linear acceleration, angular velocity, and environmental magnetic field strength. IMUs, of course, can be used as a system to capture information about multiple body segments to provide information about physiological angles of various joints. Some studies have also examined the correlation between linear acceleration and GRF with varying degrees of agreement [24-28]. Various techniques ranging from regression modeling to developing machine learning algorithms have been applied, though often using variables that may be difficult to capture on-field, such as step count and speed of action. To develop models that can be used to track events on-field, one might focus on factors that can be obtained from IMU data, and perhaps combine them with variables measured prior to testing (i.e., weight, height, etc.). In addition to GRF, knee moments are also measurements of interest. For example, many actions that can cause non-contact ACL injuries are those in which a change of direction or sudden deceleration occurs thereby applying significant orthogonal moments to the knee in the sagittal, coronal and/or transverse planes; forces in such cases may be less important than certain combinations of moments experienced by the knee [29-31]. Few studies have attempted to correlate IMU readings with knee moments; those that have primarily focused on gyroscope data

and single variable linear modeling [31, 32]. However, a multivariable model may be needed to determine knee moments more accurately.

So, the purpose of this study was to develop multivariate models using data that are available from two wearable IMU sensors, one located above and the other below the knee, in order to predict GRF and knee moments in cadaveric specimens. The rationale for using whole knees *in vitro* was that they allow us to focus on developing models to estimate impulsive forces and moments using IMUs under ideal conditions - without the inevitable soft tissue movement artefact present *in vivo* - in order to determine whether we can classify loading cycles as potentially injurious (should they be repeated enough times to cause fatigue failure of the ACL) or non-injurious. This advance, in turn, could encourage athletes, coaches, and trainers to make changes in athletic training loads in order to permit adequate rest and recovery; they could also adjust a training regimen to prevent an ACL rupture from occurring due to possible overuse.

4.3 Methods

4.3.1 Specimens, Instrumentation, & Testing Procedures

Sixteen cadaveric knee specimens were used to develop and test each constructed multivariate model (Table 4-1). Each specimen was cut to a standard length of 20 cm, dissected of tissue while leaving the ligamentous capsule and key tendons intact and then potted in polymethylmethacrylate cylinders. Prepped specimens were mounted in a custom-built and validated testing apparatus designed to simulate a one-legged landing in the presence of simulated trans-knee muscle forces (Figure 2-1) [33, 34]. Specimens were instrumented with two wearable IMUs (APDM Opal, APDM Wearable Technologies, Portland, OR), one rigidly

attached to the medial aspect of the mid-tibia and the other to the lateral aspect of the mid-femur using a combination of Coban^{TM} and elastic ties. Two 6-axis load cells (MC3A-1000, AMTI, Watertown, MA) were used to measure action and reaction forces and moments applied to the knee. A Certus optoelectronic tracking system (Optotrak Certus; Northern Digital Inc, Waterloo, Ontario, Canada), which served as the motion capture system, was used to measure knee kinematics, and to determine the moment arms for individual knee specimens about each orthogonal axis. For the flexion moment, the moment arm was the distance from the lateral epicondyle to the tibial load cell; for the abduction moment it was the distance between the medial and lateral epicondyles, while for the rotation moment it was directly measured by the tibial load cell. All models that we developed were based on the data of the Certus/load cell system (CLS). The CLS sampling rate was 2 kHz while that of the IMUs was 200 Hz.

Table 4-1 | Specimen Demographics. Total number of testing trials denotes how many trials the specimen was able to undergo before failure or completion of 100-cycle testing occurred. Trials analyzed are the number of trials where proper testing was performed; these are the trials that were used in model development/testing. Specimens denoted with "P" are paired specimen; total testing trials and trials analyzed are the sum of the pair's testing sessions.

Demographics of the Specimens Used in Model Training					
Specimen ID	**Sex**	**Age**	**Mass (kg)**	**Total Testing Trials**	**Trials Analyzed**
P1	M	33	72.6	216	200
P2	M	25	68.9	118	200
P3*	M	32	64.4	136	119
P4	M	19	71.7	226	200
P5	M	20	69.9	214	200
P6	M	25	80.3	221	100
S1	M	39	60.8	98	88
S2	M	37	77.1	110	100
S3	M	38	69.9	126	96
S4	M	33	80.3	120	100
S5	M	15	68.9	105	99
S6	F	25	86.2	105	100
S7	F	39	54.4	105	100
Demographics of the Specimens Used in Model Testing					
Specimen ID	**Sex**	**Age**	**Mass (kg)**	**Total Testing Trials**	**Trials Analyzed**
T1	M	23	72.6	105	100
T2	M	23	72.6	108	100
T3	F	26	68.9	105	96

*. Specimens that experienced a failure before the completion of 100-cycle testing

After each specimen was positioned, the IMU sensors were calibrated and initialized through the predefined calibration conditions used by the Moveo Mobility software developed by APDM, after which, the sensors continuously recorded data until testing concluded. The quadriceps, hamstring, and gastrocnemius muscles were pre-tensioned to 180 N, 70 N and 70 N, respectively (mimicking real-world values), the initial knee flexion angle adjusted to 15 degrees, and the quadriceps tendon was clamped securely in place with mechanical grips cooled by liquid nitrogen. This last step was repeated every 25 cycles to prevent tendon thawing and slippage

from the clamp; it was only during these instances that corrections of the knee angle and/or muscle tension occurred.

Landing force magnitude was fine-tuned by adjusting drop height/weight to achieve the desired sub-maximal impulsive knee loading, ranging from one to four BW applied to the tibia. A combination of paired and single knee specimens was used. Paired knee specimens had one side (either left or right) tested under lower BW conditions (1-2x BW) and the other at higher (3x+ BW), whereas single knee specimens were all tested under high sub-maximal loading conditions (3x-4x BW). Impacts were initiated by releasing a weight, guided via two parallel linear bearings, to impact the load cell at the distal end of the tibia (Figure 2-1). Based on previous studies, at least five preconditioning trials were conducted before the activation of the tibial torsional device. This allowed for any test rig adjustments and for potential uncrimping of ligament collagen fibers [33, 34].

After the preconditioning trials the tibial torsional device was then activated allowing for some of the impact force to be converted to an internal tibial torque, as can happen in a live subject when the GRF causes internal tibial rotation at the knee [33, 34] (Figure 2-1). Each specimen was then subjected to up to 100 simulated landing trials or until knee failure occurred, the latter clinically defined as anterior tibial translation (aTT) exceeding 3 mm. Peak impact force was typically reached at around 70 ms, so each trial recording consisted of 200 ms of data to ensure the peak was captured. It was assumed that the maximum vertical force, as measured by the load cells, and the maximum vertical linear acceleration, as measured by the tibial IMUs, occurred synchronously. This assumption was made based on previous studies that showed strong

correlation between GRF and linear acceleration [24]. Because both training and testing the validity of our models were needed, we separated our specimen pool to a training set (use in the development of our model; N=13) and a testing set (used in the testing of model validity; N=3).

4.3.2 Data Processing

Processing began with the removal of trials in which muscle forces and/or drop height or weight needed adjustment, where some component of the testing rig broke or malfunctioned, or where the CLS showed missing marker data (either "real" or "imaginary"). IMU data were then interpolated using the spline algorithm to match the frame rate of the sensors to the CLS. A fourth order, zero-lag, low pass Butterworth filter was applied to the data from both the tibial and femoral IMUs (linear acceleration and angular velocity). Only the training set was utilized in determining the optimal frequencies. Optimum cutoff frequency for the Butterworth low-pass digital filter was obtained by applying Winter's method as used in previous work [35, 36]. Average optimal cutoff frequencies were determined as: 9 Hz for the accelerometer (X = 9 Hz; Y= 9 Hz; Z= 9 Hz); 8 Hz for the gyroscope (X=8 Hz; Y= 8 Hz; Z= 8Hz) and were the same for the tibial and femoral IMU.

4.3.3 Model Development

We used the "Regression Learning" app developed by MATLAB to apply several types of machine learning algorithms to each metric (tibial or femoral forces; knee moments). To address the potential of overfitting and bias, a 5-fold cross-validation was performed during each model's construction; this method is like the 'leave-one-out' method but was applied five times on smaller subsets of the training set. Various adjustable modeling parameters (i.e., basis function, kernel function, isotropic nature of kernel function, number of layers, and activation function) for

each model were tuned to obtain models with the lowest root mean square error (RMSE) values with respect to the training set. Following that, a Bayesian optimization with an "expected improvement per second" acquisition function was applied for 30 iterations to tune numerical parameters (i.e., kernel scale, sigma value, epsilon value, box constraint, and layer size). We determined the best model based on two criteria: NRMSE and LoAs for the testing set. NRMSE was constructed as the RMSE value between predicted and measured values over the interquartile range of the measured value; these served as a measure of a model's accuracy as used elsewhere [27]. Based on the work of others NRMSE was limited to 20%, so only models that exhibited values at or below 20% were deemed accurate enough for further consideration [27]. LoAs were the measure of a model's reliability, and while often established *a priori* based on clinical/researcher specifications, in this study we utilized the 95% CI of the residuals. Hence the smaller the 95% CI, the more reliable the model. The model with an acceptable level of accuracy and smallest LoAs was then determined as the best fitting model. To further our analysis, BA plots were developed for descriptive analysis purposes to illustrate trends or bias that may be present. We recognize that our dependency on machine learning algorithms may preclude the development of a prediction equation (i.e., a simple model with defined variables and coefficients) and result in the "black-box" phenomenon. So, F-test graphs were used to determine the significance of each parameter to metric prediction.

A confusion matrix was constructed to determine the specificity, precision, recall, and accuracy in correctly classifying 'potentially injurious' from and 'non-injurious' loading cycles. Two matrixes were developed to compare the measured values (true class) to the predicted values (estimated class). The first compared events classified based on the vertical femoral force (Low

Risk: <3x BW; High Risk: >3x BW). The second compared events classified based on the rotation moment (Low Risk: <45.5 Nm; High Risk: >45.5 Nm). These values were determined based on previous studies examining non-contact ACL injuries [7, 37].

4.4 Results

Application of the "Regression Learning" app to each of the metrics generated a unique machine learning algorithm. These differed by: type (gaussian process regression (GPR), neural network, or support vector machine (SVM)); basis function for GPR only (zero, constant, or linear); kernel function for GPR or SVM (rational quadratic, exponential; isotropic or non-isotropic); or number of layers for neural network only (single layer, bilayer) (Table 4-2). A Gaussian process regression (GPR) model had the lowest RSME for both the vertical and resultant tibial force and flexion and abduction moment, though each had different basis and kernel functions (Table 4-2). For the vertical tibial force, a GPR with constant basis function and rational quadratic kernel function was best, whereas a GPR with zero basis function and exponential kernel function was best for resultant tibial force. A GPR with a quadratic kernel and a constant basis function was also best for abduction moment predictions, though here the kernel was non-isotropic (i.e., not Euclidean distance dependent). The optimal model to predict knee flexion moment was a GPR with a non-isotropic 3/2 Matérn kernel function and zero-basis function.

Feed forward neural networks were the best model type to predict both the vertical and resultant femoral forces, though with differing layer structures (Table 4-2). Vertical femoral force was best modeled through a single hidden layer, narrow neural network. Resultant femoral force was best modeled through a bilayer neural network that uses two hidden layers instead of one. In both cases, layer size was set to 10 nodes. Both neural networks' activation function was a rectified

linear unit (ReLU). The rotation moment was best predicted using a support vector machine algorithm (SVM), more specifically a non-linear SVM regression with a gaussian kernel function (Table 4-2).

Table 4-2 | Complete overview of the best performing models for each of the seven metrics. GPR model type is a gaussian process regression model, while SVM indicates a support vector machine learning algorithm. The activation type ReLU is the rectified linear unit.

Machine Learning Models

Model	Type	Kernel Function	Layers (Size)	Basis Function	Activation
Vertical Tibial Force	GPR	Isotropic Rational Quadratic	-	Constant	-
Vertical Femoral Force	Narrow Neural Network	-	1 (10)	-	ReLU
Resultant Tibia Force	GPR	Isotropic Exponential	-	Zero	-
Resultant Femoral Force	Bi-layered Neural Network	-	2 (10)	-	ReLU
Flexion Moment	GPR	Non-isotropic 3/2 Matern	-	Zero	-
Abduction Moment	GPR	Non-isotropic Rational Quadratic	-	Constant	-
Rotation Moment	SVM	Gaussian	-	-	-

All force models developed exhibited a very strong level of fit (R^2 range: 0.95 to 0.98) and had NRMSEs below our pre-established conditions, with the resultant femoral force model having the lowest of these values (Table 4-3; Figure 4-1). There were no discernable trends as force increased in magnitude, illustrating that at any given measured value, a predicted value has consistent variability (Table 4-2). The resultant force model tended to overestimate force; this

was evidenced by the upper bound condition being larger than the lower bound (Table 4-2). Vertical force models showed near equal tendencies for overestimations as underestimations. LoAs for the tibial models fell within ±15% while the femoral force models exceeded 20% (Table 4-3).

Table 4-3 | Results of model application for both training and testing sets across all seven metrics. RMSE, mean square error (MSE), mean absolute error (MAE), MAPE, NRMSE, LoAs are presented

Training Results (5-fold Cross-Validation)

Model	RMSE	R-Squared	MSE	MAE
Vertical Tibial Force	26.2 N	0.99	687	14.8 N
Vertical Femoral Force	102 N	0.97	10505	70.9 N
Resultant Tibial Force	28.2 N	0.98	796	13.9 N
Resultant Femoral Force	80.4 N	0.98	6468	56.8 N
Flexion Moment	1.51 Nm	0.99	2.28	0.85 Nm
Abduction Moment	1.12 Nm	0.98	1.25	0.63 Nm
Rotational Moment	1.48 Nm	0.97	2.12	0.84 Nm

Testing Results

Model	RMSE	R-Squared	MAE	MAPE	NRMSE	LoA
Vertical Tibial Force	37.9 N	0.97	29.4 N	4.42 %	11.6 %	(-70.6, 77.7) N
Vertical Femoral Force	202 N	0.95	159 N	9.14 %	12.4 %	(-413, 375) N
Resultant Tibial Force	49.6 N	0.97	40.4 N	5.34 %	13.2 %	(-53.9, 109) N
Resultant Femoral Force	145 N	0.98	111 N	6.18 %	8.93 %	(-171, 321) N
Flexion Moment	1.99 Nm	0.97	1.55 Nm	3.97 %	17.2 %	(-4.08, 3.69) Nm
Abduction Moment	0.82 Nm	0.93	0.64 Nm	6.77 %	19.9 %	(-1.41, 1.74) Nm
Rotation Moment	2.62 Nm	0.95	2.07 Nm	5.42 %	17.1 %	(-5.77, 3.61) Nm

Knee moment models all exhibited strong levels of fit (R^2 range: 0.93 to 0.97), and had NRMSE values below our pre-established condition, however, compared to the force models, the NRMSE values of the knee moment models were larger (Figure 4-1; Table 4-3). The BA plots showed varying degrees of bias and some trends. The knee flexion moment model tended to slightly underestimate the moment, and a linear slope was observed between the residuals and measured flexion moment; lower measured values tended to be overestimations, while higher values tended to be underestimations (Figure 4-2). The knee abduction moment model had an overall tendency to overestimate the value, however there was no discernable trend throughout the range of measured values; it should be noted however, that as the magnitude of the knee moment increased, variation also increased (Figure 4-2) The knee transverse plane rotation moment model tended to slightly underestimate predicted values, and a negative linear relationship between the residual and measured value was observed (Figure 4-2). The LoAs for all the moment models fell below ±20% (Table 4-3).

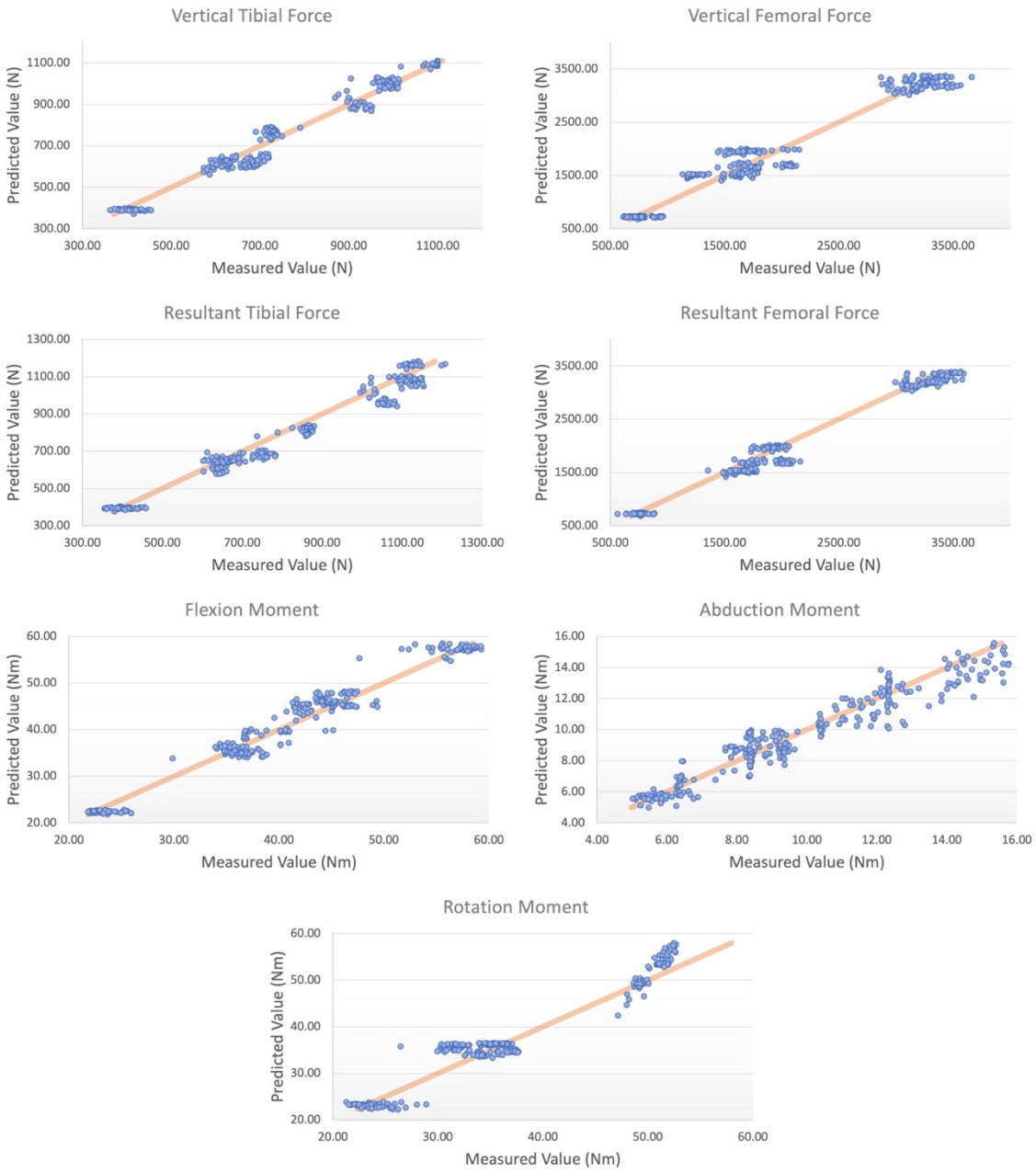

Figure 4-1 | Relationship between the predicted and measured value for each of the seven parameters

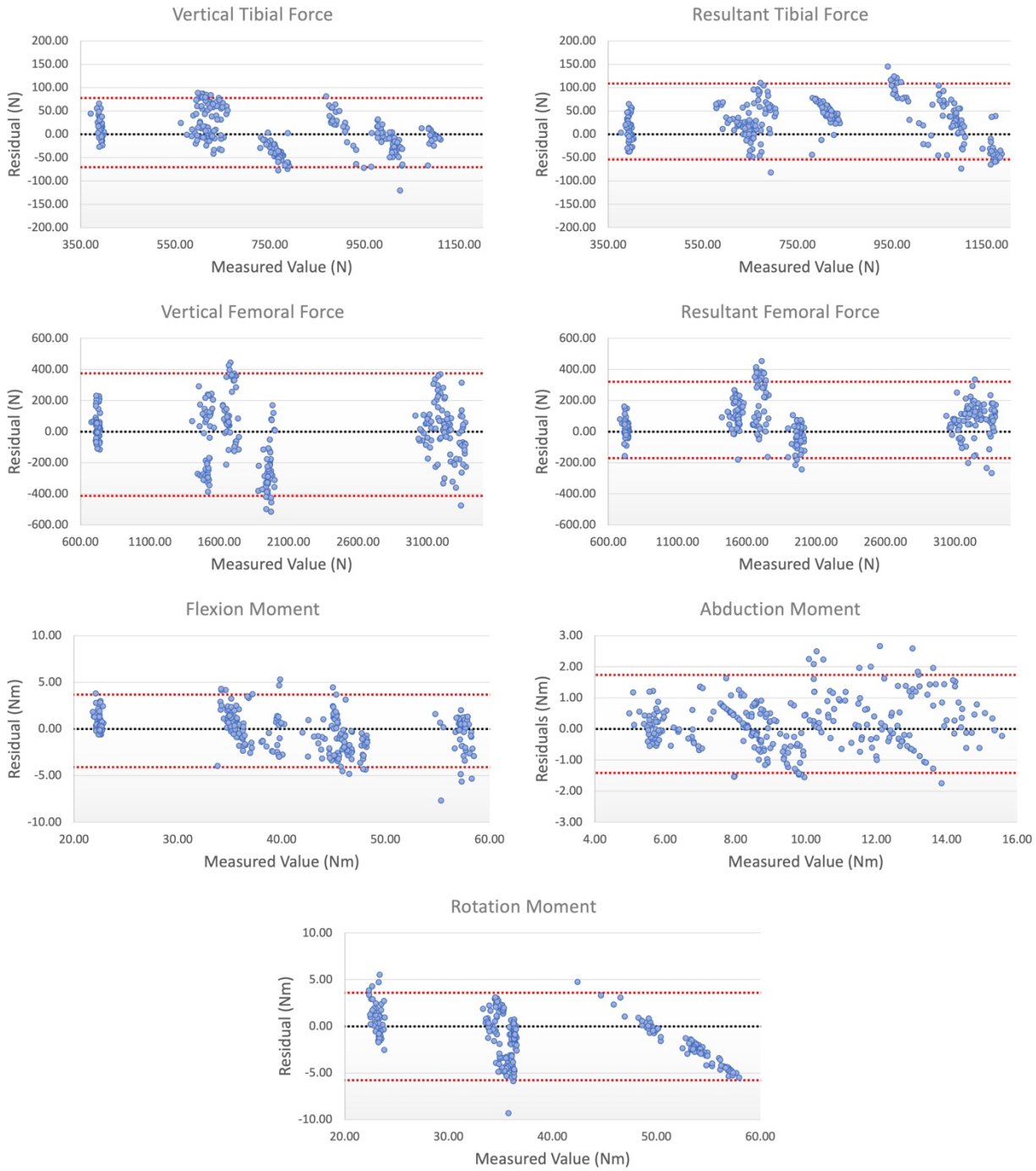

Figure 4-2 | Constructed BA-Plots for each of the parameters in where the residual difference between predicted and measured is located on the y-axis and the measured value on the x-axis. Red lines represent the LoA for the parameter, while the black line indicates the locations of the zero-difference line.

Classification of events as either “potentially injurious” or “non-injurious” was performed with a 99.7% accuracy for force classification and a 99.3% accuracy for rotation moment classification (Figure 5). In both cases, recall was 100% with no instances of false negatives. Precision for force classification was 99.0% while that of the rotation moment classification was 97.9%. Specificity for the force classification was 99.5% and 99.0% when using the rotation moment classification (Figure 4-3).

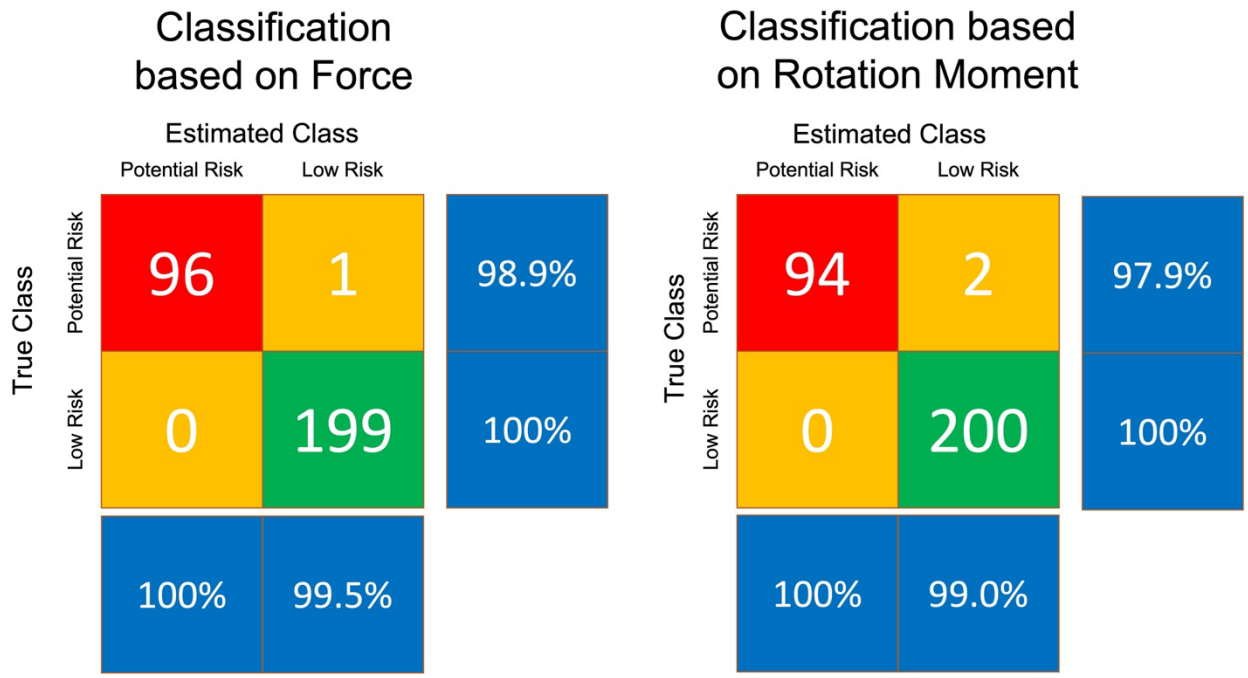

Figure 4-3 | Confusion matrixes comparing the measured classification to the estimated one. The femoral measured force (true class) is on the left and compared to the estimated femoral force (estimated class). On the right is the measured rotation moment (true class) compared to estimated rotation moment (estimated class). Column and row normalization of instances of correctly classified events are presented either to the right (column) or bottom (row) of each matrix.

4.5 Discussion: Parameter Significance & Model Performance

In the introduction we reviewed studies that utilized regression modeling techniques to establish correlations between data obtained from an IMU and metrics measured by a camera-based motion capture system. In this study, however, our goal was to develop models to predict those

metrics. To that end, we used machine learning, and considered all parameters measured by an IMU as well as mass to predict forces and knee moments during one-legged landing. We recognize that the added complexity of machine learning carries with it the benefits of increased accuracy at the cost of computational speed and potential training set dependency but given that our models are to be applied post-collection, computational speed is not a factor of concern. We applied our model to a testing set to examine their performance, thereby addressing the possibility of training set dependency. Finally, we examined whether we could accurately classify loading cycles as potentially injurious using information from a wearable sensor.

The vertical (x-axis) tibial linear acceleration was the largest contributing feature for both the tibial and femoral force models (Figure 4-3) . This was expected because of the relationship between force and acceleration. In the vertical and resultant tibia force models, other features that contributed included the flexion (z-axis) angular velocity of the tibia, x-axis femoral linear acceleration, and z-axis angular velocity of the femur. Z-axis angular velocity is correlated to ground reaction force during landing – an increase in angular velocity has been reported to decrease ground reaction force [24, 38]. As mentioned in the Results, the vertical models showed near equal tendencies for overestimations as underestimations as opposed to the resultant models which tended to overestimate the predicted value. This may be due to the more complex nature of resultant forces; while vertical force is uniaxial, resultant forces are triaxial.

Several human subjects' studies have predicted GRF from the data obtained from an IMU using different techniques and sensors [27, 39, 40]. We used cadaveric specimens to rigidly fix the sensors to the segments thereby minimizing any soft tissue artefacts that are usually present

when wearable sensors are fixed to human subjects. Even with no soft tissue, the predicted values had some error, indicating that this error may be caused by factors other than soft tissue movement. Thiel et al correlated IMU data (triaxial linear acceleration) and stride count of the subject with force using multivariable linear regression models [39]. In that study 15 subjects ran five 50 m sprints from a block start on a instrumented running track [39]. They constructed models for each individual subject, not a group, which may potentially limit the model's effectiveness for universal use on-field [39]. They reported moderate correlations between predicted and measured GRF with MAPE values ranging from 3.29% to 33.3% for each individual [39]. Although we measured tibia and femur force, not ground reaction force, in our study all force-related models had average MAPEs that were lower than these values. This may be the result of using machine learning or the mitigation of soft tissue artefact.

A study conducted by Neugebauer et al. reported strong correlations (similar to ours) in GRF (R^2=0.97) between predicted and measured values when applying mixed effect models to IMU data during gait [40]. They reported a MAPE of 5.2 ± 1.6% [40]. This study produced more accurate results than previously reported, possibly due to the added complexity of mixed effect models over generalized regression models. However, Neugebauer et al. only used linear accelerometer data; this does not consider potential angular movement contributions to forces. Angular rates were among the largest contributing factors to our models.

Lee et al. used machine learning to develop algorithms that predicted GRF as well as joint torques of the lower limbs, during normal walking using only feedforward neural networks. It was not clear whether other algorithms were considered [27]. In our study, a wide variety of learning algorithms were applied as we assumed different metrics may exhibit different

relationships with the IMU data. Lee et al. observed a very strong fit between predicted and measured GRF ($R^2 = 0.93$), which is comparable to what we found [27]. They also presented NRMSE values, normalized to the amplitude of the output for each stance phase. In the case of average GRF, a NRMSE of 6.70% was reported which is lower than any NRMSE of our study [27]. Although, the lower value could be attributable to differing normalization techniques or the lack of an exclusive testing set, they used the leave-one-out method [27]. While common in practice, the leave-one-out method may be optimistic in its accuracy when compared to the k-fold cross-validation, particularly in larger sets of data [41].

The contributions of each IMU feature to prediction differed across the moment models. Flexion moment showed the least clear divide between those of more and those of lesser importance, however the top three features were the x-axis and z-axis tibial linear accelerations and as well as the y-axis femoral linear acceleration (Figure 4-3). This shows a potentially more dependent nature of flexion moments on tibial components. Abduction moment showed a clear divide between the upper six features and the lower seven, with z-axis and x-axis tibial linear accelerations, x-axis angular velocity of both the tibia and the femur, and the z-axis and y-axis femoral linear accelerations being the largest contributing features (Figure 4-3) . Unlike most other models, the abduction moment model was equally dependent on the data from the femur IMU as the tibia IMU. The greatest divide between the importance of the features was for the rotation moment model, where y-axis angular velocity of the femur was the largest contributing feature for prediction, having an F-score nearly twice that of the next most contributing feature, mass (Figure 4-3) . This observation was counterintuitive to what we initially theorized which was that the x-axis angular velocities of both segments would be the greatest contributing

feature, however, both were ranked among the least contributing. This may be due to anatomical constraints of the knee that do not allow a significant amount of rotation.

As noted in the results, moment models exhibited larger NRMSE than those of the force models; this may be due to a larger range in force measurements, which in turn would mean an increased IQR value and ultimately a lower NRMSE value. Thus, while moment models all appear to have large NRMSE, it may be simply due to the nature of moments having smaller observed ranges. Of interest when discussing moments are the MAEs. Moment differences between predicted and measured values less than 1 Nm may effectively be negligible for clinical relevance. Studies conducted by Shin et al., Levine et al. and Kiapour et al. have tested the strain response of the anterior cruciate ligament to both abduction and rotational moments, and have reported that knee abduction moments up to 51 Nm and internal rotation moments up to 30 Nm during non-injurious landing [16, 42, 43]. High-risk injurious moments can be up to 3 times those [44, 45]. Therefore, while abduction moments illustrated the largest NRMSE, because the associated MAE was below 1 Nm, this may be clinically insignificant, as we would be able to differentiate between non-injurious and potentially “at-risk” moments.

Numerous studies have used IMU data in the development of prediction models for abduction and rotation moments, with varying success, though in most cases, low correlations were reported [27, 31, 32]. Konrath et al. created regression models using IMU data obtained from commonly performed rehabilitation activities for abduction moments. Three participants were fitted with two placed on the thigh and shank and asked to perform a stair ascent/descent as well as a sit-to-stand action. Strong, to very strong correlations between their predicted and measured values were reported which were comparable to ours [32]. They also reported very low NRSME

values, (NRMSE: SA: 0.01; SD: 0.014; StS: 0.006), though direct comparison between our NRMSE and theirs cannot be done due to our differing normalization techniques [32]. Sit-to-stand is a slower action that is not as dynamic as a jump landing and may have also contributed to the low NRMSE values. Karatsidis et al. predicted rotational moments during walking of the knee using a full body internal motion capture (IMC) method [31]. Strong correlations between their predicted and measured values were reported (R = 0.82), which were slightly lower than that observed by our study [31]. The IMC system is made up of many individual IMUs and provides information on the kinematics of the entire body, rather than the limited view of a two IMU system. However, use of an IMC system on-field may not be practical in a real-world application.

Previous studies did not present a measure of reliability. Measuring and reporting the accuracy of a model is important, but arguably of equal importance is the model's reliability of measurement. Poor reliability would indicate predications are random in nature; while some instances may be highly accurate, others could be gross over/under estimations. Using an IMU to estimate whether landing techniques could possibly be injurious requires consistency. We also note that no study applied their model to data outside of a training set. Error presented through training set predictions will be smaller than the true error, and thus may be misleading with respect to the generalizability of the model to new points. Exclusive testing data to validate a model's accuracy/reliability is needed.

In recent years, IMUs have be used as tool in risk assessment and event classification, though this has been mostly limited to lifting tasks [46, 47]. A study by Brandt et al. used a tri-axial

accelerometer and a Linear Discriminate Analysis algorithm to classify events as risky based on the Danish Working Environment Authority guidelines and reported event classification accuracy reaching 65.5% [47]. Donsis et al. also examined lifting tasks using IMUs and the NIOSH (National Institute of Occupational Safety and Health) standard to distinguish between "at risk" and "no risk" events [46]. They reported high accuracy (82.8%), sensitivity (84.8%), and specificity (80.9%) [46]. We demonstrated a 99.7% accuracy in classifying events as either "potentially injurious" or "non-injurious", which is comparable.

4.5.1 Limitations

There are several limitations in this study including the use of cadaveric specimens. If the models developed during this stage were directly applied to human subjects, there would likely be errors between predicted and measured values due to noise pollution produced by motion of the soft tissue. We also acknowledge the potential over-tuning of our models to a specific action. Due to the limitations of the rig, we were only able to simulate a one-legged jump landing. Other actions, such as cutting and sudden decelerations have also been linked to non-contact ACL injuries [4]. More types of actions would be required to develop models robust enough to predict kinematics under any on-field condition. In addition, we acknowledge that risk assessment and classification of an event as either potentially injurious or not is not based on a single variable, but instead a combination of multiple variables. While in this work we focused on correctly assessing the risk based on force and rotational moments, we did so by treating each variable separately. In reality, risk assessment could be based on the combination of the force, rotational moment, abduction moment, and the orientation of knee at the time of loading. Future testing should focus on constructing a classification system that incorporates all these variables when assessing risk.

4.6 Conclusion

For these *in vitro* studies, each model demonstrated an acceptable level of accuracy with NRMSE values less than 20% in a testing set independent of the data used for training the model. While several models exhibited some bias, most models exhibited LoAs below 20%. The femoral force models exhibited LoAs that exceeded 20%. Classification based on either force or rotation moment yielded high levels of accuracy, precision, specificity and recall force correctly classifying whether an event was potentially injurious if repeated a sufficient number of times to cause ligament fatigue failure. Future studies should examine whether such models can be applied to *in vivo* movement data that will inevitably include unavoidable soft tissue movement artefacts.

Acknowledgements

This material is based upon work supported by the National Science Foundation under grant no 2003434 and the National Institutes of Health under award number AR054821. The authors wish to thank Dr. Melanie Beaulieu for her assistance with data and Dr. Samir Rawashdeh for his assistance with the machine learning algorithms.

Conflicts of interest: the authors declare no conflict of interest

4.7 References

[1] W. Alghamdi *et al.*, "Prevalence of Cruciate Logaments Injury among Physical Education Students of Umm Al-Qura University and the Relation betwen the Dominant Body Side and Ligament Injury Side in Non-Contact Injury Type," *American Journal of Medicine and Medical Sciences,* vol. 7, no. 1, pp. 14-19, 2017.

[2] I. O. Saeed, "MRI Evaluation for Post-Traumatic Knee Joint INjuries," *Journal of Nursing and Health Science,* vol. 7, no. 2, pp. 48-51, 2018.

[3] T. E. Hewett, K. R. Ford, and G. D. Myer, "Anterior cruciate ligament injuries in female athletes: Part 2, a meta-analysis of neuromuscular interventions aimed at injury prevention," *Am J Sports Med,* vol. 34, no. 3, pp. 490-8, Mar 2006, doi: 10.1177/0363546505282619.

[4] T. E. Hewett, G. D. Myer, and K. R. Ford, "Anterior cruciate ligament injuries in female athletes: Part 1, mechanisms and risk factors," *Am J Sports Med,* vol. 34, no. 2, pp. 299-311, Feb 2006, doi: 10.1177/0363546505284183.

[5] G. D. Myer, M. V. Paterno, K. R. Ford, C. E. Quatman, and T. E. Hewett, "Rehabilitation after anterior cruciate ligament reconstruction: criteria-based progression through the return-to-sport phase," *J Orthop Sports Phys Ther,* vol. 36, no. 6, pp. 385-402, Jun 2006, doi: 10.2519/jospt.2006.2222.

[6] M. V. Paterno *et al.*, "Biomechanical measures during landing and postural stability predict second anterior cruciate ligament injury after anterior cruciate ligament reconstruction and return to sport," *Am J Sports Med,* vol. 38, no. 10, pp. 1968-78, Oct 2010, doi: 10.1177/0363546510376053.

[7] E. M. Wojtys, M. L. Beaulieu, and J. A. Ashton-Miller, "New perspectives on ACL injury: On the role of repetitive sub-maximal knee loading in causing ACL fatigue failure," *J Orthop Res,* vol. 34, no. 12, pp. 2059-2068, Dec 2016, doi: 10.1002/jor.23441.

[8] J. L. Zitnay *et al.*, "Accumulation of collagen molecular unfolding is the mechanism of cyclic fatigue damage and failure in collagenous tissues," (in eng), *Sci Adv,* vol. 6, no. 35, p. eaba2795, Aug 2020, doi: 10.1126/sciadv.aba2795.

[9] J. Kim *et al.*, "Anterior cruciate ligament microfatigue damage detected by collagen autofluorescence in situ," (in eng), *J Exp Orthop,* vol. 9, no. 1, p. 74, Jul 30 2022, doi: 10.1186/s40634-022-00507-6.

[10] K. H. Putera *et al.*, "Fatigue-driven compliance increase and collagen unravelling in mechanically tested anterior cruciate ligament," (in eng), *Commun Biol,* vol. 6, no. 1, p. 564, May 26 2023, doi: 10.1038/s42003-023-04948-2.

[11] L. Y. Griffin *et al.*, "Noncontact anterior cruciate ligament injuries: risk factors and prevention strategies," (in eng), *J Am Acad Orthop Surg,* vol. 8, no. 3, pp. 141-50, 2000 May-Jun 2000, doi: 10.5435/00124635-200005000-00001.

[12] O. E. Olsen, G. Myklebust, L. Engebretsen, and R. Bahr, "Injury mechanisms for anterior cruciate ligament injuries in team handball: a systematic video analysis," (in eng), *Am J Sports Med,* vol. 32, no. 4, pp. 1002-12, Jun 2004, doi: 10.1177/0363546503261724.

[13] J. M. Hollis, S. Takai, D. J. Adams, S. Horibe, and S. L. Woo, "The effects of knee motion and external loading on the length of the anterior cruciate ligament (ACL): a kinematic study," (in eng), *J Biomech Eng,* vol. 113, no. 2, pp. 208-14, May 1991, doi: 10.1115/1.2891236.

[14] K. L. Markolf, D. M. Burchfield, M. M. Shapiro, M. F. Shepard, G. A. Finerman, and J. L. Slauterbeck, "Combined knee loading states that generate high anterior cruciate ligament forces," (in eng), *J Orthop Res,* vol. 13, no. 6, pp. 930-5, Nov 1995, doi: 10.1002/jor.1100130618.

[15] B. Yu and W. E. Garrett, "Mechanisms of non-contact ACL injuries," (in eng), *Br J Sports Med,* vol. 41 Suppl 1, pp. i47-51, Aug 2007, doi: 10.1136/bjsm.2007.037192.

[16] C. S. Shin, A. M. Chaudhari, and T. P. Andriacchi, "Valgus plus internal rotation moments increase anterior cruciate ligament strain more than either alone," (in eng), *Med Sci Sports Exerc,* vol. 43, no. 8, pp. 1484-91, Aug 2011, doi: 10.1249/MSS.0b013e31820f8395.

[17] C. J. Anderson, C. G. Ziegler, C. A. Wijdicks, L. Engebretsen, and R. F. LaPrade, "Arthroscopically pertinent anatomy of the anterolateral and posteromedial bundles of the posterior cruciate ligament," (in eng), *J Bone Joint Surg Am,* vol. 94, no. 21, pp. 1936-45, Nov 2012, doi: 10.2106/JBJS.K.01710.

[18] M. Arif and A. Kattan, "Physical Activities Monitoring Using Wearable Acceleration Sensors Attached to the Body," (in eng), *PLoS One,* vol. 10, no. 7, p. e0130851, 2015, doi: 10.1371/journal.pone.0130851.

[19] A. G. Cutti, A. Ferrari, P. Garofalo, M. Raggi, and A. Cappello, "'Outwalk': a protocol for clinical gait analysis based on inertial and magnetic sensors," (in eng), *Med Biol Eng Comput,* vol. 48, no. 1, pp. 17-25, Jan 2010, doi: 10.1007/s11517-009-0545-x.

[20] J. Favre, X. Crevoisier, B. M. Jolles, and K. Aminian, "Evaluation of a mixed approach combining stationary and wearable systems to monitor gait over long distance," (in eng), *J Biomech,* vol. 43, no. 11, pp. 2196-202, Aug 2010, doi: 10.1016/j.jbiomech.2010.03.041.

[21] A. Ferrari *et al.*, "First in vivo assessment of "Outwalk": a novel protocol for clinical gait analysis based on inertial and magnetic sensors," (in eng), *Med Biol Eng Comput,* vol. 48, no. 1, pp. 1-15, Jan 2010, doi: 10.1007/s11517-009-0544-y.

[22] J. F. Lin and D. Kulić, "Human pose recovery using wireless inertial measurement units," (in eng), *Physiol Meas,* vol. 33, no. 12, pp. 2099-115, Dec 2012, doi: 10.1088/0967-3334/33/12/2099.

[23] P. Picerno, A. Cereatti, and A. Cappozzo, "Joint kinematics estimate using wearable inertial and magnetic sensing modules," (in eng), *Gait Posture,* vol. 28, no. 4, pp. 588-95, Nov 2008, doi: 10.1016/j.gaitpost.2008.04.003.

[24] N. G. Elvin, A. A. Elvin, and S. P. Arnoczky, "Correlation between ground reaction force and tibial acceleration in vertical jumping," (in eng), *J Appl Biomech,* vol. 23, no. 3, pp. 180-9, Aug 2007, doi: 10.1123/jab.23.3.180.

[25] R. D. Gurchiek, R. S. McGinnis, A. R. Needle, J. M. McBride, and H. van Werkhoven, "The use of a single inertial sensor to estimate 3-dimensional ground reaction force during accelerative running tasks," (in eng), *J Biomech,* vol. 61, pp. 263-268, 08 2017, doi: 10.1016/j.jbiomech.2017.07.035.

[26] U. Meyer *et al.*, "Validation of two accelerometers to determine mechanical loading of physical activities in children," (in eng), *J Sports Sci,* vol. 33, no. 16, pp. 1702-9, 2015, doi: 10.1080/02640414.2015.1004638.

[27] M. Lee and S. Park, "Estimation of Three-Dimensional Lower Limb Kinetics Data during Walking Using Machine Learning from a Single IMU Attached to the Sacrum," (in eng), *Sensors (Basel),* vol. 20, no. 21, Nov 04 2020, doi: 10.3390/s20216277.

[28] R. S. Alcantara, W. B. Edwards, G. Millet, and M. Grabowski, "Predicting continuous ground reaction forces from accelerometers during uphill and downhill running: A recurrent neural network solution," *bioRxiv,* 2021.

[29] S. G. McLean, S. W. Lipfert, and A. J. van den Bogert, "Effect of gender and defensive opponent on the biomechanics of sidestep cutting," (in eng), *Med Sci Sports Exerc,* vol. 36, no. 6, pp. 1008-16, Jun 2004, doi: 10.1249/01.mss.0000128180.51443.83.

[30] S. M. Sigward and C. M. Powers, "Loading characteristics of females exhibiting excessive valgus moments during cutting," (in eng), *Clin Biomech (Bristol, Avon),* vol. 22, no. 7, pp. 827-33, Aug 2007, doi: 10.1016/j.clinbiomech.2007.04.003.

[31] A. Karatsidis *et al.*, "Predicting kinetics using musculoskeletal modeling and inertial motion capture,"

[32] J. M. Konrath, A. Karatsidis, H. M. Schepers, G. Bellusci, M. de Zee, and M. S. Andersen, "Estimation of the Knee Adduction Moment and Joint Contact Force during Daily Living Activities Using Inertial Motion Capture," (in eng), *Sensors (Basel),* vol. 19, no. 7, Apr 2019, doi: 10.3390/s19071681.

[33] D. B. Lipps, E. M. Wojtys, and J. A. Ashton-Miller, "Anterior cruciate ligament fatigue failures in knees subjected to repeated simulated pivot landings," (in eng), *Am J Sports Med,* vol. 41, no. 5, pp. 1058-66, May 2013, doi: 10.1177/0363546513477836.

[34] D. B. Lipps, Y. K. Oh, J. A. Ashton-Miller, and E. M. Wojtys, "Effect of increased quadriceps tensile stiffness on peak anterior cruciate ligament strain during a simulated

pivot landing," (in eng), *J Orthop Res,* vol. 32, no. 3, pp. 423-30, Mar 2014, doi: 10.1002/jor.22531.

[35] B. Yu, D. Gabriel, L. Noble, and K.-N. An, "Estimate of the Optimum Cutoff Frequency for the Butterworth Low-Pass Digital Filter," *Journal of Applied Biomechanics,* vol. 15, pp. 319-329, 1999 doi: 10.1123/jab.15.3.318.

[36] M. Ajdaroski, J. A. Ashton-Miller, S. Y. Baek, P. M. Shahshahani, and A. Esquivel, "Testing a Quaternion Conversion Method to Determine Human 3D Tibiofemoral Angles During an in Vitro Simulated Jump Landing," (in eng), *J Biomech Eng,* Sep 22 2021, doi: 10.1115/1.4052496.

[37] N. A. Bates, N. D. Schilaty, C. V. Nagelli, A. J. Krych, and T. E. Hewett, "Multiplanar Loading of the Knee and Its Influence on Anterior Cruciate Ligament and Medial Collateral Ligament Strain During Simulated Landings and Noncontact Tears," (in eng), *Am J Sports Med,* vol. 47, no. 8, pp. 1844-1853, Jul 2019, doi: 10.1177/0363546519850165.

[38] B. Yu, C. F. Lin, and W. E. Garrett, "Lower extremity biomechanics during the landing of a stop-jump task," (in eng), *Clin Biomech (Bristol, Avon),* vol. 21, no. 3, pp. 297-305, Mar 2006, doi: 10.1016/j.clinbiomech.2005.11.003.

[39] D. V. Thiel *et al.*, "Predicting Ground Reaction Forces in Sprint Running Using a Shank Mounted Inertial Measurement Unit," *Proceedings,* vol. 2, no. 6, p. 199, 2018.

[40] J. M. Neugebauer, D. A. Hawkins, and L. Beckett, "Estimating youth locomotion ground reaction forces using an accelerometer-based activity monitor," (in eng), *PLoS One,* vol. 7, no. 10, p. e48182, 2012, doi: 10.1371/journal.pone.0048182.

[41] T.-T. Wong, "Performance Evaluation of Classification Algorithms by K-Fold and Leave-One-out Cross Validation," *Pattern Recogn.,* vol. 48, no. 9, pp. 2839–2846 , numpages = 8, sep 2015, doi: 10.1016/j.patcog.2015.03.009.

[42] J. W. Levine *et al.*, "Clinically relevant injury patterns after an anterior cruciate ligament injury provide insight into injury mechanisms," (in eng), *Am J Sports Med,* vol. 41, no. 2, pp. 385-95, Feb 2013, doi: 10.1177/0363546512465167.

[43] A. M. Kiapour *et al.*, "Strain Response of the Anterior Cruciate Ligament to Uniplanar and Multiplanar Loads During Simulated Landings: Implications for Injury Mechanism," (in eng), *Am J Sports Med,* vol. 44, no. 8, pp. 2087-96, Aug 2016, doi: 10.1177/0363546516640499.

[44] T. F. Besier, D. G. Lloyd, J. L. Cochrane, and T. R. Ackland, "External loading of the knee joint during running and cutting maneuvers," (in eng), *Med Sci Sports Exerc,* vol. 33, no. 7, pp. 1168-75, Jul 2001, doi: 10.1097/00005768-200107000-00014.

[45] S. G. McLean, X. Huang, A. Su, and A. J. Van Den Bogert, "Sagittal plane biomechanics cannot injure the ACL during sidestep cutting," (in eng), *Clin Biomech (Bristol, Avon),* vol. 19, no. 8, pp. 828-38, Oct 2004, doi: 10.1016/j.clinbiomech.2004.06.006.

[46] L. Donisi *et al.*, "A Logistic Regression Model for Biomechanical Risk Classification in Lifting Tasks," (in eng), *Diagnostics (Basel),* vol. 12, no. 11, Oct 29 2022, doi: 10.3390/diagnostics12112624.

[47] M. Brandt *et al.*, "Accuracy of identification of low or high risk lifting during standardised lifting situations," (in eng), *Ergonomics,* vol. 61, no. 5, pp. 710-719, May 2018, doi: 10.1080/00140139.2017.1408857.

Chapter 5: Can Wearable Sensors Identify Potentially Injurious Loading of the ACL?

This chapter was submitted for publication in the ASME Journal of Biomechanical Engineering

Mirel Ajdaroski, Ruchika Tadakala, Regina Arriola, Amanda O. Esquivel

5.1 Abstract

This research explored whether IMUs could accurately and reliably estimate metrics related to non-contact ACL injuries in humans. These included GRF, KAM, and KRM. Nine current or former athletes were recruited to perform nine sport-related movements. Four IMUs were placed on the shank and thigh of each leg. A motion capture system with a 46 retro-reflective marker schema and force plates was used to obtain measured values of each metric. Machine learning algorithms were used to analyze the IMU and subject-specific data and generated estimates for GRF, KAM, and KRM. These estimates were compared to the motion capture system's measurements and evaluated for accuracy (normalized root mean square), and reliability (Bland-Altman limits of agreement). A confusion matrix was also constructed to examine if these estimates could be used for distinguishing between low-risk and potentially injurious events. Results showed high classification accuracy, precision, specificity, and sensitivity, but poor reliability for KAM and KRM estimates. Nonetheless, the high classification accuracy and specificity may mean that IMUs can distinguish between low-risk and potentially injurious events with few false positives or negatives.

5.2 Introduction

Despite prevention efforts, the non-contact ACL injury rate continues to increase [1, 2]. It has been estimated that each year approximately one ACL tear occurs in every 50-70 female athletes [3]. The incidence of ACL tear in female high school and collegiate athletes is 2-6 times higher than in male athletes in sports involving abrupt stops, turns, and jumps [1, 2, 4] While many risk factors have been identified, sex differences in the kinematics and kinetics of the lower extremity during jump and squat tasks have been noted [5-10]. Thus, the ability to track and identify any high-risk loading conditions to the ACL could be clinically important.

ACL injury mechanisms have been categorized as 1) contact (30% of all cases) and 2) non-contact (70% of all cases) [11-14]. Non-contact ACL injuries involves the internal generation of forces and moments in response to ground reaction force and moments at the foot at the time of impact. It is not clear whether these non-contact injuries tend to be acute or fatigue failure. However, in a controlled laboratory environment, ligamentous structures have been shown to be vulnerable to fatigue failure under cyclic loading conditions [15]. Submaximal repetitive loading is known to cause cumulative micro-damage in soft tissues, most notably in the elbow [15-17]. Recognition of this injury mechanism has led to the formation of rules regarding pitch counts in youth baseball to decrease these injuries in young athletes. Recently, laboratory research has indicated that some noncontact ACL injuries that occur in female athletes may be overuse injuries due to repeated strain on the ACL [18]. A simulated jump landing at 3-4 times body weight was applied to cadaveric knees while the knee was in 15° flexion with internal tibial torque. After 100 of these severe loading cycles, mechanical failure occurred in many of the knees, providing the first evidence that the ACL is indeed susceptible to fatigue failure [19-21].

If some of these injuries are due to cyclic loading, tracking loading conditions to prevent injury may be possible. And while ground reaction force has been linked to non-contact ACL injuries, KAM and KRM have also been correlated to these injuries. [22-25].

Lower limb joint kinetics have traditionally been examined in laboratory settings using camera-based MCS and force plates. However, this system is impractical for regular usage on the field. In recent years the development of wearable sensors has emerged as an alternative to motion capture and has been employed in various applications such as gait analysis and rehabilitation assistance [26-37]. One type of sensor is the IMU, which contains accelerometers, rate gyroscopes, and magnetic field sensors which can provide information about the acceleration, velocity, and position of one body segment with respect to another and has been used to estimate various limb angles, joint moments, and GRF [27, 28, 38-46]. Wearable IMUs provide the opportunity for non-obtrusive activity monitoring in a real-world setting, however, estimates for joint moments and GRF require post-collection equations. Being able to estimate GRF and knee moments (particularly KAM and KRM) could potentially lead to the identification of high-risk loading cycles to the ACL and thus, could allow athletes, coaches, and trainers to make changes that permit for rest and recovery before a rupture can occur.

We previously developed algorithms that accurately and consistently estimated leg forces and knee moments during a simulated one-legged landing using cadaveric specimens [47]. However, due to the omission of soft tissue and the limitations of our testing rig, we theorized that these cadaveric models may not have the same level of accuracy and reliability when applied to human subjects. The present study was designed with three goals in mind: 1) test the accuracy and

reliability of the previously developed models when applied to human subjects; 2) modify the previously developed models and determine if accuracy and reliability are significantly improved when compared to unmodified models; 3) develop a classification system distinguishing "possible" and "low" risk event.

5.3 Methods

5.3.1 Subjects, Instrumentation, & Testing Procedures

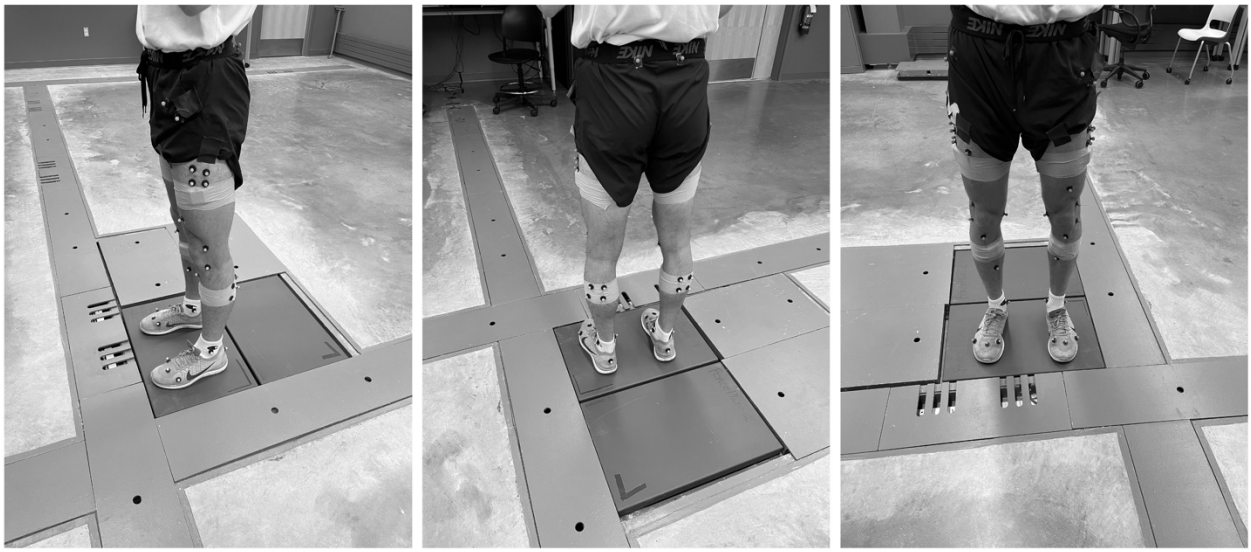

Figure 5-1 | Marker and sensor locations on participant

Before the commencement of the study, IRB approval was acquired (HUM00150719). Nine healthy volunteers (5 females, 4 males) who currently play soccer or basketball or have played in the last two years were recruited (Table 5-1). Exclusion criteria included a current lower extremity injury and BMI over 29 kg/m^2. All subjects underwent informed consent and were fitted with 46 retro-reflective spherical markers (Figure 5-1). The first 30 markers were placed based on the 30 item Rizzoli lower body protocol: (right and left) anterior and posterior superior iliac spine, greater trochanter, thigh, lateral femoral condyle, head of the fibula, anterior tibial

tuberosity, shin, lateral malleolus, calcaneus, the fifth metatarsal, first metatarsal, medial femoral epicondyle, medial malleolus, and second metatarsal head. The remaining markers were placed in clusters of four on the lateral thigh and gastrocnemius. Motion and force data were collected using a 12-camera (200 Hz) motion capture system (Prime 13 Optitrack, Corvallis, OR) and two 2000 lbf force plates (1 kHz) (FP4060-05-PT, Bertec, Columbus, OH). APDM wearable sensors (APDM Opal^{TM}, APDM Wearable Technologies, Portland, OR) were attached to the medial aspect of the tibia and the lateral aspect of the thigh of both legs using a combination of double-sided skin tape and Coban^{TM}. Data for these sensors were collected at 200 Hz and a sync device was used to synchronize these sensors with the MCS. Height, weight, thigh circumferences and distance from the midpoint of the knee to the femoral and the tibial IMUs were recorded. Participants performed seven related movements three times: a jog with a pivot, an extension leap, a sidestep cut, a crossover cut, dominant shooting, a vertical jump onto two feet and one foot (Table 5-2). These movements were selected because they are frequently performed in sports and have been linked to non-contact ACL injury [5, 7, 8, 48-51]. To quantify possible soft tissue artifact, subjects were also asked to stand still and contract their thigh muscles while still fitted with the femoral IMUs. To validate the model modifications, our population was randomly divided into a training set (N=5) and a testing set (N=4).

Table 5-1 | Subject Demographics. Sport denotes the sport a subject participated in, with dual denoting a subject had played both soccer and basketball.

Demographics of the Subjects Used in Amendment Training				
Subject ID	Sex	Mass (kg)	Height (m)	Sport
TR1	F	79.0	1.85	Soccer
TR2	F	69.0	1.78	Basketball
TR3	F	63.2	1.63	Soccer
TR4	M	78.5	1.83	Soccer
TR5	M	70.3	1.78	Soccer
Demographics of the Subjects Used in Amendment Testing				
Specimen ID	Sex	Mass (kg)	Height (m)	Sport
TE1	F	75.4	1.75	Dual
TE2	M	74.9	1.85	Soccer
TE3	F	63.7	1.73	Basketball
TE4	M	85.8	1.83	Soccer

Table 5-2 | Action performed by subjects along with descriptions. Note: dominant shooting was only performed by individuals who have played soccer

Movement	Description
Jog with pivot	Participant jogs a few steps and pushes off dominant leg to turn body towards the opposite side.
Extension Leap	Participant pushes off dominant leg while fully extending the non-dominant leg to land on force plate more than two comfortable step lengths away.
Sidestep Cut	Subject accelerates toward the direction opposite of the planted leg
Crossover Cut	Participant crosses one leg over the planted leg and accelerates in the same direction of the push off leg
Dominant Shooting	Non-dominant foot takes a firm step onto force plate to support the dominant leg swing through a “shooting” motion. (Soccer or Dual subjects only)
Jump – Land on One Foot	Subject stands with feet together, jumps maximum height and lands on one foot.
Jump – Land on Two Feet	Subject stands with feet together, jumps and lands on two feet at maximum height, 50% of maximum and 25% of maximum.

5.3.2 Data Processing

Force plate data (forces and moments) and both the tibial and femoral IMU data (linear accelerations and angular velocities) were filtered using a fourth-order, zero-lag, low-pass Butterworth filter. Optimum cutoff frequencies for the Butterworth low-pass digital filter were obtained by applying Winter's method; this method has been used in previous work [52, 53]. Only the training set was utilized in determining the optimal frequencies (Table 5-3). It was theorized that because an individual traveling at different speed in each direction, differing filter frequencies would be needed; this method has been used in previous works [53]. A 6-degree-of-freedom kinematic model of the lower extremity was created for each participant using Visual 3D software (C-motion, Germantown, MD). A motion was quantified at the knee using a Cardan angle sequence. Maximum vertical GRF was determined from the force plates. Knee joint moments were calculated using inverse dynamics and recorded at maximum vertical GRF.

Table 5-3 | The optimal cutoff frequencies determined through the application of Winter's method, for each direction. Averages of both the right and left legs are presented. All filtering frequencies are in Hz and based on a sampling rate of 200 Hz.

Optimal Cutoff Frequencies Determined for the Force Plates and IMUs

Parameter		X	Y	Z
Force Plate	Forces	15	14	13
	Moments	11	11	17
Tibial IMU	Linear Acceleration	19	20	18
	Angular Velocity	18	18	22
Femoral IMU	Linear Acceleration	17	14	16
	Angular Velocity	17	19	15

5.3.3 Previous Model Application

Previously developed models were applied to the data using all subjects and tested for accuracy (NRMSE) and reliability (LoAs). Normalization of the RMSE was calculated by dividing the RMSE value by the IQR. Based on the work of others, NRMSE was limited to 20%, so only models that exhibited values at or below 20% were deemed accurate [43]. Reliability was judged based on the LoA range, where smaller ranges indicated greater reliability. The previously developed models were not constructed to estimate GRF directly, but instead to estimate the tibial or the femoral forces [47]. Therefore, the estimated values for both were compared to the measured GRF individually and in combination.

5.3.4 Creation and Selection of Model Modifications

We used the *Regression Learning* app developed by MATLAB to apply several types of machine learning algorithms to estimate GRF and moments; this app was used previously to develop

cadaveric-based models [47]. Features used included height, mass, thigh circumference, distance from the knee midpoint to the femoral and tibial IMUs, the linear accelerations and angular velocities due to thigh muscle contraction, and the estimated values obtained by the models previously developed or the difference between the estimated value and those measured by the MCS of this study. A 5-fold cross-validation was performed during each model's construction. Various adjustable modeling parameters (such as isotropic kernel nature, activation type, etc.) for each model were tuned based on obtaining the lowest RMSE values for the training set. Following that, a Bayesian optimization where the acquisition function was expected improvement per second for 30 iterations was applied to tune numerical parameters (kernel scale, layer size, etc.). GRF was normalized using the subject's weight while the raw values for moments were used. As previously stipulated, NRMSE was limited to 20%. If a modified model was unable to fall below this limit, then the model with the lowest NRMSE was considered the most accurate. LoAs were also used to gauge estimation reliability. F-test graphs were developed to determine the significance of each parameter to metric prediction. BA plots were created to analyze trends/biases that may be present.

5.3.5 Classification Development for At-Risk Events

Because one of the goals of our study was to distinguish between low- and high-risk events, a confusion matrix was constructed to gauge the sensitivity, specificity, and accuracy in correctly identifying a class. Events were classified based on a combination of ground reaction force (Low Risk: <3x BW; High Risk: >3x BW), abduction moments (Low Risk: <150 Nm; High Risk >150 Nm), and rotation moments (Low Risk: < 45.5 Nm; High Risk: >45.5 Nm). These values were selected based on previous studies examining non-contact ACL injuries [18, 54]. Column-

normalization of the matrix was performed to determine the class-wise precision (positive predictive values) while row-normalization was performed to determine the class-wise recalls (true positive rates). Only the most accurate and reliable models were considered during the construction of the confusion matrix as their estimates would be closest to the measured risk value.

5.4 Results

5.4.1 Cadaveric (Unmodified) Models

Application of the unmodified models resulted in negligible levels of fit (R^2 range: 0.00 to 0.01), with NRMSEs exceeding our pre-established conditions and large LoAs (Table 5-4). When estimating the force, the estimated values resulted in linear trends where lower measured forces were overestimations while those higher in magnitude were underestimations (Figure 5-2). When using the tibial or femoral unmodified models separately, there was an overall tendency for underestimation, represented by the lower bound being larger than the upper bound (Figure 5-2). When adding the estimates of both models together, the upper and lower bounds were similar in magnitude, indicating equal tendencies for over/underestimation. For both the KAM and KRM unmodified models, as the magnitude of the measured moment increased, estimated moment values decreased, leading to greater underestimations; this is represented in a downward linear trend.

Table 5-4 | Results of the unmodified model applied to human subjects. NRMSE and LoA are presented. Note, all results are based on the normalized data. Because of an inability to directly compare the force related estimates of our previous work, equations developed to estimate tibial and femoral forces were compared to the measured GRF along with various combination of the two to determine the model that best estimated GRF.

Application of Cadaveric Models to Human Subjects

Model	NRME	LoA
GRF v. Tibial Force Estimates	152 %	(-2.58, 0.32) xBW
GRF v. Femoral Force Estimates	199 %	(-3.89, 2.68) xBW
GRF v. Femoral + Tibial Estimates	193 %	(-3.23, 3.53) xBW
GRF v. Femoral – Tibial Estimates	238 %	(-4.57, 1.85) xBW
Abduction Moment	102 %	(-138, 118) Nm
Rotational Moment	133 %	(-36.8, 67.3) Nm

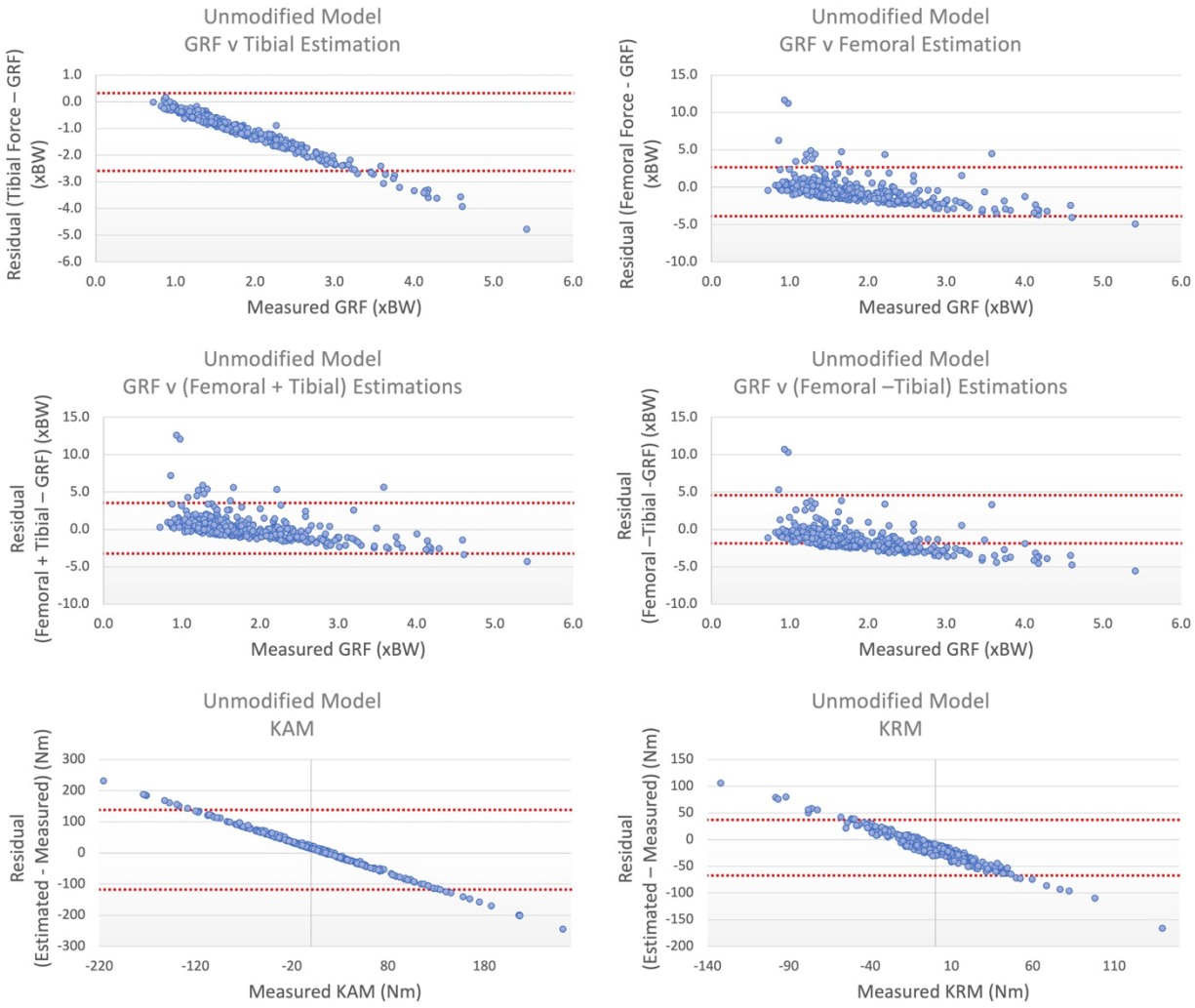

Figure 5-2 | Constructed BA-plots comparing the estimates of the unmodified models to the measured for GRF, KAM and KRM. Note: because unmodified models did not directly measure GRF, estimates using the tibial force model, femoral force model, and combinations of the two were compared to GRF

5.4.2 Modified Models

The *Regression Learning* app's application to each feature generated a unique machine learning algorithm. These differed by: type (GPR, coarse tree); kernel function for GPR (exponential, rational quadratic, 5/2 Matérn); or how the cadaveric-based models were incorporated (feature; residuals) (Table 5-5). For GRF, the estimations of both the tibial and femoral cadaveric models were incorporated as features in a GPR with a zero-basis function and an isotropic exponential

kernel function. Of all the models, this was the only one to incorporate previous models as a feature (Table 5-5). KAM and KRM models were all developed based on the residuals between MCS values and those estimated from the previously developed model. KAM was best estimated by adding a kernel approximation model with a support vector machine learner to the estimates of the unmodified abduction moment model. For KRM, a GPR with a zero-basis function and an isotropic exponential kernel function added to the estimates of the unmodified rotation moment model yielded the best estimations. Application of these modified models resulted in very strong fits (R^2 range: 0.92 to 0.96) with NRMSEs below our pre-established conditions (Table 5-6). However, in all models, large LoAs were observed in the KAM and KRM estimations. The BA graphs of the GRF modified model showed no discernable trend for estimations (Figure 5-3). Both the KAM and KRM modified models showed slight trends - as the magnitude of the measured moment increased, the variability of the estimation increased.

Table 5-5 | Overview of the best performing models for GRF, flexion, abduction, and rotation moments. GPR model type is a Gaussian process regression model while SVM indicates a support vector machine learning algorithm.

Machine Learning Models

Model	Unmodified Model Application	Type	Kernel Function	Basis Function	Learner
GRF	Feature	GPR	Isotropic Exponential	Zero	-
KAM	Difference	Kernel	-	-	SVM
KRM	Difference	GPR	Isotropic Exponential	Zero	-

Table 5-6 | Results of amended model application for both training and testing sets across GRF, flexion, abduction, and rotation moments. RMSE, MAE, MAPE, NRMSE, LoA, and model fit (R-squared) are presented. Note, all results are based on the normalized data.

Training Results (5-fold Cross-Validation)

Model	RMSE	R-Squared	MAPE	MAE
GRF	0.19 xBW	0.95	7.91 %	0.14 xBW
KAM	8.94 Nm	0.99	10.3 %	6.30 Nm
KRM	4.24 Nm	0.98	43.7%	3.08 Nm

Testing Results

Model	RMSE	R-Squared	MAE	MAPE	NRMSE	LoA
GRF	0.20 xBW	0.92	0.15 xBW	8.90 %	18.2 %	(-0.35, 0.40) xBW
KAM	10.7 Nm	0.96	7.82 Nm	34.7%	19.6%	(-21.8, 21.9) Nm
KRM	4.71 Nm	0.95	3.53 Nm	53.5%	17.8%	(-9.78, 9.39) Nm

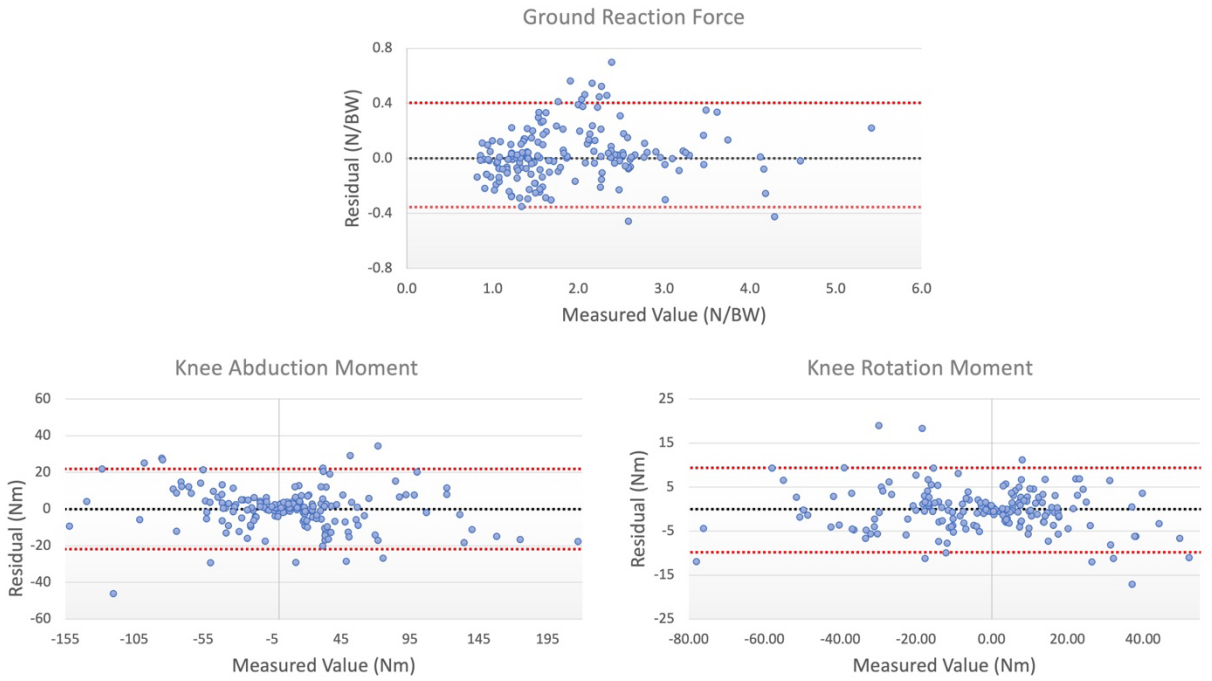

Figure 5-3 | Constructed BA-Plots for modified models for force (GRF), knee abduction, and knee rotation moments in where the residual difference between estimated and measured is located on the y-axis and the measured value on the x-axis. Red lines indicate the limits of agreement and black line the location of the zero-difference line

5.4.3 Classifying Risk Based on Estimations

Because the modified models yielded more accurate estimates (lower NRMSE), construction of the confusion matrix was done using the modified model estimations. Classification as either "possible" or "low" risk was performed with a 96.5% accuracy. Both the precision and recall of classifying a possible risk event was 78.6%. while that of a low-risk event was 98.1% (Figure 5-4).

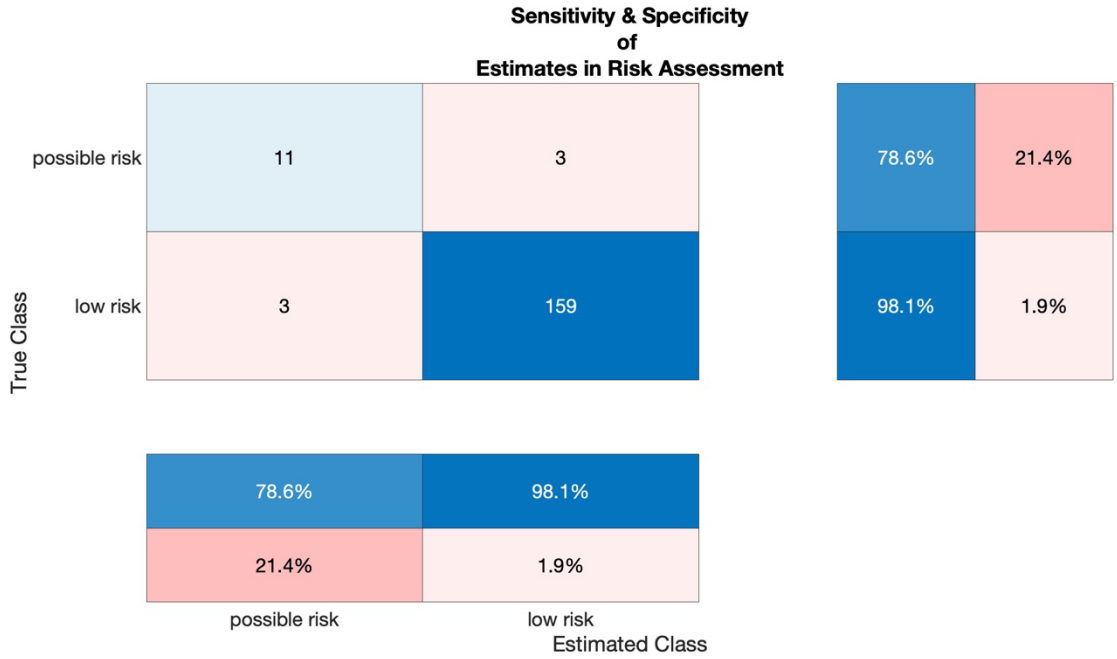

Figure 5-4 | Confusion matrix comparing the measured classifications to the estimated classifications. Right columns are the column-normalized instances of correctly classified events by the estimated class. Bottom rows are the row-normalized instances of correctly classified events by true class

5.5 Discussion

Various studies have utilized some form of modeling technique to correlate IMU data to the forces/moments measured by an MCS [41-46]. While this is important, the overall goal of this study was to determine whether IMU data could be used to reliably estimate forces and moments and classify loading cycles as potentially injurious or benign.

Previously, cadaveric specimens were used to estimate metrics where the effect of soft tissue was mitigated [47]. We had theorized that, due to the absence of soft tissue, the application of our cadaveric model to human subject data would result in estimates that were not acceptably reliable or accurate. Our theory was supported when all cadaveric models yielded high NRMSE and large LoAs, indicating questionable accuracy and reliability. Thus, model modifications to

account for a variety of dynamic movements and possible soft tissue artifact were examined. Machine learning was used to develop these modifications using the estimates of the previously developed models, along with the subject's thigh circumferences, linear accelerations, and angular velocities associated with thigh muscle contractions, mass, height, and IMU placements. This resulted in improved NRMSE values and smaller LoAs than that of the unmodified models across all measurements. Studies by Hossain et al. and Lee et al. have both estimated GRF for several activities of daily living (ADL), such as walking at various speeds on a level surface and stair ascending, with levels of accuracy exceeding that of our study using either machine learning (Lee et al.; feedforward neural networks) or deep learning (Hossain et al.; *Kinetics-FM-DLR-Ensemble-Net*) [43, 55]. KAM and KRM were also examined in these studies. The method by Lee et al. estimated KAM and KRM with low fit levels and NRMSE values greater than our 20% limits; however, this may be attributed to the use of the feedforward neural network, as we previously found that algorithm to be among the worst performing for moment predictions [43]. The deep learning method used by Hossain et al. estimated KAM with greater accuracy than our modified algorithm (KAM NRMSE: 8.27% compared to 19.6%), however, this may be due to their examination of activities representative of daily life and not sports[55]. Application of the Hossain et al. method to the more rigorous activities common in sports may yield poorer results as the algorithm may not be equipped to handle factors such as excess noise contamination due to soft tissue artifact. Neither the Hossain et al. or the Lee et al. studies presented a measure of reliability. While the accuracy of a model is important, neither study presented a method to measure reliability; reliability is of equal importance, because poor reliability would indicate predictions are random in nature. If IMUs are to be implemented to track injuries on-field, consistency is required.

Due to the “black box” phenomenon, F-tests were performed to gauge the contribution of each feature. The femoral force was the largest contributing feature to the GRF model (Figure 5-5). This was expected because, during cadaveric testing, the force measured by the femoral load cell was what was used when establishing xBW testing conditions [47]. Tibial force estimates also significantly contributed to GRF estimates (Figure 5-5). All other features used in GRF estimations did not significantly contribute (Importance Score < 20; $p > 0.05$). In both moment models, no one feature significantly contributed to the estimations. However, this may be due to the limitations of F-scoring. F-scores evaluate the importance of each feature independently from all other features. Thus, F-scoring does not account for the combined effect of multiple features [56].

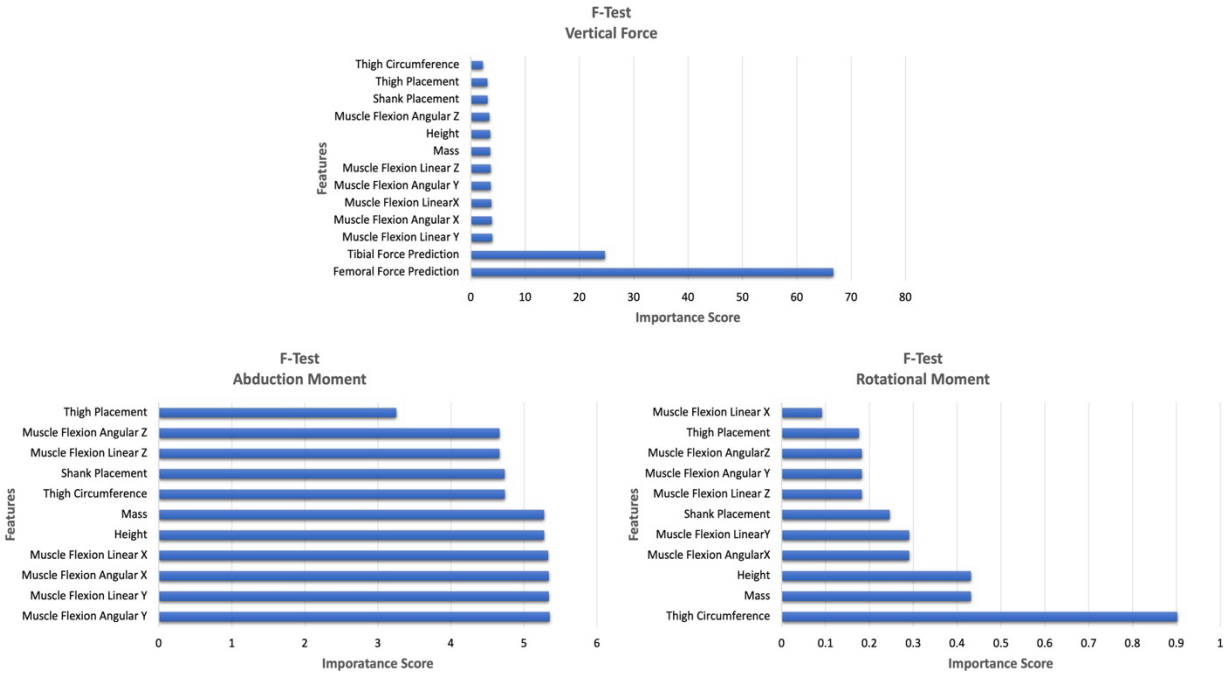

Figure 5-5 | F-test graphs used in determining the significance of a variable to a prediction model. On the y-axis are the differing features used in the construction of the model while on the x-axis are the importance scores. Larger scores indicate a more significant feature.

The third, and arguably most vital purpose of our study was to assess the ability to correctly distinguish between possible and low-risk events. Because of the poor performance of all the unmodified models, only the modified model estimates were used to estimate risk. Risk value was correctly identified with a high level of accuracy, precision, and recall which may mean we can correctly distinguish between possible and low-risk events. In recent years, the use of IMUs as a tool in determining biomechanical risk classification has grown, though, with most of these studies focusing on lifting tasks [57, 58]. Brandt et al. used a combination of surface electromyography and tri-axial accelerometer measurements in a Linear Discriminant Analysis algorithm to classify lifting events as risky or not based on The Danish Working Environment Authority guidelines [58]. They were able to reach accuracies of up to 65.5%, lower than that observed in our classification model [58]. Donsis et al. constructed a confusion matrix based on the estimations of a binary logistic regression model to assess the risk class based on the NIOSH (National Institute of Occupational Safety and Health) standard and demonstrated a good ability to distinguish between "risk" and "no risk" NIOSH classes with high accuracy (82.8%), sensitivity (84.8%), and specificity (80.9%); while our algorithm had a higher accuracy (96.5%), sensitivity was similar (78.6%) [57]. Although the tasks evaluated in these two studies are not like the dynamic actions of our study, they do reinforce the potential that IMUs must classify risk.

5.5.1 Limitations

This study has several limitations, including the use of a controlled laboratory setting. Due to the limited space to perform the required tasks, data collected may not be indicative of on-field conditions. The floor, being stiffer than common surfaces in sports may have also limited our

results as studies conducted have tracked the effects of surface stiffness on energy absorption and biomechanics, and it may be possible that greater errors would be present if our models were used to track on-field activities [59, 60]. The low instances of "risky" events is another limitation, as this may mean the precision determined in our study is skewed, and the addition of more "risky" events may see the precision for this classification lowered. Our use of multiple sensors may also be a hindrance to on-field application, as athlete's comfort and ability to perform needs to be considered. This may mean that IMU placement and/or the number of IMUs available would change during on-field application; as such, new models may be needed to account for these changes. The effects of dermal thickness and tissue composition is another limitation of this work, as various works have alluded to the potential effects each may have on sensor measurement reliability [61, 62]. Measuring skin fold thickness, or subcutaneous fat levels under where the IMUs were placed should be examined as to understand their effects and develop possible filtering algorithms to account for possible sensor movement.

5.6 Conclusion

There were three goals for this study. The first was to assess the performance of our cadaveric models when applied to human subject data. This yielded a poor level of accuracy (high NRMSE) and reliability (large LoA), which may have been due to testing limitations and the absence of soft tissue during model construction. Model modifications to account for dynamic movements and possible soft tissue artifact were needed. Thus, the second purpose of our study was to develop these modifications to our original models. These consisted of subject-specific data (thigh circumferences, muscle contraction, mass, and height), IMU placements, and our unmodified model estimates. All modified models demonstrated NRMSE below 20% and

therefore had acceptable levels of accuracy. However, the large LoAs associated with KAM and KRM estimates may mean a possible lack of consistency. While it was challenging to consistently estimate knee moments, the accuracy and consistency of a risk estimate may be more important for injury tracking purposes. Hence, the third purpose of our study was to develop a classification system distinguishing “possible” and “low” risk estimated events. High levels of accuracy, precision, specificity, and sensitivity indicated that while the individual estimated values may be questionable, estimated risk is near that of measured risk. This ability to classify events may be crucial for injury tracking purposes. Future studies should examine the effect that different surfaces may have on model estimates, and the potential use of these models to track GRF and knee moments on the field.

5.7 References

[1] A. L. Gornitzky, A. Lott, J. L. Yellin, P. D. Fabricant, J. T. Lawrence, and T. J. Ganley, "Sport-Specific Yearly Risk and Incidence of Anterior Cruciate Ligament Tears in High School Athletes: A Systematic Review and Meta-analysis," *Am J Sports Med,* Dec 11 2015, doi: 10.1177/0363546515617742.

[2] J. M. Hootman, R. Dick, and J. Agel, "Epidemiology of collegiate injuries for 15 sports: summary and recommendations for injury prevention initiatives," *J Athl Train,* vol. 42, no. 2, pp. 311-9, Apr-Jun 2007.

[3] G. D. Myer, K. R. Ford, and T. E. Hewett, "Preventing ACL Injuries in Women," *The Journal of Musculoskeletal Medicine,* vol. 1, pp. 12-38, 2006.

[4] A. P. Toth and F. A. Cordasco, "Anterior cruciate ligament injuries in the female athlete," *J Gend Specif Med,* vol. 4, no. 4, pp. 25-34, 2001.

[5] P. Fauno and B. Wulff Jakobsen, "Mechanism of anterior cruciate ligament injuries in soccer," *Int J Sports Med,* vol. 27, no. 1, pp. 75-9, Jan 2006, doi: 10.1055/s-2005-837485.

[6] T. E. Hewett *et al.*, "Biomechanical measures of neuromuscular control and valgus loading of the knee predict anterior cruciate ligament injury risk in female athletes: a prospective study," *Am J Sports Med,* vol. 33, no. 4, pp. 492-501, Apr 2005, doi: 10.1177/0363546504269591.

[7] R. J. Schmitz, A. S. Kulas, D. H. Perrin, B. L. Riemann, and S. J. Shultz, "Sex differences in lower extremity biomechanics during single leg landings," *Clin Biomech (Bristol, Avon),* vol. 22, no. 6, pp. 681-8, Jul 2007, doi: 10.1016/j.clinbiomech.2007.03.001.

[8] B. Yu, C. F. Lin, and W. E. Garrett, "Lower extremity biomechanics during the landing of a stop-jump task," *Clin Biomech (Bristol, Avon),* vol. 21, no. 3, pp. 297-305, Mar 2006, doi: 10.1016/j.clinbiomech.2005.11.003.

[9] B. L. Zeller, J. L. McCrory, W. B. Kibler, and T. L. Uhl, "Differences in kinematics and electromyographic activity between men and women during the single-legged squat," *Am J Sports Med,* vol. 31, no. 3, pp. 449-56, May-Jun 2003.

[10] D. L. Miranda, P. D. Fadale, M. J. Hulstyn, R. M. Shalvoy, J. T. Machan, and B. C. Fleming, "Knee biomechanics during a jump-cut maneuver: effects of sex and ACL surgery," *Med Sci Sports Exerc,* vol. 45, no. 5, pp. 942-51, May 2013, doi: 10.1249/MSS.0b013e31827bf0e4.

[11] T. E. Hewett, K. R. Ford, and G. D. Myer, "Anterior cruciate ligament injuries in female athletes: Part 2, a meta-analysis of neuromuscular interventions aimed at injury prevention," *Am J Sports Med,* vol. 34, no. 3, pp. 490-8, Mar 2006, doi: 10.1177/0363546505282619.

[12] T. E. Hewett, G. D. Myer, and K. R. Ford, "Anterior cruciate ligament injuries in female athletes: Part 1, mechanisms and risk factors," *Am J Sports Med,* vol. 34, no. 2, pp. 299-311, Feb 2006, doi: 10.1177/0363546505284183.

[13] G. D. Myer, M. V. Paterno, K. R. Ford, C. E. Quatman, and T. E. Hewett, "Rehabilitation after anterior cruciate ligament reconstruction: criteria-based progression through the return-to-sport phase," *J Orthop Sports Phys Ther,* vol. 36, no. 6, pp. 385-402, Jun 2006, doi: 10.2519/jospt.2006.2222.

[14] M. V. Paterno *et al.*, "Biomechanical measures during landing and postural stability predict second anterior cruciate ligament injury after anterior cruciate ligament reconstruction and return to sport," *Am J Sports Med,* vol. 38, no. 10, pp. 1968-78, Oct 2010, doi: 10.1177/0363546510376053.

[15] G. M. Thornton, T. D. Schwab, and T. R. Oxland, "Cyclic loading causes faster rupture and strain rate than static loading in medial collateral ligament at high stress," *Clin Biomech (Bristol, Avon),* vol. 22, no. 8, pp. 932-40, Oct 2007, doi: 10.1016/j.clinbiomech.2007.05.004.

[16] J. R. Dugas, "Valgus extension overload: diagnosis and treatment," *Clin Sports Med,* vol. 29, no. 4, pp. 645-54, Oct 2010, doi: 10.1016/j.csm.2010.07.001.

[17] G. M. Thornton, T. D. Schwab, and T. R. Oxland, "Fatigue is more damaging than creep in ligament revealed by modulus reduction and residual strength," *Ann Biomed Eng,* vol. 35, no. 10, pp. 1713-21, Oct 2007, doi: 10.1007/s10439-007-9349-z.

[18] E. M. Wojtys, M. L. Beaulieu, and J. A. Ashton-Miller, "New perspectives on ACL injury: On the role of repetitive sub-maximal knee loading in causing ACL fatigue failure," *J Orthop Res,* vol. 34, no. 12, pp. 2059-2068, Dec 2016, doi: 10.1002/jor.23441.

[19] D. B. Lipps, E. M. Wojtys, and J. A. Ashton-Miller, "Anterior cruciate ligament fatigue failures in knees subjected to repeated simulated pivot landings," *Am J Sports Med,* vol. 41, no. 5, pp. 1058-66, May 2013, doi: 10.1177/0363546513477836.

[20] K. H. Putera *et al.*, "Fatigue-driven compliance increase and collagen unravelling in mechanically tested anterior cruciate ligament," (in eng), *Commun Biol,* vol. 6, no. 1, p. 564, May 26 2023, doi: 10.1038/s42003-023-04948-2.

[21] J. Kim *et al.*, "Anterior cruciate ligament microfatigue damage detected by collagen autofluorescence in situ," (in eng), *J Exp Orthop,* vol. 9, no. 1, p. 74, Jul 30 2022, doi: 10.1186/s40634-022-00507-6.

[22] J. M. Hollis, S. Takai, D. J. Adams, S. Horibe, and S. L. Woo, "The effects of knee motion and external loading on the length of the anterior cruciate ligament (ACL): a kinematic study," (in eng), *J Biomech Eng,* vol. 113, no. 2, pp. 208-14, May 1991, doi: 10.1115/1.2891236.

[23] K. L. Markolf, D. M. Burchfield, M. M. Shapiro, M. F. Shepard, G. A. Finerman, and J. L. Slauterbeck, "Combined knee loading states that generate high anterior cruciate ligament forces," (in eng), *J Orthop Res,* vol. 13, no. 6, pp. 930-5, Nov 1995, doi: 10.1002/jor.1100130618.

[24] B. Yu and W. E. Garrett, "Mechanisms of non-contact ACL injuries," (in eng), *Br J Sports Med,* vol. 41 Suppl 1, pp. i47-51, Aug 2007, doi: 10.1136/bjsm.2007.037192.

[25] C. S. Shin, A. M. Chaudhari, and T. P. Andriacchi, "Valgus plus internal rotation moments increase anterior cruciate ligament strain more than either alone," (in eng), *Med Sci Sports Exerc,* vol. 43, no. 8, pp. 1484-91, Aug 2011, doi: 10.1249/MSS.0b013e31820f8395.

[26] S. Ananthanarayan, M. Sheh, A. Chien, H. Profita, and K. A. Siek, "Designing Wearable Interfaces for Knee Rehabilitation," in *Proceedings of the 8th International Conference on Pervasive Computing Technologies for Healthcare*, Oldenburg, Germany, 2014.

[27] M. Arif and A. Kattan, "Physical Activities Monitoring Using Wearable Acceleration Sensors Attached to the Body," (in eng), *PLoS One,* vol. 10, no. 7, p. e0130851, 2015, doi: 10.1371/journal.pone.0130851.

[28] S. Bakshi, M. H. Mahoor, and B. S. Davidson, "Development of a Body Joint Angle Measurement System Using IMU Sensors," in *33rd Annual International Conference of the IEEE EMBS*, Boston, MA, 2011.

[29] S. J. Bamberg, A. Y. Benbasat, D. M. Scarborough, D. E. Krebs, and J. A. Paradiso, "Gait analysis using a shoe-integrated wireless sensor system," *IEEE Trans Inf Technol Biomed,* vol. 12, no. 4, pp. 413-23, Jul 2008, doi: 10.1109/TITB.2007.899493.

[30] J. A. Barrios, K. M. Crossley, and I. S. Davis, "Gait retraining to reduce the knee adduction moment through real-time visual feedback of dynamic knee alignment," *J Biomech,* vol. 43, no. 11, pp. 2208-13, Aug 10 2010, doi: 10.1016/j.jbiomech.2010.03.040.

[31] K. H. Chen, P. C. Chen, K. C. Liu, and C. T. Chan, "Wearable sensor-based rehabilitation exercise assessment for knee osteoarthritis," *Sensors (Basel),* vol. 15, no. 2, pp. 4193-211, 2015, doi: 10.3390/s150204193.

[32] C. J. Anderson, C. G. Ziegler, C. A. Wijdicks, L. Engebretsen, and R. F. LaPrade, "Arthroscopically pertinent anatomy of the anterolateral and posteromedial bundles of the posterior cruciate ligament," (in eng), *J Bone Joint Surg Am,* vol. 94, no. 21, pp. 1936-45, Nov 2012, doi: 10.2106/JBJS.K.01710.

[33] A. G. Cutti, A. Ferrari, P. Garofalo, M. Raggi, and A. Cappello, "'Outwalk': a protocol for clinical gait analysis based on inertial and magnetic sensors," (in eng), *Med Biol Eng Comput,* vol. 48, no. 1, pp. 17-25, Jan 2010, doi: 10.1007/s11517-009-0545-x.

[34] J. Favre, X. Crevoisier, B. M. Jolles, and K. Aminian, "Evaluation of a mixed approach combining stationary and wearable systems to monitor gait over long distance," (in eng), *J Biomech,* vol. 43, no. 11, pp. 2196-202, Aug 2010, doi: 10.1016/j.jbiomech.2010.03.041.

[35] A. Ferrari *et al.*, "First in vivo assessment of "Outwalk": a novel protocol for clinical gait analysis based on inertial and magnetic sensors," (in eng), *Med Biol Eng Comput,* vol. 48, no. 1, pp. 1-15, Jan 2010, doi: 10.1007/s11517-009-0544-y.

[36] J. F. Lin and D. Kulić, "Human pose recovery using wireless inertial measurement units," (in eng), *Physiol Meas,* vol. 33, no. 12, pp. 2099-115, Dec 2012, doi: 10.1088/0967-3334/33/12/2099.

[37] P. Picerno, A. Cereatti, and A. Cappozzo, "Joint kinematics estimate using wearable inertial and magnetic sensing modules," (in eng), *Gait Posture,* vol. 28, no. 4, pp. 588-95, Nov 2008, doi: 10.1016/j.gaitpost.2008.04.003.

[38] C. Strohrmann, H. Harms, C. Kappeler-Setz, and G. Troster, "Monitoring kinematic changes with fatigue in running using body-worn sensors," *IEEE Trans Inf Technol Biomed,* vol. 16, no. 5, pp. 983-90, Sep 2012, doi: 10.1109/TITB.2012.2201950.

[39] T. Watanabe and H. Suito, "Tests of Wireless Wearable Sensor System in Joint Angle Measurement of Lower Limbs," in *33rd Annual International Conference of the IEEE EMBS*, Boston, MA, 2011.

[40] N. G. Elvin, A. A. Elvin, and S. P. Arnoczky, "Correlation between ground reaction force and tibial acceleration in vertical jumping," *J Appl Biomech,* vol. 23, no. 3, pp. 180-9, Aug 2007.

[41] D. V. Thiel *et al.*, "Predicting Ground Reaction Forces in Sprint Running Using a Shank Mounted Inertial Measurement Unit," *Proceedings,* vol. 2, no. 6, p. 199, 2018.

[42] J. M. Neugebauer, D. A. Hawkins, and L. Beckett, "Estimating youth locomotion ground reaction forces using an accelerometer-based activity monitor," (in eng), *PLoS One,* vol. 7, no. 10, p. e48182, 2012, doi: 10.1371/journal.pone.0048182.

[43] M. Lee and S. Park, "Estimation of Three-Dimensional Lower Limb Kinetics Data during Walking Using Machine Learning from a Single IMU Attached to the Sacrum," (in eng), *Sensors (Basel),* vol. 20, no. 21, Nov 04 2020, doi: 10.3390/s20216277.

[44] J. Favre, A. V. Dowling, and T. P. Andriacchi, "The Relationship between Segment Angular Velocity and Knee Abduction Moment during a Drop Jump:Implications for ACL Injury Risk Prediction," in *11th Annual Orthopaedic Research Society*, 2010.

[45] J. M. Konrath, A. Karatsidis, H. M. Schepers, G. Bellusci, M. de Zee, and M. S. Andersen, "Estimation of the Knee Adduction Moment and Joint Contact Force during Daily Living Activities Using Inertial Motion Capture," (in eng), *Sensors (Basel),* vol. 19, no. 7, Apr 2019, doi: 10.3390/s19071681.

[46] A. Karatsidis *et al.*, "Predicting kinetics using musculoskeletal modeling and inertial motion capture,"

[47] M. Ajdaroski, S. Y. Baek, J. A. Ashton-Miller, and A. O. Esquivel, "Predicting forces and knee moments using IMUs: an in vitro study," 2023.

[48] B. P. Boden, G. S. Dean, J. A. Feagin, Jr., and W. E. Garrett, Jr., "Mechanisms of anterior cruciate ligament injury," *Orthopedics,* vol. 23, no. 6, pp. 573-8, Jun 2000.

[49] D. T. Kirkendall and W. E. Garrett, Jr., "The anterior cruciate ligament enigma. Injury mechanisms and prevention," *Clin Orthop Relat Res,* no. 372, pp. 64-8, Mar 2000.

[50] M. J. Decker, M. R. Torry, D. J. Wyland, W. I. Sterett, and J. Richard Steadman, "Gender differences in lower extremity kinematics, kinetics and energy absorption during landing," *Clin Biomech (Bristol, Avon),* vol. 18, no. 7, pp. 662-9, Aug 2003.

[51] E. Pappas, M. Hagins, A. Sheikhzadeh, M. Nordin, and D. Rose, "Biomechanical differences between unilateral and bilateral landings from a jump: gender differences," *Clin J Sport Med,* vol. 17, no. 4, pp. 263-8, Jul 2007, doi: 10.1097/JSM.0b013e31811f415b.

[52] B. Yu, D. Gabriel, L. Noble, and K.-N. An, "Estimate of the Optimum Cutoff Frequency for the Butterworth Low-Pass Digital Filter," *Journal of Applied Biomechanics,* vol. 15, pp. 319-329, 1999 doi: 10.1123/jab.15.3.318.

[53] M. Ajdaroski, J. A. Ashton-Miller, S. Y. Baek, P. M. Shahshahani, and A. Esquivel, "Testing a Quaternion Conversion Method to Determine Human 3D Tibiofemoral Angles During an in Vitro Simulated Jump Landing," (in eng), *J Biomech Eng,* Sep 22 2021, doi: 10.1115/1.4052496.

[54] N. A. Bates, N. D. Schilaty, C. V. Nagelli, A. J. Krych, and T. E. Hewett, "Multiplanar Loading of the Knee and Its Influence on Anterior Cruciate Ligament and Medial Collateral Ligament Strain During Simulated Landings and Noncontact Tears," (in eng), *Am J Sports Med,* vol. 47, no. 8, pp. 1844-1853, Jul 2019, doi: 10.1177/0363546519850165.

[55] M. S. B. Hossain, Z. Guo, and H. Choi, "Estimation of Lower Extremity Joint Moments and 3D Ground Reaction Forces Using IMU Sensors in Multiple Walking Conditions: A Deep Learning Approach," (in eng), *IEEE J Biomed Health Inform,* vol. PP, Mar 29 2023, doi: 10.1109/JBHI.2023.3262164.

[56] Y. Chen and C. Lin, *Combining SVMs with Various Feature Selection Strategies*. Berlin, Heidelberg: Springer Berlin Heidelberg, 2006, pp. 315--324.

[57] L. Donisi *et al.*, "A Logistic Regression Model for Biomechanical Risk Classification in Lifting Tasks," (in eng), *Diagnostics (Basel),* vol. 12, no. 11, Oct 29 2022, doi: 10.3390/diagnostics12112624.

[58] M. Brandt *et al.*, "Accuracy of identification of low or high risk lifting during standardised lifting situations," (in eng), *Ergonomics,* vol. 61, no. 5, pp. 710-719, May 2018, doi: 10.1080/00140139.2017.1408857.

[59] T. R. Derrick, J. Hamill, and G. E. Caldwell, "Energy absorption of impacts during running at various stride lengths," (in eng), *Med Sci Sports Exerc,* vol. 30, no. 1, pp. 128-35, Jan 1998, doi: 10.1097/00005768-199801000-00018.

[60] D. P. Ferris, M. Louie, and C. T. Farley, "Running in the real world: adjusting leg stiffness for different surfaces," (in eng), *Proc Biol Sci,* vol. 265, no. 1400, pp. 989-94, Jun 1998, doi: 10.1098/rspb.1998.0388.

[61] L. K. Smalls, R. Randall Wickett, and M. O. Visscher, "Effect of dermal thickness, tissue composition, and body site on skin biomechanical properties," (in eng), *Skin Res Technol,* vol. 12, no. 1, pp. 43-9, Feb 2006, doi: 10.1111/j.0909-725X.2006.00135.x.

[62] L. Q. Vu, K. H. Kim, L. J. H. Schulze, and S. L. Rajulu, "Lumbar posture assessment with fabric strain sensors," (in eng), *Comput Biol Med,* vol. 118, p. 103624, Mar 2020, doi: 10.1016/j.compbiomed.2020.103624.

Chapter 6: Can Wearable Sensors Provide Accurate and Reliable 3D Tibiofemoral Angle Estimates During Dynamic Actions?

This chapter has been accepted for publication in Sensors and should be referred to as:

Ajdaroski M, Esquivel A. Can Wearable Sensors Provide Accurate and Reliable 3D Tibiofemoral Angle Estimates during Dynamic Actions? *Sensors*. 2023; 23(14):6627. https://doi.org/10.3390/s23146627

6.1 Abstract

The ability to accurately measure tibiofemoral angles during various dynamic activities is of clinical interest. The purpose of this study was to determine if IMUs can provide accurate and reliable angle estimates during dynamic actions. A tuned quaternion conversion (TQC) method tuned to dynamics actions was used to calculate Euler angles based on IMU data and these calculated angles were compared to a motion capture system (our "gold" standard) and a commercially available sensor fusion algorithm. Nine healthy athletes were instrumented with APDM Opal IMUs and asked to perform nine dynamic actions; five participants were used in training the parameters of the TQC method with the remaining four used to test validity. Accuracy was based on the RMSE and reliability was based on the LoA. Improvement across all three orthogonal angles was observed as the TQC method was able to more accurately (lower RMSE) and more reliably (smaller LoA) estimate an angle than the commercially available algorithm. No significant difference was observed between the TQC method and the motion capture system in any of the three angles ($p < 0.05$). It may be feasible to use this method to track

tibiofemoral angles with higher accuracy and reliability than the commercially available sensor fusion algorithm.

6.2 Introduction

There has been a discernible rise in non-contact ACL injuries among athletes, despite the implementation of preventive measures [1, 2]. These injuries are of particular concern among young female athletes, with rates higher than their male counterparts in similar sports [1-3]. These injuries can be expensive to treat, with ACL reconstruction procedures ranging from $27,000 to $35,000 in cost, in addition, there is an increased risk of early-onset osteoarthritis of the knee following these operations [4-6]. Studies have identified sex-based differences in anatomy, hormones, and movement patterns as possible risk factors for ACL injury susceptibility [7-16]. While anatomical and hormonal factors cannot be controlled, identifying, and modifying movement patterns that may contribute to ACL injury or reducing exposure to severe loading cycles is possible.

Traditionally, camera-based MCS in laboratory are used to measure kinematics. These systems are comprised of multiple cameras and load cells which make them difficult to use ‘in the field’. An IMU is a wearable sensor made up of accelerometers, rate gyroscopes, and magnetic field sensors that measure the linear acceleration, angular velocity, and magnetic field strength of a particular body part. By using a specialized sensor fusion algorithm, the device can track the orientation of the body part in inertial space. Additionally, combining the IMU data of two adjacent body segments can be done to determine the Euler angles of a joint. These sensors have

been utilized in different scenarios, including gait analysis, and rehabilitation assistance with success [17-28].

Research conducted in laboratory settings on cadaveric models has suggested that some ACL injuries are due to overuse and repetitive strain placed on the ACL [29]. Numerous scenarios can lead to these high-strain conditions, however, one theory that is commonly accepted suggests that such injuries occur when the knee is externally rotated with a slight flexion and a slight valgus angle at the time of the incident [13, 30]. In theory, once these specific conditions are fulfilled, and the knee is subjected to a ground reaction force, a strong quadriceps contraction might occur, resulting in the tibia moving anteriorly to the femur; this movement could potentially cause the ACL to experience strain beyond its injury threshold [13, 30]. The ground reaction and quadriceps forces, as well as the orientation of the knee, are crucial factors in this scenario [13, 31]. Recently, a study has explored and created algorithms for calculating ground reaction forces with IMUs, with encouraging results [32]. However, accurately estimating 3D tibiofemoral angles has been more challenging. [33-37] and we believe that commercially available IMU algorithms may not be accurate for more dynamic activities like sports, where larger changes in joint angles, velocities, and accelerations can occur; this theory was corroborated through the results of our previous work [38]. Through testing with cadaveric specimens, we discovered that adjusting the settings of a sensor fusion algorithm led to improved performance compared to a commercially available version [38]. However, the use of cadaveric specimens excludes the effect soft tissue artifact may have on estimated angle accuracy. Thus, our goal in this study was to use the algorithm previously developed, but to adjust it for use in live human subjects and determine if the tuned algorithm demonstrates improved accuracy and

reliability when measuring tibiofemoral (knee) angles in all three orthogonal directions during more dynamic activities.

6.3 Materials and Methods

6.3.1 Subjects, Instrumentation, & Testing Procedures

Before the commencement of the study, we received IRB approval (HUM00150719). Nine healthy (5 females, 4 males) current or former (within two years) soccer or basketball athletes were recruited (Table 5-1). Participants with a BMI over 29 kg/m^2 or who had a current lower extremity injury were excluded. Instrumentation and testing procedures have been described previously [32]. Briefly, informed consent was obtained before a participant was fitted with 46 retro-reflective spherical markers; the first 30 markers were placed according to the 30 Rizzoli lower body protocol, with the remaining placed in clusters of fours on the lateral thigh and gastrocnemius (Figure 5-1). Motions were collected using a 12-camera motion capture system (Prime 13 Optitrack, Corvallis, OR) and two APDM wearable sensors (APDM Opal, APDM Wearable Technologies, Portland, OR); the wearable sensors were placed similarly to previous works [32, 38]. All data were collected at 200 Hz and a sync device was used to synchronize the recordings. IMUs were calibrated before each session through the predefined calibration conditions used by the Moveo Mobility software (version 1.0.0) developed by APDM. Participants were asked to complete seven related tests three times: a jog with a pivot, an extension leap, a sidestep cut, a crossover cut, dominant shooting, a vertical jump onto two feet, and a vertical jump onto one foot (Table 5-2). Because both training and testing the validity of our tuned algorithm were needed, we randomly separated our subject pool based on average

subject weight, into a training set (used in tuning; N=5) and a testing set (used in the testing of validity; N=4).

6.3.2 Data Processing

For the MCS, a six-degree-of-freedom kinematic model of the lower extremity was created for each participant, including the pelvis, thigh, shank, and foot, using Visual 3D software (C-Motion, Germantown, MD). A static trial was collected to determine the participant's anatomic neutral. Joint angles at maximum ground reaction force were calculated in Visual 3D using a Cardan rotation sequence (CRS). Joint angles are the relative orientation of one local coordinate system to another and can be represented by three rotations about a unique axis. Emphasis is placed on the order of these rotations. Within this study, a CRS XYZ was implemented, with a lateral rotational matrix determined first, followed by an anterior, and finally a vertical rotational matrix; this process has been used in previous work [33]. Angles obtained through this kinematic model were normalized to the femur through the Visual 3D software. For the IMU, two methods were used to obtain the tibiofemoral angles: 1) APDM proprietary algorithm (denoted as the IMU method); 2) a tuned quaternion conversion algorithm (denoted as the TQC method). Angles obtained through the IMU method were not subjected to additional processing.

IMU data were filtered using a fourth-order, zero-lag, low-pass Butterworth filter. Optimum cutoff frequencies for the Butterworth digital filter were obtained by applying Winter's method; this method has been used in previous works [38, 39]. Only the training set was utilized in determining the optimal frequencies (Table 5-3). Following filtering, a nine-axis indirect Kalman filter using the quaternion conversion of the IMU accelerometer, gyroscope, and magnetometer

data was used. This process is detailed at greater length in our previous work and the paper by Stanley et al [38, 40]. Briefly, this process began through the estimation of a sensor's current orientations from the angular changes of the previous orientation with the initial alignment estimated to be NED. Once obtained, this estimated orientation was converted to a quaternion format. Next, quaternion conversion estimations of the gravitational and magnetic field measurements were obtained using linear acceleration and angular velocity. These estimates were used to correct the gravitational and magnetic field data obtained from the previous orientation and magnetometer. The corrected orientation and magnetometer estimates became the innovation for the indirect Kalman filter. As mentioned by Stanley et al., the indirect Kalman filter attempts to track errors rather than orientation as the data is updated through a recursive process [40]. Additionally, this process being recursive meant that the *a priori* estimates of the error process and the state transitions models were set to zero, thereby allowing for the application of the reduced Kalman equations [40]. Because orientation was in a quaternion format, the subtraction of the data from adjacent segments was mathematically valid. Therefore, the data attributed to the tibial IMU sensor was subtracted from the femoral IMU sensor. The resulting values were then converted into Euler angles, similar to what was done before [38].

6.3.3 Parameters Used in the TQC Method

Parameter adjustment followed what was previously done [38]. Briefly, several unique parameters used in the covariance of the observation model noise and predicted estimate covariance were required; all the required parameters can be viewed in greater length in the work by Stanley et al [40]. APDM Opal documentation provided the values for accelerometer noise, gyroscope noise, and magnetometer noise. Gyroscope drift noise, linear acceleration noise, and

magnetic disturbance noise were not detailed in the documentation, so the default values based on the FRDM-FXS-Multi family of sensor boards (as used by the Freescale Toolbox of MATLAB) were used; this was done in our previous work [38]. The use of these default values was implemented due to the potential value range being theoretically infinite such that a process of trial and error would not be possible.

The LADF and MDDF were unknown parameters that accounted for the effects of drift in either the linear acceleration or magnetic disturbance. Because their theoretical values ranged from 0 to 1, and because through previous testing, differences less than 0.0001 resulted in no distinguishable change between subsequent LADF/MDDF, values for the LADF/MDDF were theoretically finite. Using the training set of data, a trial-and-error approach was taken where adjustments to the LADF and/or MDDF were performed in increments of 0.0001 from 0.0001 to 0.9999 to minimize the difference in angles between the TQC method and the MCS. These adjustments were performed on each axe, resulting in 3 unique LADF and 3 unique MDDF values per trial. An average for both the LADF and MMDF was determined and used when calculating the angles of the testing set for validation. A trial-and-error approach has been used in previous work [38].

6.3.4 Statistical Analysis

A repeated measured ANOVA with a pairwise comparison was performed on both the training and testing sets to determine whether there was a difference between the TQC method and MCS and the IMU method and MCS. A Bonferroni correction was used to correct for multiple comparisons. Differences were considered significant if $p < 0.05$. LoAs were constructed for the

testing set to assess each method's reliability. LoAs were taken as the 95% confidence interval of the residual difference between a sensor method (either the TQC or IMU) and the MCS. To assess each method's accuracy, the RMSE was determined between the MCS and either the IMU or TQC methods. BA plots were developed for descriptive analysis and used to comment on trends/biases that may exist; this was based on whether angles estimated using the IMU exhibited a tendency to over/underestimate true angles or whether there was an increase or decrease in variability as the angle increased in magnitude.

6.4 Results

6.4.1 Training Set

Among all comparisons within the training set, flexion angle differences between the MCS and IMU as well as IMU and TQC were the only ones that were statistically significant (Figure 6-1). The training set showed a mean difference in flexion/extension between the MCS and IMU of -9.94° (95% CI: -13.9° to -5.96°) while that between the MCS and TQC was -0.18° (95% CI: -4.16° to -3.80°). For abduction/adduction, a mean difference of -0.47° (95% CI: -2.71° to 1.77°) between the MCS and IMU was observed, while the mean difference between the MCS and TQC was -0.13° (95% CI: -2.37° to 2.11°) (Figure 6-1). The mean difference in rotation between the MCS and IMU was -0.71° (95% CI: -4.01° to 2.60°); between the MCS and TQC, the difference was -0.10 (95% CI: -3.41° to 3.21°). Across all cases, the LoA and RMSE of MCS vs TQC were determined to be smaller, indicating increases in both accuracy and reliability in the TQC (Table 6-1).

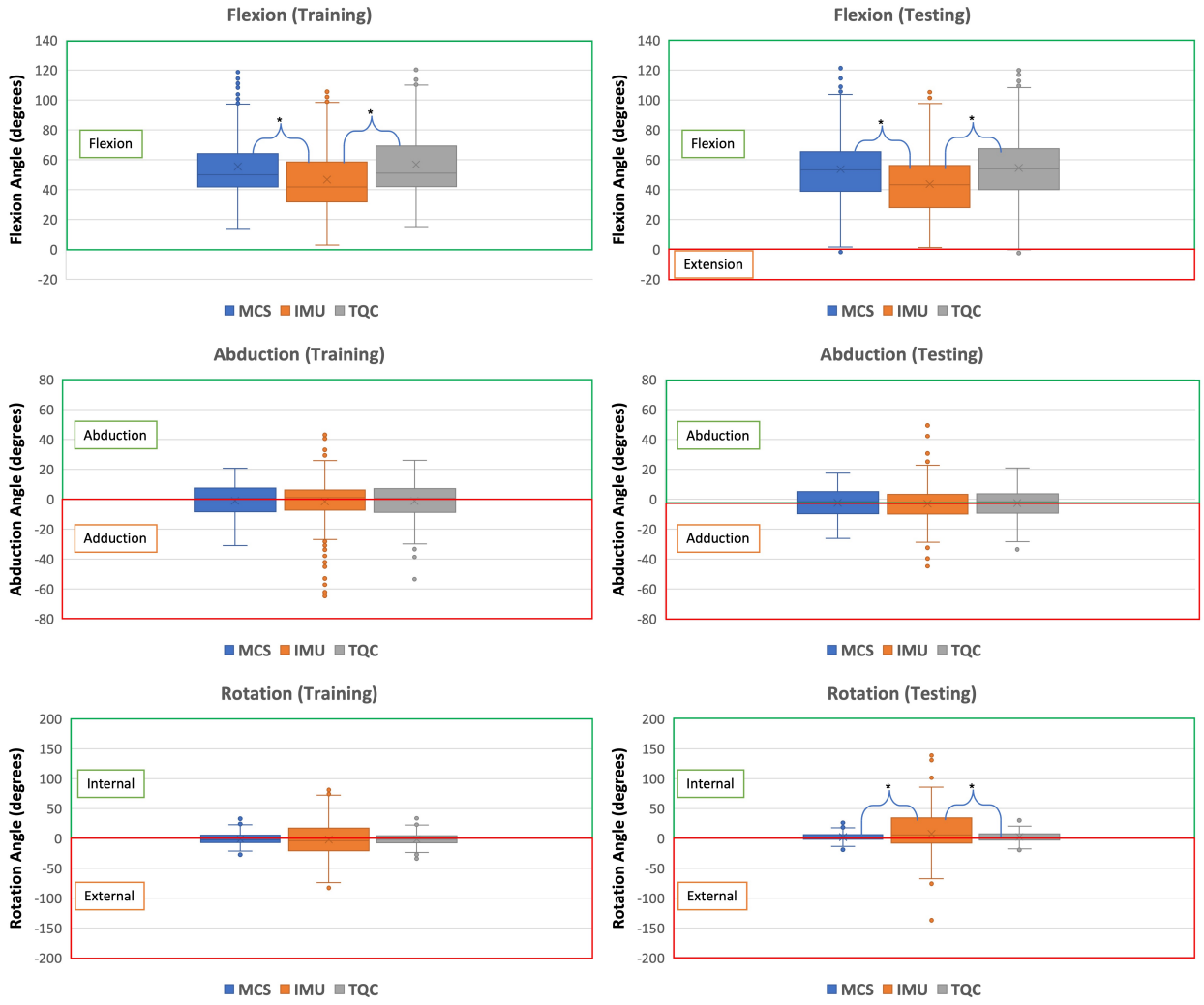

Figure 6-1 | Box-and-whisker plots comparing the values of the motion capture system (MCS), the sensor fusion algorithm of the IMU (IMU), and the tune quaternion conversion method (TQC) for flexion (**top**), abduction (**middle**), and rotation (**bottom**). Differences that were determined to be significant are denoted by *.

Table 6-1 Comparisons of the angles estimated using either the IMU or TQC method to those of the MCS. Presented are the RMSE and LoA bound (taken as the difference between upper and lower bound). Diff. is taken as the difference of MCS vs. TQC values or MCS vs. IMU.

Comparisons of the IMU and TQC Methods to MCS

		Training Set		Testing Set	
	Comparison	RMSE	LoA (Upper – Lower)	RMSE	LoA (Upper – Lower)
Flexion	MCS v IMU	16.6°	52.0°	19.0°	68.1°
	MCS v TQC	7.48°	29.3°	8.00°	32.9°
	Diff.	-9.08°	-22.6°	-11.0°	-35.2°
Abduction	MCS v IMU	11.9°	46.6°	8.59°	33.4°
	MCS v TQC	3.51°	13.8°	3.14°	12.9°
	Diff.	-8.37°	-32.8°	-5.44°	-22.4°
Rotation	MCS v IMU	25.5°	100°	29.7°	121°
	MCS v TQC	4.39°	17.2°	3.63°	15.0°
	Diff.	-21.2°	82.9°	-26.1°	105°

6.4.2 Testing Set

Flexion and rotation angles between the MCS and IMU as well as IMU and TQC were determined to be statistically significant (Figure 6-1). A mean difference in flexion/extension of -9.96° (95% CI: -14.3 to -5.64) was determined between the MCS and IMU, while that between the MCS and TQC was determined to be 0.80° (95% CI: -3.52 to 5.12). For abduction/adduction, the mean difference between the MCS and IMU was -0.68° (95% CI: -2.58 to 1.23) while the mean difference between the MCS and TQC was -0.49° (95% CI: -2.39 to 1.42) (Figure 6-1).

For rotation, the mean difference between the MCS and IMU was 5.42° (95% CI: 1.68 to 9.17) and 0.04° (95% CI: -3.70 to 3.79) between the MCS and TQC. Across all comparisons, differences between the MCS and IMU resulted in larger RMSE values as well as larger LoA (Table 6-1).

The BA plots comparing the MCS and IMU differences showed varying degrees of bias and trends. For flexion/extension, there tended to be an underestimation of the angle by the IMU, and a linear slope was observed between the residuals and the measured flexion/extension angle; lower measured values skewed towards overestimations while higher values tended to be underestimations (Figure 6-2). Within the abduction/adduction BA plot between the MCS and IMU, as the magnitude of the measured angle increased (regardless of whether abduction or adduction), estimated values by the IMU decreased (Figure 6-2) . For rotational angles between the MCS and IMU, the IMU tended to overestimate the magnitude of the angle, regardless of whether it was internal or external rotation. Comparing the MCS and the TQC, differences in flexion/extension as well as rotation showed no discernable trends. With the abduction/addiction BA plot between the MCS and IMU, as the magnitude of the measured angle increased, there was an increase in the variability of TQC estimates.

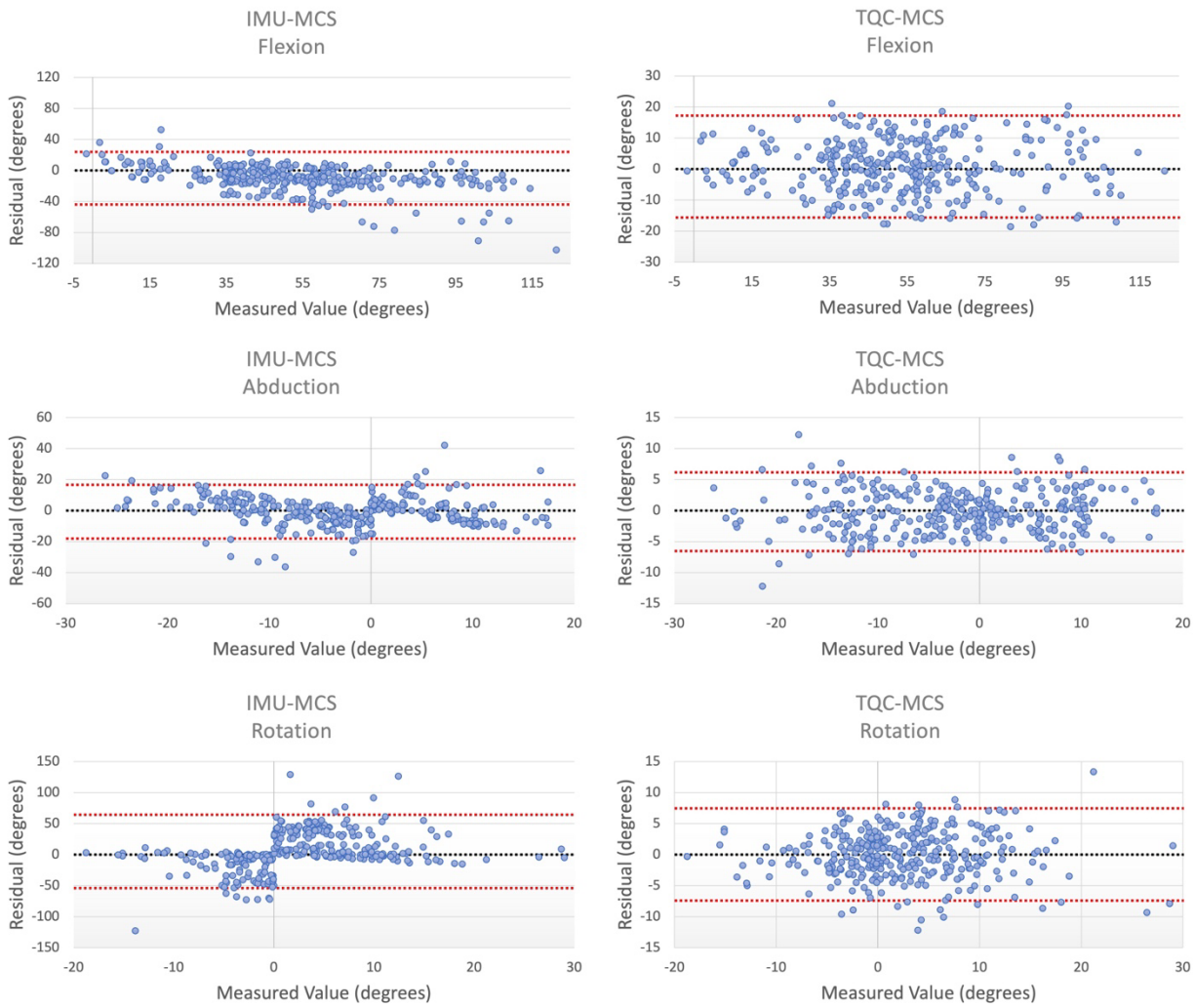

Figure 6-2 | Bland–Altman plots associated with the residuals for flexion (**top**), abduction (**middle**), and rotation (**bottom**) between the motion capture system (MCS) and either the sensor fusion algorithm (IMU; **left**) or the tuned quaternion conversion method (TQC; **right**). Residuals were plotted against the measured values of the MCS. Limits of agreement (LoAs) are shown in red while the line of zero difference is shown in black.

6.5 Discussion

We hypothesized that, the sensor fusion algorithm employed by commercially available wearable sensors may not necessarily be accurate when used in dynamic activities such as sports where larger changes in joint angles, velocities, and accelerations occur. Previous cadaveric testing supported this theory, as the tuning of certain parameters of a quaternion conversion algorithm

resulted in more accurate and reliable angle estimates over an IMU's sensor fusion algorithm [38]. However, we recognized several limitations in this previous work, such as a lack of soft tissue and a lack of variability in the motion. The purpose of this study was to use the algorithm previously developed but retune it for use in human subjects in a variety of action types and determine if this tuned algorithm demonstrated improved accuracy and reliability in angle estimations. In all cases for the testing set, differences between the TQC and MCS were determined to be statistically insignificant, while differences between the IMU and MCS were observed as being significant in both flexion and rotation. Whether or not these differences are clinically relevant is dependent on the particular scenario. A review paper examining ACL tear in athletes reported flexion angle differences of 10°-21.7° between injured and un-injured knees and a laboratory study observed abduction angle increases of 8° in athletes who went on to injure their ACL [8, 41]. Therefore, while differences between the IMU and MCS were observed as being statistically significant in flexion, clinically this may be negligible. Across all comparisons, the RMSE values associated with the differences between the TQC and MCS were smaller than those between the IMU and MCS, with the largest difference occurring in the testing set rotational angles (3.63° compared to 29.7°); this was similarly observed during our cadaveric testing [38]. In every case, the LoA associated with the difference between the TQC and MCS were smaller than those between the IMU and MCS, indicating a smaller range in differences and a better degree of reliability.

Various studies have calculated joint angles, particularly those of the knee, using IMU-derived data, and then compared the results to those obtained through an MCS [34-37, 42-45]. However, the focus of many of these studies has been on examining differences in flexion angles, possibly

due to the knee flexion angle exhibiting the largest change during an action, and consequently being easiest to measure reliably. However, being able to accurately measure abduction and rotation angles is important because of the potential effects these angles may play in knee injuries, specifically, ACL injuries. Many studies have proposed there is a correlation between ACL strain and the abduction/adduction and rotational orientation of the joint [16, 46-52]. Because of this possible correlation, to improve knee injury tracking, it becomes important to track all three knee angles. Furthermore, the method by which joint angles are determined through IMUs also varies widely from study to study, with some taking the integration of angular rates while others using Euler angles. Studies such as those by Watanabe et al., Tong et al., and Bakhshi et al calculated knee joint angles by taking the integration of angular rates, without the conversion to Euler angles and limiting themselves to only determining flexion angles [35, 36, 42]. This process may be problematic as angles obtained do not describe the orientation of the joint to a fixed coordinate system, but rather to some arbitrary coordinate system. As such, each study's estimated angles may not represent the knee's true orientation, and comparisons between estimated and MSC-measured values may not be accurate. However, these studies have shown their methods to be accurate in knee flexion estimates as the least accurate of these studies (Tong et al.) demonstrated an RMSE value below that which we reported between the MCS and TQC (our best case within flexion comparisons) (RMSE of 6.4° compared to 7.48°) [36]. This comparison may warrant criticism, as these studies observed actions associated with rehabilitation, which can be less dynamic than those in our study, but it may be that, due to possible increases in both angular velocities and linear accelerations, the results of our study were more prone to noise pollution and thus inaccuracies. Various studies have noted the potential effects of soft tissue artifact on the validity of results [53-55].

Bell et al and Zügner et al compared angles estimated via a sensor's proprietary sensor fusion algorithm and those of an MCS [43, 44]. In these cases, the sensor fusion algorithm was used to calculate the Euler angles of the knee joint. In the study by Bell et al, RMSE values between estimated and measured knee flexion angles were lower than any previously mentioned study and lower than that of our study (RMSE of between 2° and 2.9° compared to 7.48°) [44]. While this shows a high accuracy for flexion angle estimates, the accuracy of abduction/adduction or rotational estimates was not reported which are important if IMUs are to be used for injury prevention. Zügner et al reported that they found no significance in the mean difference between estimated and measured knee flexion angles ($p=0.7$) and determined a high ICC ($ICC>0.8$) [43]. Mean difference comparisons and ICC compare data sets as groups, and as such, mitigate the effects of gross differences; if the algorithm over- and underestimates angles similarly, the mean difference would be relatively small and may be misleading to the performance of an algorithm. Approaches such as RMSE or mean absolute percent errors remove this pitfall and may be much better indicators of accuracy.

In a previous study done using APDM Opal sensors, highly dynamic activities (jumps) were observed and comparisons of all three knee angles were reported [38]. It was concluded that for both abduction/adduction and rotation, the APDM Opal algorithm was able to perform well under certain conditions, particularly those of smaller angle displacements, and experienced greater variability as the magnitude of the measured angle increased [38]. We observed a very similar trend when comparing the IMU to the MCS across both abduction/adduction and rotation angles, but only within the abduction/adduction comparison between TQC and MCS was a similar trend noted, however, the extent of this increase in the variability of the increase in angle

magnitude was not as prominent. In both this and our previous study, the mean difference between the IMU estimated abduction/adduction angle and that of the MCS was not significant, although, the RMSE reported in our study was greater (RMSE of 8.59° compared to 4.91°) [38]. Several factors may have influenced this, however, such as the limited range of action previously observed (limited to only vertical jumping). Differing action types, including cutting maneuvers that induce more abduction/adduction and rotation, were examined in this study. Normalization of both RMSE values may provide a better means of comparison. Across all cases, the RMSE values between the TQC and MCS were smaller than those reported by our previous study, illustrating that perhaps the TQC may estimate angles more accurately. Furthermore, comparing the BA plots showed that the TQC demonstrated an overall greater degree of reliability as both lesser trends and smaller LoAs were observed.

6.5.1 Limitations

This study has several limitations, including the use of a controlled laboratory setting. Due to the limited space and potential lack of comfort, participants may not have been able to perform actions exactly as they would on-field. The floor, being stiffer than common surfaces in sports may have also impacted our results as several studies have tracked the effects of surface stiffness on energy absorption and biomechanics; it may be possible that greater errors/variations would be present to track in on-field activities where surface stiffness may vary greatly [56, 57]. The small population size (N=9) of our study is a limitation. Additional participants with more varying age, weight, height, etc. may be needed to assess the true accuracy and reliability of the TQC. The way our sensors were affixed may also be a limitation, to using this in the field, as on-field use of these sensors may preclude them from being similarly placed on athletes. Either due

to game rules or athlete comfort, sensor placement may need to be adjusted. Studies conducted have correlated the relationship between sensor position and orientation with errors in estimations, showing a reduction of accuracy up to 20.8% [58]. Thus, while using the current sensor placement, we reported high levels of accuracy and reliability when implementing the TQC, changes in either sensor orientation/placement may adversely affect our results. Additionally, the duration of each test may have omitted, or greatly reduced, the potential effect drift and error accumulation may have on angle estimates. While the TQC accounts for gyroscopic drift in a recursive process, test actions were performed in several seconds. During on-field implementation, the sensor may need to be recording for upwards of two hours, depending on the sport being examined. The effects of prolonged recording on the accuracy/reliability of the TQC warrants additional research.

6.6 Conclusions

Our goal in this study was to ascertain the potential improvement in accuracy and reliability of a tuned quaternion conversion algorithm when compared to the sensor fusion algorithm often provided by the manufacturers. The theory was, that due to their popularity in rehabilitation settings, various parameters within the sensor fusion algorithm are tuned to less dynamic actions and therefore may not be robust enough for implementation in sports-related activities. Tuning a quaternion conversion algorithm and using dynamic actions, we recorded improvement across all three angle types, as the TQC was able to more accurately (lower RMSE) and more reliably (smaller LoA) estimate an angle than the IMU. It may be feasible to use this algorithm to identify and track knee angle measurements that may be associated with ACL injury. However, further testing into the effect surface-of-play may have, optimal placement of sensors to ensure

adherence to rules and player comfort, and the effects drift may have on the prolonged recording will be needed before an on-field application is possible.

Author Contributions: Conceptualization, A.E.; Methodology, M.A. and A.E.; Investigation/Data Collection, AE and M.A.; Software, M.A.; Formal Analysis, MA; Writing—original draft, M.A.; Writing—review & editing, A.E.; Supervision, A.E.

Funding: This material is based upon work supported by the National Science Foundation under grant no 22044908.

Institutional Review Board Statement: The study was conducted in accordance with the Declaration of Helsinki, and approved by the Institutional Review Board (or Ethics Committee) of University of Michigan (HUM00150719)

Informed Consent Statement: Informed consent was obtained from all subjects involved in the study

Acknowledgments: The authors would like to thank the all the subjects who volunteered to participate for their enthusiasm and interest in the study.

Conflicts of Interest: The authors declare no conflict of interest.

6.7 References

[1] A. L. Gornitzky, A. Lott, J. L. Yellin, P. D. Fabricant, J. T. Lawrence, and T. J. Ganley, "Sport-Specific Yearly Risk and Incidence of Anterior Cruciate Ligament Tears in High School Athletes: A Systematic Review and Meta-analysis," *Am J Sports Med,* Dec 11 2015, doi: 10.1177/0363546515617742.

[2] J. M. Hootman, R. Dick, and J. Agel, "Epidemiology of collegiate injuries for 15 sports: summary and recommendations for injury prevention initiatives," *J Athl Train,* vol. 42, no. 2, pp. 311-9, Apr-Jun 2007.

[3] A. P. Toth and F. A. Cordasco, "Anterior cruciate ligament injuries in the female athlete," *J Gend Specif Med,* vol. 4, no. 4, pp. 25-34, 2001.

[4] B. M. Saltzman, G. L. Cvetanovich, B. U. Nwachukwu, N. A. Mall, C. A. Bush-Joseph, and B. R. Bach, Jr., "Economic Analyses in Anterior Cruciate Ligament Reconstruction: A Qualitative and Systematic Review," *Am J Sports Med,* Apr 30 2015, doi: 10.1177/0363546515581470.

[5] H. N. Ladenhauf, J. Graziano, and R. G. Marx, "Anterior cruciate ligament prevention strategies: are they effective in young athletes - current concepts and review of literature," *Curr Opin Pediatr,* vol. 25, no. 1, pp. 64-71, Feb 2013, doi: 10.1097/MOP.0b013e32835ad208.

[6] A. von Porat, E. M. Roos, and H. Roos, "High prevalence of osteoarthritis 14 years after an anterior cruciate ligament tear in male soccer players: a study of radiographic and patient relevant outcomes," *Ann Rheum Dis,* vol. 63, no. 3, pp. 269-73, Mar 2004.

[7] P. Fauno and B. Wulff Jakobsen, "Mechanism of anterior cruciate ligament injuries in soccer," *Int J Sports Med,* vol. 27, no. 1, pp. 75-9, Jan 2006, doi: 10.1055/s-2005-837485.

[8] T. E. Hewett *et al.*, "Biomechanical measures of neuromuscular control and valgus loading of the knee predict anterior cruciate ligament injury risk in female athletes: a prospective study," *Am J Sports Med,* vol. 33, no. 4, pp. 492-501, Apr 2005, doi: 10.1177/0363546504269591.

[9] R. J. Schmitz, A. S. Kulas, D. H. Perrin, B. L. Riemann, and S. J. Shultz, "Sex differences in lower extremity biomechanics during single leg landings," *Clin Biomech (Bristol, Avon),* vol. 22, no. 6, pp. 681-8, Jul 2007, doi: 10.1016/j.clinbiomech.2007.03.001.

[10] B. Yu, C. F. Lin, and W. E. Garrett, "Lower extremity biomechanics during the landing of a stop-jump task," *Clin Biomech (Bristol, Avon),* vol. 21, no. 3, pp. 297-305, Mar 2006, doi: 10.1016/j.clinbiomech.2005.11.003.

[11] B. L. Zeller, J. L. McCrory, W. B. Kibler, and T. L. Uhl, "Differences in kinematics and electromyographic activity between men and women during the single-legged squat," *Am J Sports Med,* vol. 31, no. 3, pp. 449-56, May-Jun 2003.

[12] D. L. Miranda, P. D. Fadale, M. J. Hulstyn, R. M. Shalvoy, J. T. Machan, and B. C. Fleming, "Knee biomechanics during a jump-cut maneuver: effects of sex and ACL surgery," *Med Sci Sports Exerc,* vol. 45, no. 5, pp. 942-51, May 2013, doi: 10.1249/MSS.0b013e31827bf0e4.

[13] L. Y. Griffin *et al.*, "Noncontact anterior cruciate ligament injuries: risk factors and prevention strategies," (in eng), *J Am Acad Orthop Surg,* vol. 8, no. 3, pp. 141-50, 2000 May-Jun 2000, doi: 10.5435/00124635-200005000-00001.

[14] C. Y. Wild, J. R. Steele, and B. J. Munro, "Why do girls sustain more anterior cruciate ligament injuries than boys?: a review of the changes in estrogen and musculoskeletal structure and function during puberty," (in eng), *Sports Med,* vol. 42, no. 9, pp. 733-49, Sep 2012, doi: 10.1007/BF03262292.

[15] L. Yin, D. Sun, Q. C. Mei, Y. D. Gu, J. S. Baker, and N. Feng, "The Kinematics and Kinetics Analysis of the Lower Extremity in the Landing Phase of a Stop-jump Task," (in eng), *Open Biomed Eng J,* vol. 9, pp. 103-7, 2015, doi: 10.2174/1874120701509010103.

[16] B. Yu and W. E. Garrett, "Mechanisms of non-contact ACL injuries," (in eng), *Br J Sports Med,* vol. 41 Suppl 1, pp. i47-51, Aug 2007, doi: 10.1136/bjsm.2007.037192.

[17] S. Ananthanarayan, M. Sheh, A. Chien, H. Profita, and K. A. Siek, "Designing Wearable Interfaces for Knee Rehabilitation," in *Proceedings of the 8th International Conference on Pervasive Computing Technologies for Healthcare*, Oldenburg, Germany, 2014.

[18] M. Arif and A. Kattan, "Physical Activities Monitoring Using Wearable Acceleration Sensors Attached to the Body," *PLoS One,* vol. 10, no. 7, p. e0130851, 2015, doi: 10.1371/journal.pone.0130851.

[19] S. Bakshi, M. H. Mahoor, and B. S. Davidson, "Development of a Body Joint Angle Measurement System Using IMU Sensors," in *33rd Annual International Conference of the IEEE EMBS*, Boston, MA, 2011.

[20] S. J. Bamberg, A. Y. Benbasat, D. M. Scarborough, D. E. Krebs, and J. A. Paradiso, "Gait analysis using a shoe-integrated wireless sensor system," *IEEE Trans Inf Technol Biomed,* vol. 12, no. 4, pp. 413-23, Jul 2008, doi: 10.1109/TITB.2007.899493.

[21] J. A. Barrios, K. M. Crossley, and I. S. Davis, "Gait retraining to reduce the knee adduction moment through real-time visual feedback of dynamic knee alignment," *J Biomech,* vol. 43, no. 11, pp. 2208-13, Aug 10 2010, doi: 10.1016/j.jbiomech.2010.03.040.

[22] K. H. Chen, P. C. Chen, K. C. Liu, and C. T. Chan, "Wearable sensor-based rehabilitation exercise assessment for knee osteoarthritis," *Sensors (Basel),* vol. 15, no. 2, pp. 4193-211, 2015, doi: 10.3390/s150204193.

[23] C. J. Anderson, C. G. Ziegler, C. A. Wijdicks, L. Engebretsen, and R. F. LaPrade, "Arthroscopically pertinent anatomy of the anterolateral and posteromedial bundles of the

posterior cruciate ligament," (in eng), *J Bone Joint Surg Am,* vol. 94, no. 21, pp. 1936-45, Nov 2012, doi: 10.2106/JBJS.K.01710.

[24] A. G. Cutti, A. Ferrari, P. Garofalo, M. Raggi, and A. Cappello, "'Outwalk': a protocol for clinical gait analysis based on inertial and magnetic sensors," (in eng), *Med Biol Eng Comput,* vol. 48, no. 1, pp. 17-25, Jan 2010, doi: 10.1007/s11517-009-0545-x.

[25] J. Favre, X. Crevoisier, B. M. Jolles, and K. Aminian, "Evaluation of a mixed approach combining stationary and wearable systems to monitor gait over long distance," (in eng), *J Biomech,* vol. 43, no. 11, pp. 2196-202, Aug 2010, doi: 10.1016/j.jbiomech.2010.03.041.

[26] A. Ferrari *et al.*, "First in vivo assessment of "Outwalk": a novel protocol for clinical gait analysis based on inertial and magnetic sensors," (in eng), *Med Biol Eng Comput,* vol. 48, no. 1, pp. 1-15, Jan 2010, doi: 10.1007/s11517-009-0544-y.

[27] J. F. Lin and D. Kulić, "Human pose recovery using wireless inertial measurement units," (in eng), *Physiol Meas,* vol. 33, no. 12, pp. 2099-115, Dec 2012, doi: 10.1088/0967-3334/33/12/2099.

[28] P. Picerno, A. Cereatti, and A. Cappozzo, "Joint kinematics estimate using wearable inertial and magnetic sensing modules," (in eng), *Gait Posture,* vol. 28, no. 4, pp. 588-95, Nov 2008, doi: 10.1016/j.gaitpost.2008.04.003.

[29] E. M. Wojtys, M. L. Beaulieu, and J. A. Ashton-Miller, "New perspectives on ACL injury: On the role of repetitive sub-maximal knee loading in causing ACL fatigue failure," *J Orthop Res,* vol. 34, no. 12, pp. 2059-2068, Dec 2016, doi: 10.1002/jor.23441.

[30] O. E. Olsen, G. Myklebust, L. Engebretsen, and R. Bahr, "Injury mechanisms for anterior cruciate ligament injuries in team handball: a systematic video analysis," (in eng), *Am J Sports Med,* vol. 32, no. 4, pp. 1002-12, Jun 2004, doi: 10.1177/0363546503261724.

[31] P. Renstrom *et al.*, "Non-contact ACL injuries in female athletes: an International Olympic Committee current concepts statement," (in eng), *Br J Sports Med,* vol. 42, no. 6, pp. 394-412, Jun 2008, doi: 10.1136/bjsm.2008.048934.

[32] M. Ajdaroski, S. Y. Baek, J. A. Ashton-Miller, and A. O. Esquivel, "Predicting forces and knee moments using IMUs: an in vitro study," 2023.

[33] M. Ajdaroski, R. Tadakala, L. Nichols, and A. Esquivel, "Validation of a Device to Measure Knee Joint Angles for a Dynamic Movement," (in eng), *Sensors (Basel),* vol. 20, no. 6, Mar 2020, doi: 10.3390/s20061747.

[34] J. M. Barrett, D. Viggiani, J. Park, and J. P. Callaghan, "Expressing angles relative to reference postures: A mathematical comparison of four approaches," (in eng), *J Biomech,* vol. 104, p. 109733, May 2020, doi: 10.1016/j.jbiomech.2020.109733.

[35] T. Watanabe and H. Saito, "Tests of wireless wearable sensor system in joint angle measurement of lower limbs," (in eng), *Annu Int Conf IEEE Eng Med Biol Soc,* vol. 2011, pp. 5469-72, 2011, doi: 10.1109/IEMBS.2011.6091395.

[36] K. Tong and M. H. Granat, "A practical gait analysis system using gyroscopes," (in eng), *Med Eng Phys,* vol. 21, no. 2, pp. 87-94, Mar 1999, doi: 10.1016/s1350-4533(99)00030-2.

[37] R. Takeda, S. Tadano, A. Natorigawa, M. Todoh, and S. Yoshinari, "Gait posture estimation using wearable acceleration and gyro sensors," (in eng), *J Biomech,* vol. 42, no. 15, pp. 2486-94, Nov 2009, doi: 10.1016/j.jbiomech.2009.07.016.

[38] M. Ajdaroski, J. A. Ashton-Miller, S. Y. Baek, P. M. Shahshahani, and A. Esquivel, "Testing a Quaternion Conversion Method to Determine Human 3D Tibiofemoral Angles During an in Vitro Simulated Jump Landing," (in eng), *J Biomech Eng,* Sep 22 2021, doi: 10.1115/1.4052496.

[39] B. Yu, D. Gabriel, L. Noble, and K.-N. An, "Estimate of the Optimum Cutoff Frequency for the Butterworth Low-Pass Digital Filter," *Journal of Applied Biomechanics,* vol. 15, pp. 319-329, 1999 doi: 10.1123/jab.15.3.318.

[40] M. Pedley, M. Stanley, and Z. Baranski, "Freescale Sensor Fusion Kalman Filter," ed: Freescale S emiconductor 2014.

[41] J. Larwa, C. Stoy, R. S. Chafetz, M. Boniello, and C. Franklin, "Stiff Landings, Core Stability, and Dynamic Knee Valgus: A Systematic Review on Documented Anterior Cruciate Ligament Ruptures in Male and Female Athletes," (in eng), *Int J Environ Res Public Health,* vol. 18, no. 7, 04 2021, doi: 10.3390/ijerph18073826.

[42] S. Bakhshi, M. H. Mahoor, and B. S. Davidson, "Development of a body joint angle measurement system using IMU sensors," (in eng), *Annu Int Conf IEEE Eng Med Biol Soc,* vol. 2011, pp. 6923-6, 2011, doi: 10.1109/IEMBS.2011.6091743.

[43] R. Zügner, R. Tranberg, J. Timperley, D. Hodgins, M. Mohaddes, and J. Kärrholm, "Validation of inertial measurement units with optical tracking system in patients operated with Total hip arthroplasty," (in eng), *BMC Musculoskelet Disord,* vol. 20, no. 1, p. 52, Feb 2019, doi: 10.1186/s12891-019-2416-4.

[44] K. M. Bell *et al.*, "Verification of a Portable Motion Tracking System for Remote Management of Physical Rehabilitation of the Knee," (in eng), *Sensors (Basel),* vol. 19, no. 5, Feb 2019, doi: 10.3390/s19051021.

[45] B. Fan, H. Xia, J. Xu, Q. Li, and P. B. Shull, "IMU-based knee flexion, abduction and internal rotation estimation during drop landing and cutting tasks," (in eng), *J Biomech,* vol. 124, p. 110549, Jul 19 2021, doi: 10.1016/j.jbiomech.2021.110549.

[46] K. L. Markolf, D. M. Burchfield, M. M. Shapiro, M. F. Shepard, G. A. Finerman, and J. L. Slauterbeck, "Combined knee loading states that generate high anterior cruciate

ligament forces," (in eng), *J Orthop Res,* vol. 13, no. 6, pp. 930-5, Nov 1995, doi: 10.1002/jor.1100130618.

[47] T. E. Hewett, G. D. Myer, and K. R. Ford, "Anterior cruciate ligament injuries in female athletes: Part 1, mechanisms and risk factors," (in eng), *Am J Sports Med,* vol. 34, no. 2, pp. 299-311, Feb 2006, doi: 10.1177/0363546505284183.

[48] T. E. Hewett, K. R. Ford, and G. D. Myer, "Anterior cruciate ligament injuries in female athletes: Part 2, a meta-analysis of neuromuscular interventions aimed at injury prevention," (in eng), *Am J Sports Med,* vol. 34, no. 3, pp. 490-8, Mar 2006, doi: 10.1177/0363546505282619.

[49] C. S. Shin, A. M. Chaudhari, and T. P. Andriacchi, "Valgus plus internal rotation moments increase anterior cruciate ligament strain more than either alone," (in eng), *Med Sci Sports Exerc,* vol. 43, no. 8, pp. 1484-91, Aug 2011, doi: 10.1249/MSS.0b013e31820f8395.

[50] S. G. McLean, S. W. Lipfert, and A. J. van den Bogert, "Effect of gender and defensive opponent on the biomechanics of sidestep cutting," (in eng), *Med Sci Sports Exerc,* vol. 36, no. 6, pp. 1008-16, Jun 2004, doi: 10.1249/01.mss.0000128180.51443.83.

[51] S. M. Sigward and C. M. Powers, "Loading characteristics of females exhibiting excessive valgus moments during cutting," (in eng), *Clin Biomech (Bristol, Avon),* vol. 22, no. 7, pp. 827-33, Aug 2007, doi: 10.1016/j.clinbiomech.2007.04.003.

[52] M. L. Beaulieu, J. A. Ashton-Miller, and E. M. Wojtys, "Loading mechanisms of the anterior cruciate ligament," (in eng), *Sports Biomech,* vol. 22, no. 1, pp. 1-29, Jan 2023, doi: 10.1080/14763141.2021.1916578.

[53] A. Peters, B. Galna, M. Sangeux, M. Morris, and R. Baker, "Quantification of soft tissue artifact in lower limb human motion analysis: a systematic review," (in eng), *Gait Posture,* vol. 31, no. 1, pp. 1-8, Jan 2010, doi: 10.1016/j.gaitpost.2009.09.004.

[54] T. Y. Tsai, T. W. Lu, M. Y. Kuo, and C. C. Lin, "Effects of soft tissue artifacts on the calculated kinematics and kinetics of the knee during stair-ascent," (in eng), *J Biomech,* vol. 44, no. 6, pp. 1182-8, Apr 2011, doi: 10.1016/j.jbiomech.2011.01.009.

[55] L. B. Wood and H. Asada, "Low variance adaptive filter for cancelling motion artifact in wearable photoplethysmogram sensor signals," (in eng), *Annu Int Conf IEEE Eng Med Biol Soc,* vol. 2007, pp. 652-5, 2007, doi: 10.1109/IEMBS.2007.4352374.

[56] T. R. Derrick, J. Hamill, and G. E. Caldwell, "Energy absorption of impacts during running at various stride lengths," (in eng), *Med Sci Sports Exerc,* vol. 30, no. 1, pp. 128-35, Jan 1998, doi: 10.1097/00005768-199801000-00018.

[57] D. P. Ferris, M. Louie, and C. T. Farley, "Running in the real world: adjusting leg stiffness for different surfaces," (in eng), *Proc Biol Sci,* vol. 265, no. 1400, pp. 989-94, Jun 1998, doi: 10.1098/rspb.1998.0388.

[58] T. Tan, D. P. Chiasson, H. Hu, and P. B. Shull, "Influence of IMU position and orientation placement errors on ground reaction force estimation," (in eng), *J Biomech,* vol. 97, p. 109416, Dec 2019, doi: 10.1016/j.jbiomech.2019.109416.

Chapter 7: Summary, Pitfalls, and Future Directions

7.1 Summary of Our Work

The increase in the incidence of ACL injuries is a growing concern, and the need to be able to prevent them has garnered much attention in sports medicine. By nature, most ACL injuries are non-contact and, in some cases, possibly due to ligament overuse. Fortunately, if overuse is the reason, the tracking of parameters such as ground reaction force, knee moments, and knee angles may provide a means to prevent them. While traditional tracking methods have limited use outside the laboratory, IMUs may be a viable on-field approach to monitor kinematics in athletes during gameplay events. However, IMUs only record linear acceleration and angular velocity of a segment and therefore require the application of post-collection equations to estimate relevant parameters.

The first stage of this study used *in vitro* models to estimate the values of GRF, knee moments, and angles during single-legged simulated landings. A QC method estimated the 3D tibiofemoral angles using data obtained from the IMUs. We utilized nine cadaveric knee specimens during the training (N=4) and validation (N=5) of the method. We compared the estimated angles using our new method to those obtained from a commercially available sensor fusion algorithm (APDM OPAL) and those calculated from the active marker motion capture system. We found significant differences in some orthogonal angles when comparing the QC method and commercially available algorithm to the MCS data ($p<0.01$). However, differences between the QC method and the MCS in the testing set for flexion and rotation angles were less than those of the

commercially available algorithm and the MCS, indicating improvement. Smaller limits of agreement between the QC method and the MCS indicate improved reliability in angle estimations. We used machine learning algorithms in the next stage to estimate the values of the forces and moments. Here, we used 24 specimens; 21 were used for training each model, while three were used for testing accuracy (normalized root mean square error) and reliability (Bland-Altman limits of agreement). The results showed that the models estimated the forces and knee moments with acceptable levels of error and reliability, although several exhibited some form of bias. Our Stage 1 testing showed the potential of IMUs to estimate forces, knee moments, and knee angles accurately and reliably in cadaveric models, thus allowing us to proceed to Stage 2: estimating various parameters such as GRF, KAM, KRM, and knee angles using IMU data for human subjects.

In the second stage of this study, we recruited nine healthy volunteers (five females, four males) who currently play soccer or basketball or have played in the last two years. We fitted four IMUs on each subject (placed on the shank and thigh of either leg) and instructed them to perform nine sport-related movements three times each. A motion capture system including force plates allowed us to measure kinematics and force, we used Visual 3D software to calculate knee joint moments using inverse dynamics. We recorded KAM, KRM, and knee angle measurements at the maximum vertical GRF; a sync box allowed for taking IMU data at this same time frame. The second stage used a similar method found in the first to estimate knee angles; however, we returned to the QC method for human subjects. We used the data of five participants to re-tune the algorithm, with the remaining four used to test the algorithm's validity. The results of the new algorithm were then compared to those of the commercially available algorithm and the MCS. In

all three angle types, the new algorithm was more accurate (lower RMSE) and more reliable (smaller LoA) in angle estimation than the commercially available software. In the second stage, we again used machine learning to estimate the forces and moments; however, the models here used the first-stage model estimations and subject-specific metrics to develop modified models. We compared the modified models' estimated values to the MCS and tested for accuracy (normalized root mean square) and reliability (Bland-Altman limits of agreement). We also developed a confusion matrix to examine if these estimates could distinguish between low-risk and potentially injurious events. Results showed high classification accuracy, precision, specificity, and sensitivity but poor reliability for the KAM and KRM estimates. Nonetheless, the modified models show promise in distinguishing between low-risk and potentially injurious events.

Over both stages of our study, we found that IMUs can be used to estimate ground reaction forces, knee moments, and knee angles with moderate levels of accuracy, and even though we found some poor reliability during our human subject testing, estimated values could still distinguish between low-risk and potentially injurious events with high accuracy. Our results show that we may be able to use IMUs to track these conditions on-field, inform coaches and team doctors of potentially injurious events, and have athletes rest and recover appropriately. However, over the course of our work, several limitations have been noted that could warrant further research.

7.2 Pitfalls, Limitations, and Future Pursuits

We discovered several limitations during testing in either stage that may have skewed our results or impeded our ability to develop robust models. During the first stage, we recognized that our use of cadaveric specimens meant we developed the algorithm and models under ideal circumstances; omitted were the possible effects of soft tissue. However, this was less of a limitation and more of designing this stage with a particular goal: developing models that related the IMU data to the mechanics of a performed action. If we proceeded directly toward the second stage and performed human testing, we would be unable to state with any certainty if errors between measured and estimated values were due to the inability of IMU data to model a phenomenon or if other factors (such as soft tissue artifact) were to blame. Stage one showed that it was possible to use IMU data to model an action; thus, we were confident that errors arising in the second stage were attributable to other factors. Cadaveric specimen use was not the only limitation of the first testing stage, as a lack of action variability can also be a potential limitation. This lack of variability may have meant the models were overly tuned for jump-landing actions. However, our modifications during the second stage accounted for both soft tissue and included a variety of actions. Although, which factor (the soft tissue or actions variation effects) these modifications more heavily account for is unclear. Reperforming stage one testing with a different rig that can mimic various actions would give us insight into this question. Though the high performance in the second stage may mean additional testing is not warranted.

During the second stage, the limited space and potential lack of inability to perform tasks in the 'natural setting' may have meant participants did not perform actions exactly as they would on-

field. Therefore, the models developed during this second stage may provide less accurate and reliable estimates when applied on-field. The stiffer floor of the laboratory may also skew our models' abilities, as several studies have related the effects of floor stiffness to energy absorption and biomechanics [1, 2]. Reperforming the second stage on softer surfaces more akin to field conditions, such as turf, may alleviate this issue. Likewise, adding a third stage in which we develop modifications based on differing play surfaces may also be a research avenue to pursue. How we affixed our sensors onto a participant during stage two is also an issue of concern, as on-field rules and regulations and an athlete's comfort may preclude placing them similarly during gameplay. We may need to adjust sensor placement or find different ways to integrate the sensors without violating rules or compromising comfort. For example, additional research into developing a sensor-embedded shin guard for soccer athletes may allow for tracking of injurious events while unaffecting the core gameplay. However, this would mean we would need to develop new models based on the data of these new sensors. Though, the procedure and results of this study would provide a framework for how to model the new sensor data. In terms of basketball, sensor-embedded shoes may be the alternative to how our sensors were placed, though again, we would need to construct new models.

The possible effects of prolonged recording were never examined during human subject testing, thus proving to be another limitation of this study. The actions participants performed during our human subject testing were done so in quick secession; all actions lasted no longer than a minute. This small duration of each test may have omitted or reduced the effects of gyroscopic drift and possible error accumulation within the sensor readings. We understand that implementing a sensor to record events during gameplay may require the sensor to be active for hours, depending

on the sport. How this continuous activation affects sensor recording is unclear and warrants additional research. A possible avenue to pursue is to observe how the sensor recordings are affected by the time when left within a neutral environment (i.e., placed on a level surface and free of any outside movement). Examining the effects of time independently from any other factor may provide a means to develop additional model modifications to account for its influence. Another pursuit may be to implement our sensors during game practice events. Not only would the effects of time be present, but without game rules and regulations, we would be able to place our sensors as we did during our human subject testing. Pursuing this course would allow for modifications based on the duration and the surface of play and allow for observing actions more comparable to those during competitive gameplay. As we did not account for the effects of dermal thickness and tissue composition during human subject this, this may pose another limitation of our work. Various works have alluded to the potential effects tissue may have on sensor measurement reliability [3, 4]. Measuring skin fold thickness, or subcutaneous fat levels where the IMUs were placed should be examined to understand their effects and develop possible filtering algorithms to account for possible sensor movement.

7.3 Final Conclusions

Over the course of our work, we have demonstrated that IMUs can be used to estimate ground reaction force, knee moments, and knee angles with some accuracy. And though during the human testing, we determined a deficiency in reliability in knee moment estimates, we used our models' estimates to classify the risk of an event with high accuracy, precision, specificity, and sensitivity. Our results show the potential of IMUs for tracking gameplay events and distinguishing between low-risk and potentially-risky events. While we acknowledged several

limitations within our work, we also provided several research avenues to pursue in addressing and correcting them. Ultimately, we believe that IMUs may be used to aid coaches and clinicians in preventing some athletes from sustaining ACL injuries.

7.4 References

[1] T. R. Derrick, J. Hamill, and G. E. Caldwell, "Energy absorption of impacts during running at various stride lengths," (in eng), *Med Sci Sports Exerc,* vol. 30, no. 1, pp. 128-35, Jan 1998, doi: 10.1097/00005768-199801000-00018.

[2] D. P. Ferris, M. Louie, and C. T. Farley, "Running in the real world: adjusting leg stiffness for different surfaces," (in eng), *Proc Biol Sci,* vol. 265, no. 1400, pp. 989-94, Jun 1998, doi: 10.1098/rspb.1998.0388.

[3] L. K. Smalls, R. Randall Wickett, and M. O. Visscher, "Effect of dermal thickness, tissue composition, and body site on skin biomechanical properties," (in eng), *Skin Res Technol,* vol. 12, no. 1, pp. 43-9, Feb 2006, doi: 10.1111/j.0909-725X.2006.00135.x.

[4] L. Q. Vu, K. H. Kim, L. J. H. Schulze, and S. L. Rajulu, "Lumbar posture assessment with fabric strain sensors," (in eng), *Comput Biol Med,* vol. 118, p. 103624, Mar 2020, doi: 10.1016/j.compbiomed.2020.103624.